THE INFLUENCE OF WATER COMPOSITION ON THE PITTING BEHAVIOUR OF A STAINLESS STEEL

by

A.E. Capendale

A thesis submitted to the Faculty of Engineering, University of Cape Town in fulfilment of the degree of Master of Science in Applied Science.

Department of Materials Engineering, University of Cape Town.

December 1985

ACKNOWLEDGEMENTS

I wish to express my appreciation to the following people who have assisted me during this research project:

My supervisor, Mr Robert Noël, who was a constant source of guidance and encouragement.

Mrs Helgard Böhm and Mrs Sue Betz for their assistance and co-operation in the laboratory and in the final preparation of the manuscript.

Mr Nick Dreze and Mr Andrew Rapley for their technical expertise in the workshop.

Mr Bernie Greeves for his help and advice with the photographic material.

Miss Tracey Leveton for the many hours which she devoted to the typing of this thesis.

All my fellow students who have helped to make the duration of this study a pleasant experience.

This thesis was based on the results of the collaborative programme of work undertaken as part of the research and development programme of the Research Organisation of the Chamber of Mines of South Africa.

ABSTRACT

The new concept of hydropower has been found to be technically feasible in South African gold mines. Chilled mine service water is piped from the surface to deep level stopes where the hydrostatic pressure provides power for stoping machinery. This water varies widely in composition and acidity. High concentrations of sulphate, chloride and nitrate are present. These ions are derived from the leaching of oxidised sulphides from the broken rock, the fissure water and the dissolution of blasting fumes.

In order to minimise the deterioration of stoping machinery by corrosion and synergistic corrosive abrasive effects, a compromise between selecting a suitable corrosion resistant material and treating the mine service water to an acceptable level of corrosiveness is being sought.

The potentiodynamic polarization technique has been used to determine the corrosion behaviour of AISI 431 stainless steel in synthetic mine water solutions. The construction of an experimentally determined E-pH diagram showed that AISI 431 is passive in solutions with a pH equal to and greater than 3.8. As expected the presence of chloride ions was found to be responsible for pitting corrosion during the potentiodynamic polarization tests. The chloride concentration at which the breakdown of passivity changes from being uniform (transpassivity) to localized (pitting), was defined to be the critical chloride concentration, $[Cl^-]_{crit}$. The corrosion potential, the pitting or breakdown potential and the protection potential were plotted as a function of chloride concentration for solutions with various combinations of pH and nitrate concentration. It was found that increasing pH and nitrate ion concentration inhibited pitting corrosion of AISI 431 by increasing the $[Cl^-]_{crit}$. A limited series of tests showed that sulphate ions inhibit pitting corrosion of AISI 431 to a lesser extent than nitrate ions. For the limited range of concentrations reported in mine waters, linear relationships were found to exist between inhibitor ion concentration and $[Cl^-]_{crit}$.

The results have been discussed in terms of their practical application to the real mine water situation. The increase in corrosion potential in real mine

waters due to microbial activity, the presence of oxidisers and other factors is thought to play an important role in the occurrence of pitting corrosion of mining equipment. It is suggested that careful control of the chemistry of the mine water will be as important as alloy selection in minimising the corrosion problems which are likely to be encountered in the hydropower system.

A GLOSSARY OF SYMBOLS AND ABBREVIATIONS

a	- activity
β	- Tafel constant
$[Cl^-]_{crit}$	- critical chloride concentration
E	- electrode potential
E^o	- standard electrode potential
E_b	- breakdown potential corresponding to uniform breakdown of passivity due to transpassive dissolution
E_{corr}	- corrosion potential
E_F	- Flade potential
E_p	- pitting potential corresponding to localized breakdown of passivity due to pitting corrosion
E_{pp}	- primary passive potential
E_x	- protection potential
F	- Farraday's constant = 9.64870 x 10^4 C mol^{-1}
ΔG	- change in free energy
h.e.r.	- hydrogen evolution reaction
i_o	- exchange current density
i_{corr}	- corrosion current density
I_c	- critical anodic current density
I_{pass}	- passive current density
o.r.r.	- oxygen reduction reaction
n	- number of electrons involved in a reaction
η	- overvoltage
pH	- log $1/[H^+]$
π	- osmotic pressure
ppm	- concentration in parts per million
r	- rate of reaction
R	- molar gas constant = 8.3143 $J.mol^{-1}K^{-1}$
R.W.R.	- relative wear resistance
S.C.E.	- saturated calomel electrode
S.H.E.	- standard hydrogen electrode
τ	- induction time for pit initiation
T.D.S.	- total dissolved solids

CONTENTS

PAGE

PAGE

CHAPTER 1

INTRODUCTION

The development of mechanised stoping techniques in order to increase the productivity and profitability of South African gold mines requires the introduction of machines for the mining and transportation of quartzitic rock. The two most challenging problems facing the mechanization programme are:

i) To devise suitable methods of powering stoping machinery.
ii) To achieve adequate reliability of stoping machinery.

The limited efficiency, high maintenance costs and other factors associated with the traditional use of pneumatic and electric power have necessitated the search for an alternative source of power for underground operations. The high costs of mineral oils and pollution of the working area resulting from spillage excludes the use of conventional hydraulics. Hydraulically powered systems, using an emulsion (known as 5:95), which consists of 95 per cent water and 5 per cent additive, as the hydraulic fluid, have therefore been developed for use in the mines. A new concept, known as hydropower, involves utilizing the energy made available by the hydrostatic pressure in a column of water leading from the surface to deep level stopes. The high pressure water will be used in the form of water jets to assist in mechanical rock breaking and stope cleaning. It is intended that the hydraulic machinery currently operating on 5:95 emulsions will ultimately be converted for powering by hydropower water. A further attraction is that, by cooling the water at the surface, the hydropower system could contribute to the overall cooling of the mines. An increase in the corrosivity of the water due to contamination by the mining environment will necessitate that the water undergoes a treatment process before it is re-used (Manager MAB, (1983)).

Corrosion and abrasion have been identified as the major causes of material degradation resulting in the unreliable performance of underground machinery. In-situ studies and laboratory tests have shown that stainless steels have superior wear resistance to mild steel and proprietary wear resistant alloys

in a situation where both corrosion and abrasion are encountered. The relative wear reistance (R.W.R.):

$$R.W.R. = \frac{\text{Volume loss of mild steel}}{\text{Volume loss of material X}}$$

of a series of corrosion resistant steels is compared to mild steel and a number of proprietary wear resistant alloys in Figure 1.1 (Noël, Allen and Ball, (1984)).

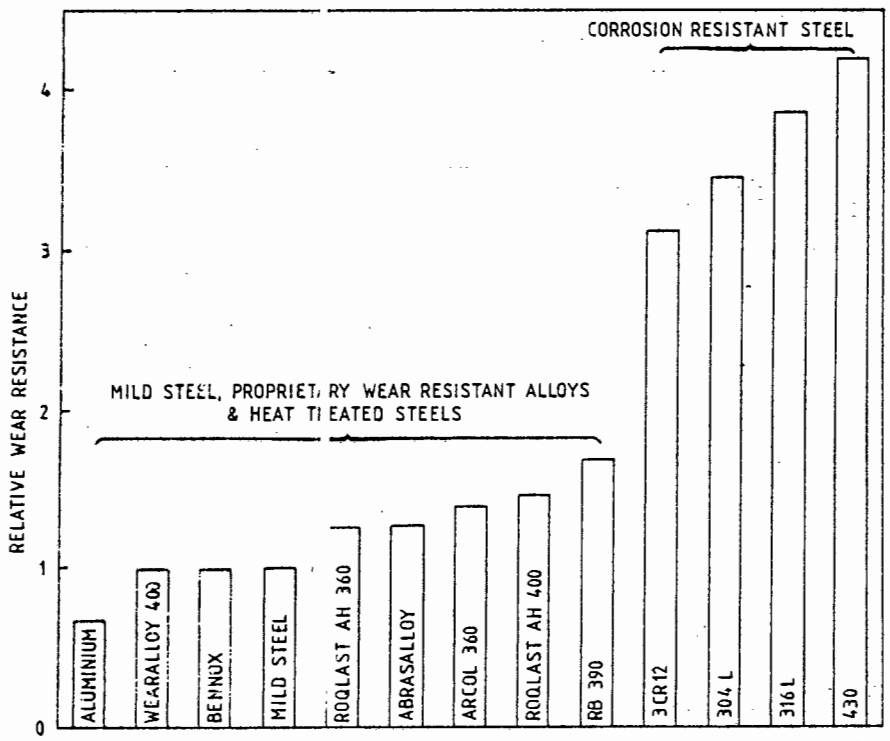

FIGURE 1.1 : The relative wear resistance of corrosion resistant steels compared to mild steel and proprietary wear resistant steels (after Noël, Allen and Ball (1984)).

This work clearly highlighted the need for a "stainless" type steel with good abrasion resistance, however conventional stainless steels are expensive and do not have the required mechanical properties. Chromium-containing martensitic steels are therefore regarded as being potential materials for the manufacture of mining equipment. Chromium provides corrosion resistance while a martensitic microstructure provides abrasion resistance and the desired mechanical properties.

The design of machinery to function on treated mine water and the development of new materials with suitable mechanical properties and corrosion resistance is vital for the successful implementation of the hydropower concept. By simultaneous interactive research in the fields of alloy development, water treatment, corrosion and wear, the Chamber of Mines aims to determine a practical and cost-effective compromise between alloy composition and water-quality (Manager MAB, (1983)).

CHAPTER 2

AN OUTLINE OF THE PROBLEM

2.1 THE AIM OF THE CHAMBER OF MINES RESEARCH ORGANISATION

Ultimately the Chamber of Mines Research Organisation aims to develop cost-effective "stainless" type materials which will remain passive in treated mine waters. This is schematically represented in Figure 2.1. To achieve this aim it is necessary to identify those factors relating to the quality of mine water and the composition of the steel in order that appropriate treatment of the water can be undertaken and suitable steels may be developed.

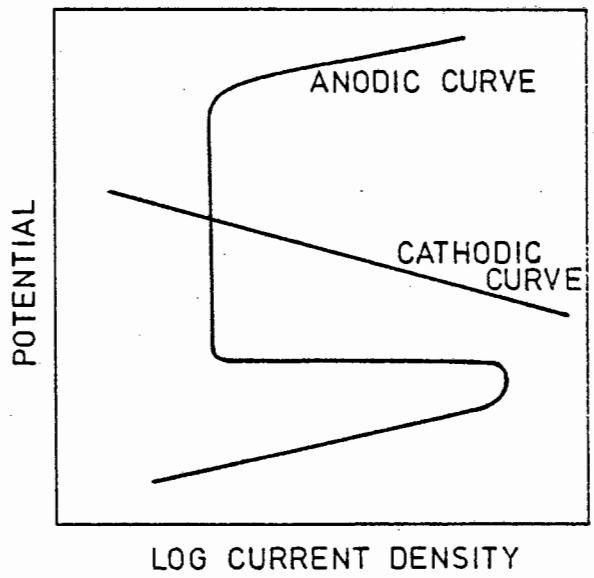

FIGURE 2.1 : A representation of the relative positions of the anodic and cathodic curves necessary for a material to be passive in a particular solution

2.2 THE WATER

2.2.1 Water Quality

A survey of the water in gold mines conducted by the Chamber of Mines indicated that the composition of the waters varied widely

from one mine to another. Furthermore variations were found in the composition of water sampled at different points in a particular mine as well as in samples taken from the same point at different times. Table 2.1 lists the average concentrations of the predominant ions present as well as the hardness, conductivity and pH of some selected mine waters. The survey was more comprehensive than shown in Table 2.1 and included minor species such as bicarbonate, fluoride, nitrite, potassium, cupric and ferric ions. A complete analysis of a wider range of mine waters is presented in Appendix A.

TABLE 2.1 : Mine water compositions (Manager MAB, (1983))

MINE	pH	CONDUCTIVITY mS/m	TOTAL DISSOLVED SOLIDS (ppm)	TOTAL HARDNESS AS $CaCO_3$ (ppm)	Cl^- (ppm)	SO_4^{2-} (ppm)	NO_3^- (ppm)	Na^+ (ppm)
Mine A	6.0	252	1944	753	85	1035	158	263
Mine B	6.5	490	3038	635	1203	265	144	790
Mine C	6.1	614	3790	448	1865	153	65	1040
Mine D	6.5	255	2184	518	39	829	327	290
Mine E	6.3	700	4975	1034	1812	821	228	1130
Mine F	5.8	1200	10870	3689	2766	2008	1650	1520
Mine G	6.3	192	4180	769	1220	901	191	900
Mine H	7.6	175	1820	738	103	677	188	104
Mine I	6.9	240	2824	1526	36	1586	10	70
Mine J	6.5	850	6756	1785	1564	2176	1185	1480

Due to the variability of the concentration of the ions these figures should only be regarded as an approximate indication of the composition range expected for a particular mine water. Table 2.1, for instance, indicates a pH range of 5 to 8, whereas pH values as low as 2.1 were recorded during the survey. Reference to Table 2.1 and the map in Figure 2.2 shows that the mine waters of the Orange Free State have higher total dissolved solids (T.D.S.) contents, and in particular higher chloride concentration than those of the Transvaal.

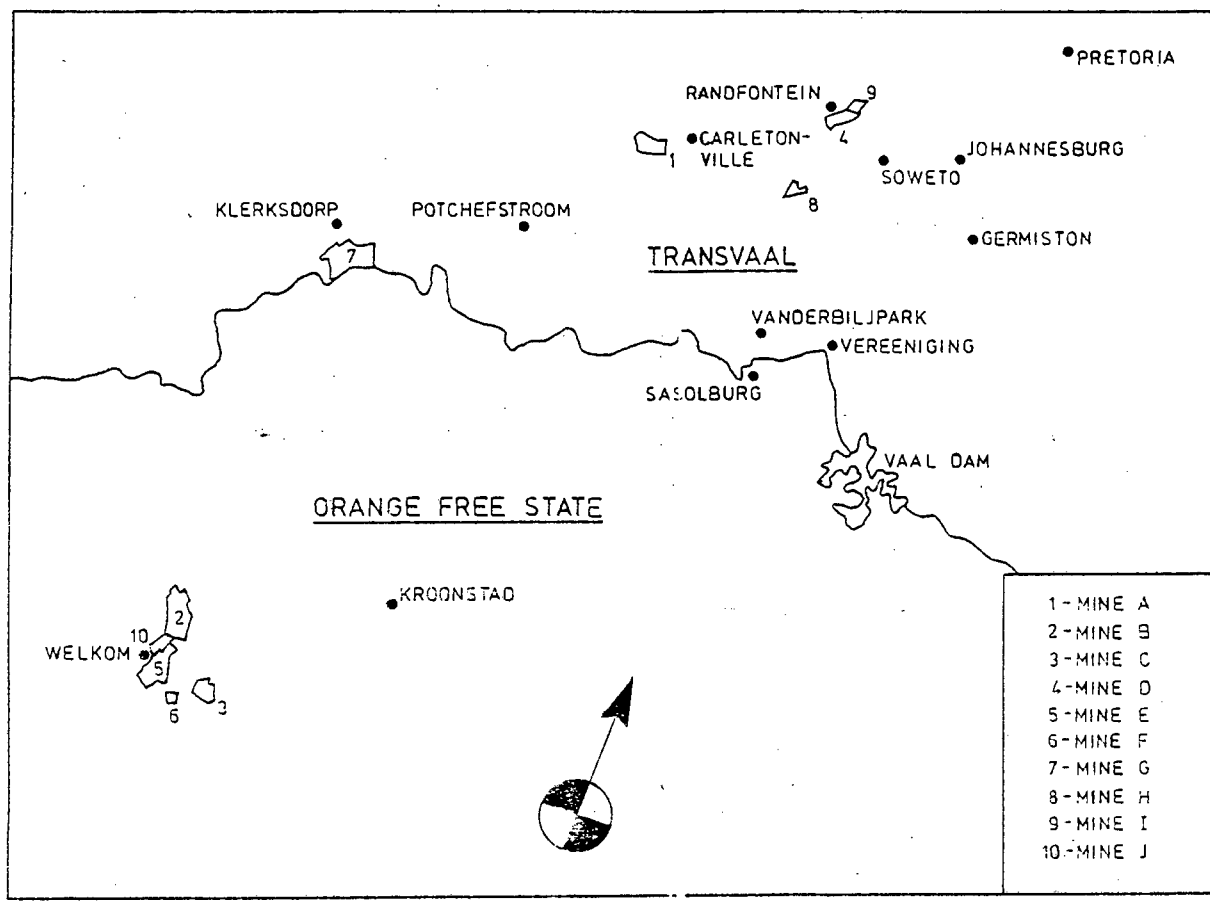

FIGURE 2.2 : Locations of mines included in the survey (after Higginson and White, (1983))

The oxygen concentration of the water was generally found to be close to saturation level. In the case of crevices and stagnant situations however it is probable that the water would be depleted of oxygen which would result in the hydrogen evolution reaction being the major cathodic process.

Higginson and White (1983) measured mine water temperatures ranging from 10°C to 42°C. Temperature affects the kinetics of corrosion reactions and also determines the solubility of oxygen in water. A temperature of 30°C is considered to be a reasonable average for mine water.

Microbial activity affects the corrosivity of mine waters in a number of ways. The bacteria species Thiobacillus thio-oxydans and Thiobacillus ferro-oxidans are known to accelerate the oxidation of pyrites ore which results in sulphuric acid formation and a corresponding decrease in pH (Rawat, (1976)). Tiller (1982) has suggested that these and other organisms are able to

metabolically utilize cathodic hydrogen and thus influence the corrosion rate.

Scotto et al (1983) reported that microbial activity on the surface of stainless steel in natural sea water resulted in an increase in the corrosion potential as shown in Figure 2.3. They suggested that this effect was due to the alteration of the cathodic kinetics by the microbes. It is possible that microbial activity in areas where stagnant water is encountered in the mines may result in a similar effect.

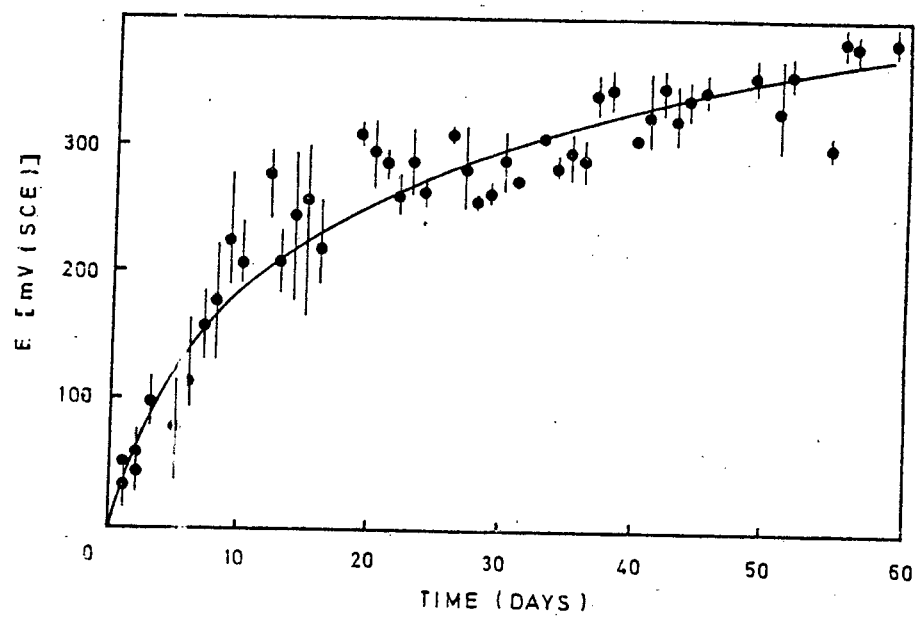

FIGURE 2.3 : E_{corr} as a function of time for a 21 Cr - 3 Mo stainless steel in natural sea water (after Scotto et al, (1983))

The complexity and variability of mine waters makes it difficult to determine which constituents are responsible for the corrosive nature of the water. Subrahmanyam and Hoey (1975) investigated the corrosion behaviour of mild steel in synthetic acid mine waters using both weight loss and electrochemical techniques. They found that the corrosion rate of mild steel was increased by the presence of ferric and cupric ions which were reduced in a cathodic process. They also determined that the corrosion rate was predominantly governed by diffusion control of the cathodic

processes. Rawat (1976) reported that the corrosion rate of mild steel in Indian coal mines increased with increasing concentration of chloride and sulphate ions. He could not find any correlation between the corrosion rate and the saturation index (Appendix B).

Higginson and White (1983) determined the corrosion rate of mild steel in South African gold mine waters using Tafel plots. They found that above a pH of 5 deaeration resulted in a decrease in the corrosion rate, and that the corrosion rate was independent of pH in this range. Below a pH of 5 they found that the corrosion rate increased approximately linearly with decreasing pH, and that the corrosion rate was lower in the deaerated solutions. These results led to the conclusion that in waters with a pH greater than 5 the diffusion controlled oxygen reduction reaction was the predominant cathodic process, while in solutions of pH less than 5 the hydrogen evolution reaction and the oxygen reduction reaction competed for the cathodic process. In deaerated solutions with saturation index less than negative 3 they found that the corrosion rate increased with decreasing saturation index. In an investigation of synthetic waters Higginson (1984) reported that the corrosion rate of mild steel was essentially independent of the concentration of nitrate, chloride or sulphate ions.

2.2.1.1 Summary

This review has highlighted a number of important factors which should be taken into consideration when studying the effect of water quality on the corrosivity of mine waters. These factors have been summarized in Table 2.2.

TABLE 2.2 : Important factors in mine waters and the levels at which they are present

FACTOR	LEVEL/(Concentration in ppm)
Chloride concentration	50 - 2000
Nitrate concentration	50 - 1500
Sulphate concentration	100 - 2000
Dissolved oxygen	Generally saturated
Presence of oxidisers	Traces of Fe^{3+} and Cu^{2+}
Microbes	Suspected to be present
Temperature	30°C average
pH	4 - 9

2.2.2 Hydropower Water Cycle and Water Treatment

A cycle of hydropower water through a mine would result in contamination of the water by the underground mining environment. The sources of contamination have been identified and are illustrated in Figure 2.4 which is a schematic representation of the hydropower water concept. Chemical and bacterial oxidation of the pyrites ore culminating in the formation of sulphuric acid leads to a decrease in pH as well as an increase in the sulphate content of the water. Lime is added to the water to increase the pH, and thus the T.D.S. is further increased. Blasting fumes and products dissolve in the water thereby increasing the nitrate concentration. The chloride ion concentration of the water is increased by the assimilation of fissure water into the system. A further overall increase in the T.D.S. is anticipated due to evaporation which is estimated at 10 per cent during a cycle. It is intended that by treating the water after each cycle the total dissolved solids content and pH will be maintained within an acceptable prescribed range.

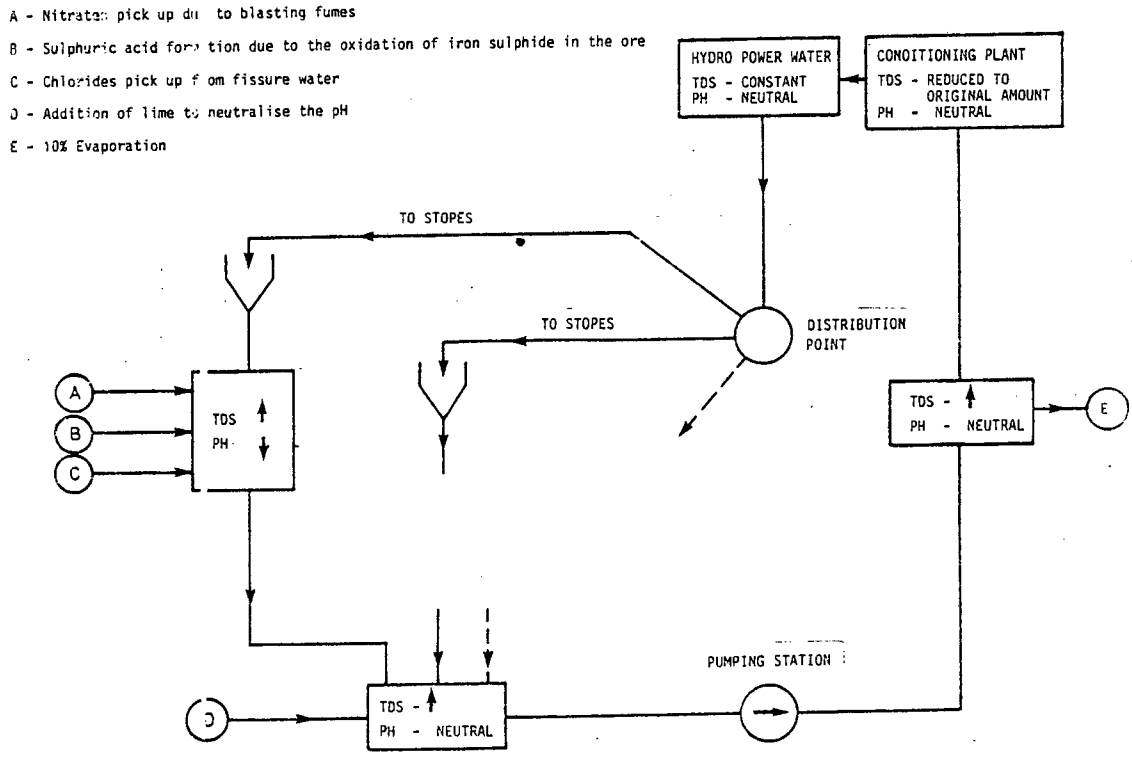

FIGURE 2.4 : The hydropower water cycle indicating sources of water contamination

The following water treatment practices are commonly employed for the treatment of mine service waters:

i) Biocidal treatment for prevention of biological fouling
ii) Sterilisation for potability
iii) Water conditioning for neutralisation and clarification
iv) Anti-fouling treatment for prevention of scaling
v) Addition of corrosion inhibitors

These procedures are necessitated by the deterioration in the quality of the water during recycling (White, 1985).

The Chamber of Mines is currently investigating the feasibility of desalinating mine water using a seeded reverse osmosis technique. (Harries, (1984)). Osmosis is a natural process whereby pure water flows through a semi-permeable membrane from a dilute solution to a more concentrated solution as shown in Figure 2.5(a). The membrane is selective in that water can pass through it whereas dissolved solids cannot.

An equilibrium situation is achieved when the chemical potential of the solutions are equal on both sides of the membrane. The difference in heads on either side of the membrane at equilibrium is equal to the osmotic pressure, π. Now, as shown in case (b), if a pressure greater than π is applied to the solution the chemical potential of the solvent in the solution is increased and the natural flow can be reversed thereby resulting in "reverse osmosis" (Gooding,(1985)).

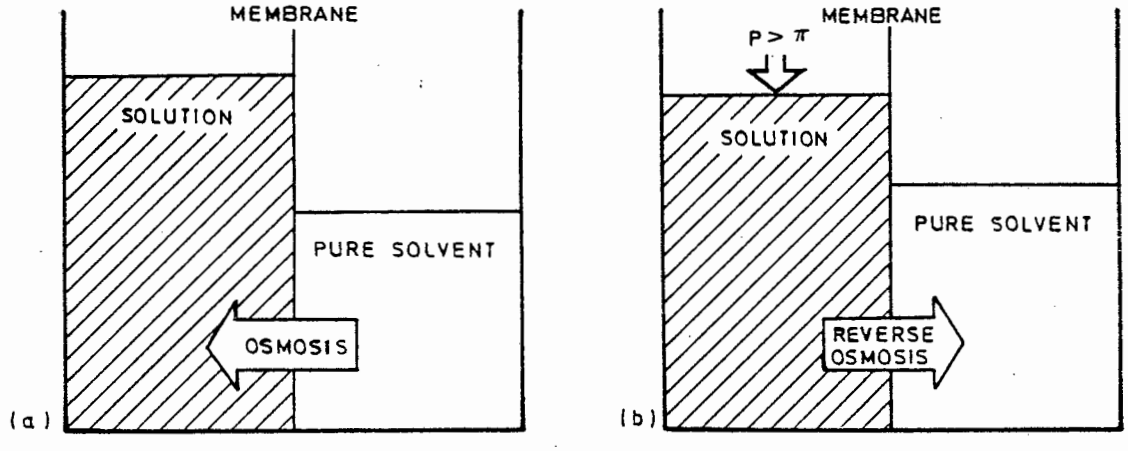

FIGURE 2.5 : The principle of (a) osmosis and (b) reverse osmosis (after Gooding, (1985))

The Chamber of Mines has overcome the problem of scale formation on the reverse osmosis membranes when desalinating mine waters with high concentrations of calcium sulphate. The scaling has been solved by introducing calcium sulphate seed crystals, which provide preferential precipitation sites, into the feed water. The cellulose acetate membranes are sensitive to temperature and pH and hence appropriate conditioning of the water prior to treatment by seeded reverse osmosis is necessary. A pilot seeded reverse osmosis plant has been successfully operated and it has been shown that about 70 per cent of the total dissolved solids can be removed from the mine water. It was found that all ions are removed in almost equal proportions (Harries, (1984)).

2.3 MATERIALS SELECTION

2.3.1 A 'Stainless' Type Steel

The selection of a material for use in the mining industry requires a careful design of all the material's properties if it is to perform satisfactorily in the harsh service conditions encountered underground. Mechanical properties, ease of fabrication, corrosion resistance and wear resistance have to be balanced against cost to achieve an economically acceptable material. It has been proposed by the Chamber of Mines that a 'stainless' type steel containing 8 to 12 per cent chromium with a dual phase microstructure, consisting of 95 per cent martensite and 5 per cent retained austenite, will be a viable solution. An intensive research program investigating the metallurgical, mechanical and corrosion-abrasion resistance properties of such alloys is in progress (Manager MAB, 1983)). Barker (1985) has shown that these alloys have superior corrosion-abrasion resistance which infers high hardness, toughness and strength and good corrosion resistance. As the alloys are generally used in the quenched and tempered condition it is interesting to note the effect of tempering time and tempering temperature on the corrosion resistance of a 13.2 per cent chromium steel as shown in Figure 2.6 (Truman, (1976)). Determining the ultimate heat treatment is therefore also of great importance.

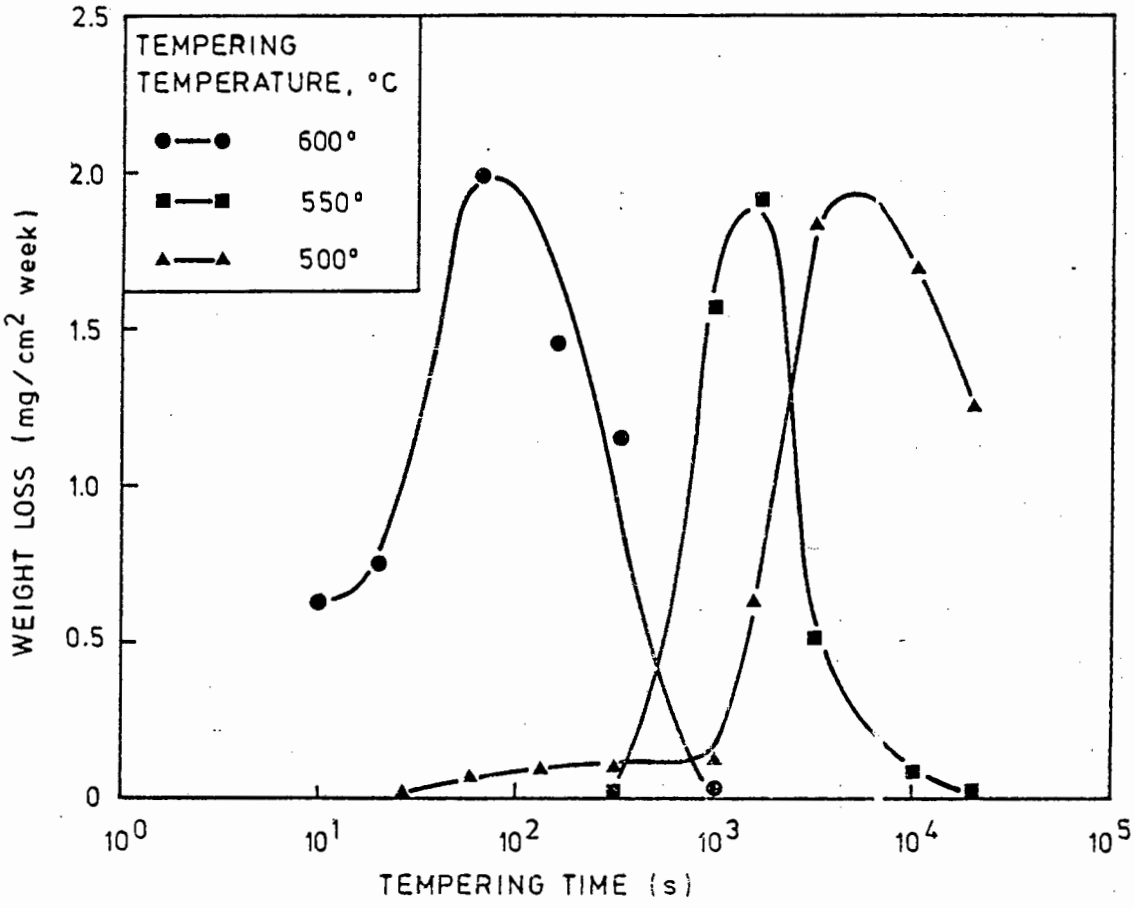

FIGURE 2.6 : The effect of tempering time and tempering temperature on the corrosion resistance of a 13.2 per cent chromium steel in aerated water (after Truman, (1976))

2.3.2 The Choice of a Standard Material for this Project

As no final alloy selection had been made at the time of commencement of this project it was necessary to select a suitable standard material which would be comparable to the experimental alloys.

The alloying elements present affect the polarization behaviour of stainless steels as shown in Figure 2.7 (Sedriks, (1984)). Thus, it was neccessary to choose a standard material with similar alloying elements to those being considered for the experimental alloys.

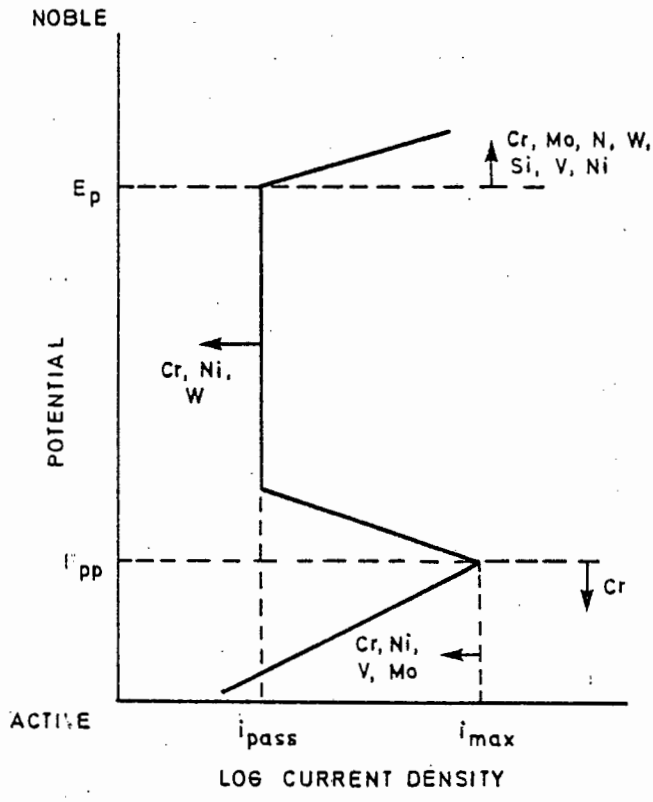

FIGURE 2.7 : The effect of alloying elements on the anodic polarization behaviour of stainless steels (after Sedriks (1984))

AISI 431 which contains 16.5 per cent Cr, 1.8 per cent Ni and 0.18 per cent C, and has a martensitic microstructure was chosen as the standard test material. The complete composition, mechanical properties and microstructure are shown in Appendix C. The reasons for choosing AISI 431 are as follows:

i) The Chamber of Mines recommended AISI 431 as an initial choice for many of the moving components in mining machinery operating on mine water.

ii) AISI 431 has a martensitic microstructure and although it contains more chromium than the type of alloy which is likely to emerge from the current alloy development program, it is still reasonably representative of such an alloy. Once the experimental alloys do become available the effect of chromium content on the corrosion resistance may be determined.

iii) Immersion testing conducted by the Chamber of Mines showed that pitting corrosion of AISI 431 occurred in some Orange Free State mine waters (Manager MAB, (1983)). It is therefore important to investigate the factors which cause pitting of a typical martensitic stainless steel in mine water.

2.4 THE AIM OF THIS PROJECT

The Chamber of Mines has employed a unique approach in combining alloy development, corrosion research and water treatment practice to solve a problem. An economical and practical solution will require constructive input and a certain degree of compromise from each discipline involved.

The aim of this project is to establish an electrochemical technique to assess the influence of the composition of synthetic mine water on the corrosion behaviour of a martensitic stainless steel. Of particular interest is the identification of which ions are responsible for localized pitting corrosion, and the determination of the concentration levels below which these ions may be tolerated. The effect of the interaction between the various ions present on the corrosivity of the solutions, will also be studied. It is intended that the results will be taken into account by water treatment engineers and that the newly developed alloys will be similarly tested in order that their corrosion behaviour might be compared to that of AISI 431.

Clearly this project cannot cover the whole range of problems discussed in the preceding sections, rather it must be seen as a contribution to an ongoing research program.

CHAPTER 3

LITERATURE REVIEW

3.1 THERMODYNAMIC ASPECTS OF AQUEOUS CORROSION

3.1.1 Basic Electrochemistry and Thermodynamics

Aqueous corrosion is predominantly an electrochemical process and hence it is necessary to employ electrochemical thermodynamics to evaluate the energy changes involved in these reactions (Pourbaix, (1973)).

The spontaneous direction of a reaction is indicated by a negative change in free energy, this concept is demonstrated by a mechanical analogy in Figure 3.1. The ball in position 2 has lower energy than in position 1 and therefore according to the principles of thermodynamics is more stable (Fontana and Greene, (1967)).

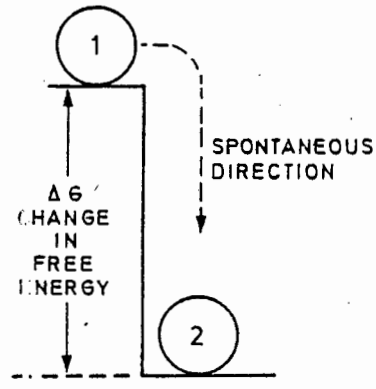

FIGURE 3.1 : Mechanical analogy of free energy (after Fontana and Greene, (1967))

The simple corrosion reaction of zinc with acid, represented in the following manner:

$$Zn + 2H^{+} = Zn^{2+} + H_2$$

can be separated into the half-cell reactions:

1. $Zn = Zn^{2+} + 2e^-$ oxidation half-cell reaction
2. $2H^+ + 2e^- = H_2$ reduction half-cell reaction

Half-cell reaction 1 produces electrons and is known as the oxidation half-cell reaction while half-cell reaction 2 consumes electrons and is known as the reduction half-cell reaction. The potential of many half-cell reactions have been measured with respect to the standard hydrogen half-cell reaction as illustrated in Figure 3.2. The inert platinum electrode acts as a substrate for the hydrogen reaction (Fontana and Greene, (1967)).

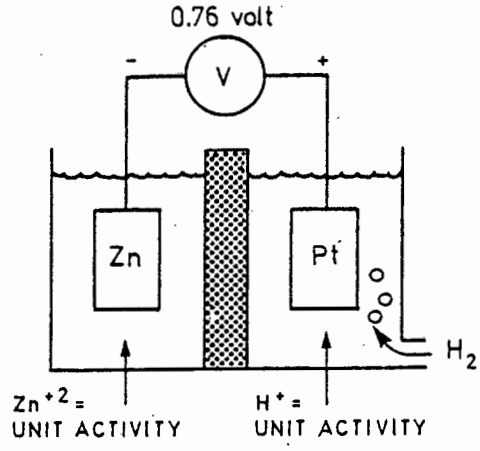

FIGURE 3.2 : Determination of half-cell reaction potentials (after Fontana and Greene, (1967))

The electrode potentials are measured in conditions of unit activity at 25°C and tables of values including most electrochemical half-cell reactions are available. A more negative half-cell potential indicates that the reaction will be the oxidation reaction while a more positive half-cell potential indicates a reduction reaction. In non-standard conditions the Nernst equation can be used to calculate the potential of the reaction:

$$E = E^\circ + 2.3\ {}^{RT}/_{nF}\ \log\ (a_{oxid}/a_{red})$$

E° = standard half-cell potential

E = half-cell potential
R = gas constant
T = absolute temperature
n = number of electrons involved
F = Farraday's constant
a_{oxid}, a_{red} = activity (concentration) of oxidised and reduced species respectively

The change in free energy, ΔG, accompanying a half-cell reaction is related to the electrode potential by the following equation:

$$\Delta G_{\frac{1}{2}\ cell} = -nFE$$

If the change in free of the total reaction:

$$\Delta G_{reaction} = \Delta G_{red} - \Delta G_{oxid}$$

is negative, the reaction will proceed as written (Fontana and Greene, (1967)).

3.1.2 E-pH Diagrams

The two predominant reduction reactions involved in aqueous corrosion, the hydrogen evolution reaction (h.e.r.) and the oxygen reduction reaction (o.r.r.), may be expressed by the following equations which relate pH to potential at 1 atm and 25°C:

a) hydrogen evolution:

$$2H^+ + 2e^- \rightarrow H_2$$

$$E^\circ = 0.00 - 0.591\ pH$$

b) oxygen reduction:

$$O_2 + 4H^+ + 4e^- \rightarrow 2H_2O$$

$$E^\circ = 1.228 - 0.691\ pH$$

Figure 3.3 is a graphical representation of these two equations illustrating the domain of thermodynamic stability of water. In the region below the line "a" hydrogen evolution occurs, between line "a" and line "b" the reduction of oxygen occurs and above line "b" the evolution of oxygen takes place (Pourbaix and de Zoubov, (1966)[1]).

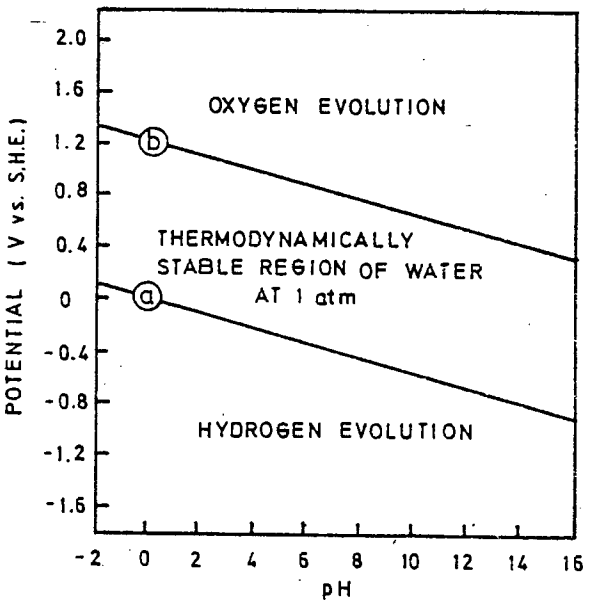

FIGURE 3.3 : E-pH diagram for H_2O (Pourbaix and de Zoubov (1966)[1])

By applying these principles, in conjunction with solubility data, Pourbaix and his co-workers constructed E-pH diagrams for many metal/aqueous systems. These diagrams are used to predict domains of corrosion, immunity and passivity for the specific system. A region of corrosion represents a stable soluble metal species, immunity a stable insoluble metal surface and passivity a stable insoluble metal oxide, hydroxide or hydride which forms a protective adherent film on the metal surface thereby restricting the dissolution of metal (Pourbaix, (1966)).

The simplified E-pH diagram for iron in aqueous solution is depicted in Figure 3.4. In acidic solutions, pH 2, iron may be oxidised by either the h.e.r. or the o.r.r. Between pH 2 and 9.5 the h.e.r. will oxidise iron while the o.r.r. could result in either corrosion or passivation. Between pH 9.5 and 12.5 passivation of the metal surface by formation of either Fe_2O_3 or Fe_3O_4 will occur. Above pH 12.5 iron could either be oxidised by

the h.e.r. or alternatively at higher potentials, passivated by the o.r.r. (Pourbaix and de Zoubov, (1966)[2]).

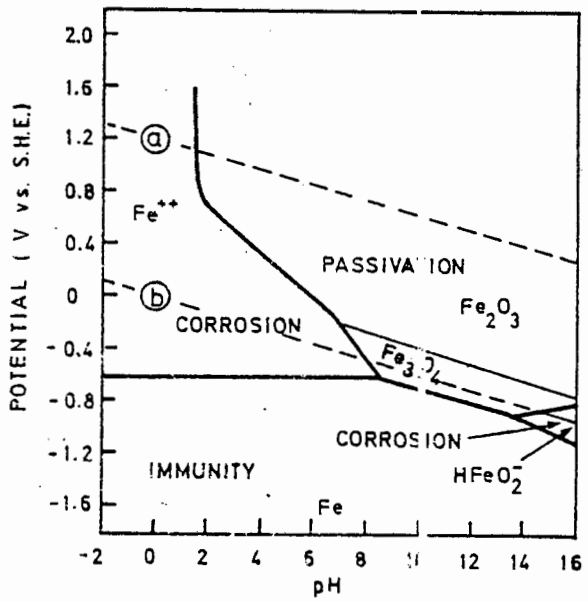

FIGURE 3.4 : Simplified E-pH diagrams of Fe-H_2O system (after Pourbaix and De Zoubov (1966)[2])

Pourbaix (1966) himself has repeatedly drawn attention to the applications and limitations of E-pH diagrams and has stressed the necessity for their correct interpretation if they are to be of any practical significance. E-pH diagrams apply to pure metals (unless otherwise stated) in aqueous solutions not containing substances which may form soluble complexes with the metal. The diagrams are applicable to equilibrium conditions of potential and pH measured at the metal-solution interface. Passivation can be of varying efficiency depending on the extent of adherence of the solid film to the metal surface. E-pH diagrams only express whether a condition is energetically possible, they do not indicate if an energetically favourable reaction will occur, or at what rate it will occur. These diagrams must therefore be seen primarily as a guide to the execution and interpretation of experimental studies (Pourbaix, (1966)).

3.2 KINETICS OF CORROSION

3.2.1 Principles of Kinetics

An equilibrium hydrogen electrode existing on a platinum surface is shown in Figure 3.5. The rate of reduction, r_{red}, equals the rate of oxidation, r_{oxid}. The rate of interchange of hydrogen ions and hydrogen molecules is known as the exchange current density, i_o, and is related to r_{oxid} and r_{red} by the following equation:

$$r_{oxid} = r_{red} = i_o/nF$$

There is no nett current flow and the electrode is at its equilibrium potential (Fontana and Greene, (1967)).

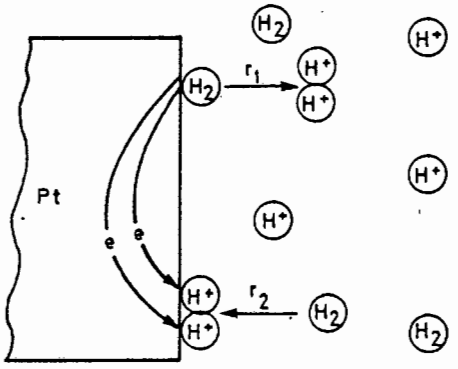

FIGURE 3.5 : Hydrogen electrode on a platinum surface (after Fontana and Greene, (1967))

In a corrosion reaction however, the electrons produced by an oxidation (anodic) reaction are consumed by a reduction (cathodic) reaction and the participating electrodes will be polarized from their equilibrium potentials. The amount of polarization is referred to as the overvoltage, η. Two types of polarization are encountered:

1) Activation polarization which is controlled by a slow rate determining step in the reaction. Activation polarization is described by the Tafel equation:

$$\eta_a = \pm \beta \log {}^{i}/_{io}$$

η_a = overvoltage
β = constant
i = rate of anodic or cathodic reaction

2) Concentration polarization which is controlled by diffusion of a species to or from the metal surface. Concentration polarization is described by the following equation:

$$\eta_c = 2.3\, {}^{RT}/_{nF} \log (1 - {}^{i}/_{iL})$$

where i_L is the limiting diffusion current density.

Usually both activation and concentration polarization occur at an electrode which could then be represented as shown in Figure 3.6 (Fontana and Greene, (1967)).

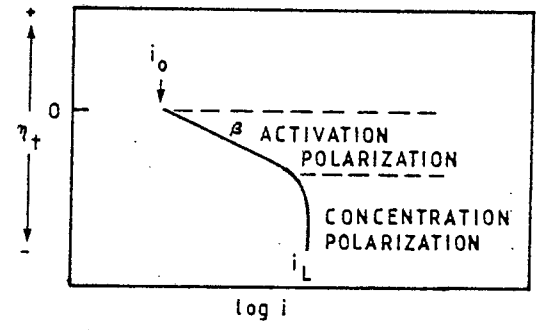

FIGURE 3.6 : An electrode displaying both activation and concentration polarization (after Fontana and Greene, (1967))

3.2.2 Mixed Electrodes

A plot of E against log i for the corrosion of iron by acid is represented by Figure 3.7 The hydrogen half-cell reaction is polarized in a negative direction from its equilibrium potential E_{H_2/H^+} and the iron half-cell reaction is polarized in a positive direction from its equilibrium potential $E_{Fe/Fe^{2+}}$. At

the point where both half-cell potentials have a potential of E_{corr}, conservation of charge is achieved and the system thus assumes E_{corr} as its equilibrium corrosion potential and i_{corr} as its corrosion current density (Fontana and Greene, (1967)).

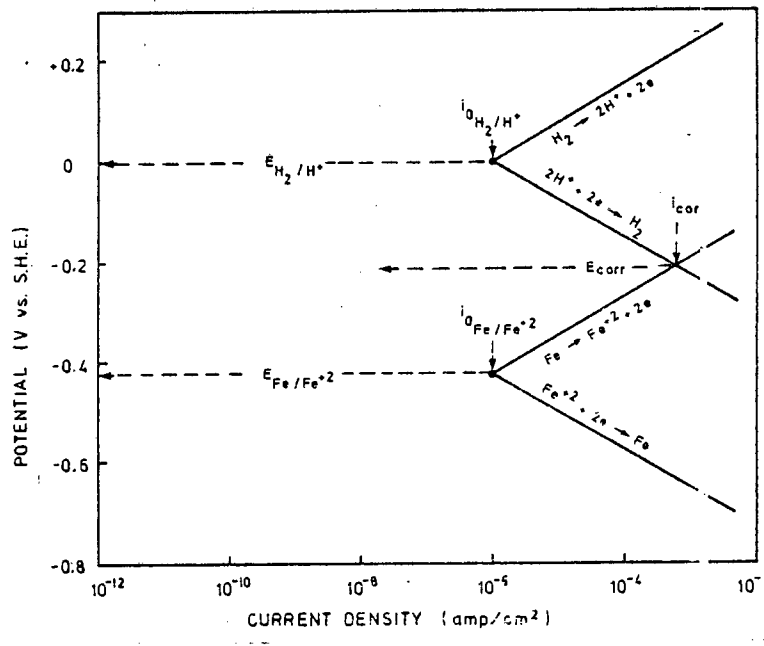

FIGURE 3.7 : E log i behaviour of Fe/Fe^{2+} and H/H^+ (after Fontana and Greene, (1967))

3.2.3 Kinetics of Cathodic Reactions in Aqueous Systems

3.2.3.1 Hydrogen Evolution Reaction

The cathodic hydrogen evolution reaction is an activation controlled process. A corrosion reactior in which the h.e.r. is the cathodic component is controlled by the activation overvoltage of charge transfer. The kinetics of the h.e.r. are therefore affected by temperature, pH (a measure of concentration of the reactant) and exchange current density of the h.e.r. on the metal considered (Shreir, (1979)).

3.2.3.2 Oxygen Reduction Reaction

Diffusion involving the transport of oxygen to the metal surface results in the o.r.r. being a predominantly

concentration polarization controlled process. The kinetics of the o.r.r. are therefore controlled by temperature, oxygen concentration in the solution, and the degree of agitation of the solution. An increase in temperature results in two contradictory effects: (1) lower solubility of oxygen in the solution and hence lower concentration of oxygen and (2) an increase in the diffusion coefficient of oxygen in the solution. Figure 3.8 demonstrates the effect of concentration polarization at increasing solution velocity. In each case a limiting cathodic current (i_L), due to concentration polarization, is reached. The i_L increases with increasing agitation because of enhanced transport of oxygen to the metal surface (Shreir, (1979)).

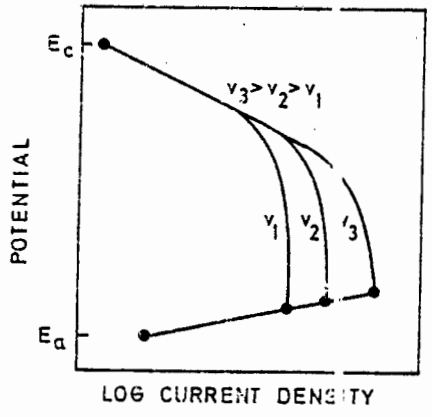

FIGURE 3.8 : Effect of velocity on the oxygen reduction reaction kinetics (after Shreir, (1979))

3.2.4 The Anodic Kinetics of Stainless Steel

The anodic behaviour of stainless steel is characterized by an active to passive transition, the excellent corrosion resistance in the passive state is due mainly to chromium enrichment of the oxide layer (El-Basiouny and Haruyama, (1976)).

Figure 3.9 is a graphical representation of the anodic dissolution of a typical stainless steel. As the potential is increased in the active region a current maximum, the critical anodic current

density (I_c), is reached at a potential referred to as the primary passive potential (E_{pp}). At potentials greater than E_{pp} the current density decreases to the passive current density (I_{pass}), which is independent of potential. The passive potential range represents the existence of a stable oxide on the surface of the stainless steel. The breakdown potential, E_b, is the potential above which the oxide layer is transformed to a soluble species and the current increases due to transpassive corrosion (Greene, (1962)).

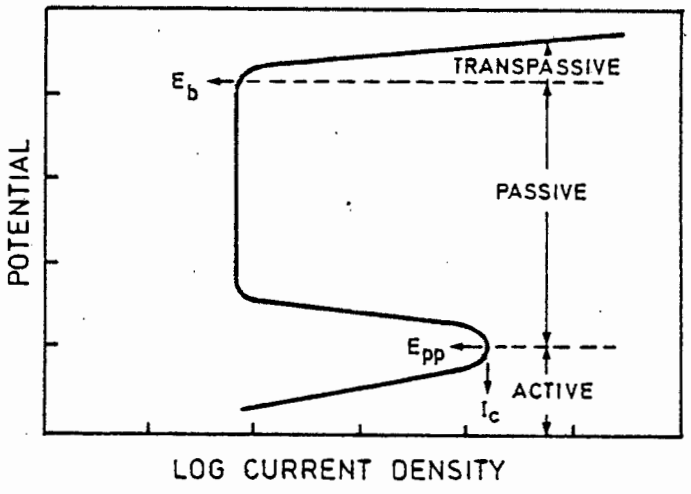

FIGURE 3.9 : Anodic dissolution of stainless steel (after Greene, (1962))

3.2.5 The Effect of the Relative Positions of the Cathodic and Anodic Curves and the Corrosion Behaviour of Stainless Steel

The point of intersection of the cathodic and anodic curves determines the rate of corrosion of a metal. Figure 3.10 represents three examples of intersection each of which will result in a different type of corrosion. In case "1" the intersection of the curves is at a point of active dissolution and the metal will corrode at a rate i_{corr}. Three points of intersection b, c and d occur in case "2". Point b falls within the range of active dissolution and point d within the passive state (Greene, (1962)). Edelnau (1958) has reported that the potential of a system with its intersection at point c rapidly decreases and the metal assumes the corrosion rate corresponding

to point b, the intersection at point c is hence an unstable state. Case "2", despite the possibility of passivation, is undesirable as a slight change in the environmental conditions could result in a transition from passive to active corrosion. Case "3" would result in a stable passive metal surface, therefore it is a desirable situation (Greene, (1962)).

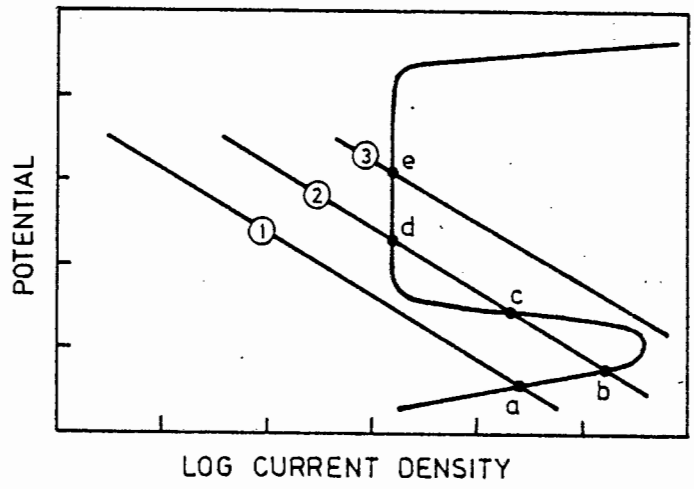

FIGURE 3.10 : Three possible cases of intersection of the anodic and cathodic curves (after Greene, (1962))

3.2.6 Experimental Polarization Curves

Anodic or cathodic polarization curves can be measured by the application of an external current using a potentiostat. The applied current is however equivalent to the difference between the rate of the anodic and cathodic process and hence the true polarization behaviour is not determined.

The experimentally determined anodic polarization curves which would be measured for cases "1", "2" and "3" in Figure 3.10, are represented in Figure 3.11. Case "1" shows the active-passive transition with distortion in the region of E_{corr} due to the proximity of the anodic and cathodic curves. Case "2" demonstrates the stability of both the active and the passive state. The dashed line, referred to as the "negative loop" by Edelnau (1958), represents the region where the cathodic current is greater than the anodic current (due to log scale the negative

sign of the current is not evident). In case "3" the metal is in the passive state and the active region of the anodic curve is completely obscured by the cathodic reaction (Greene, (1962)).

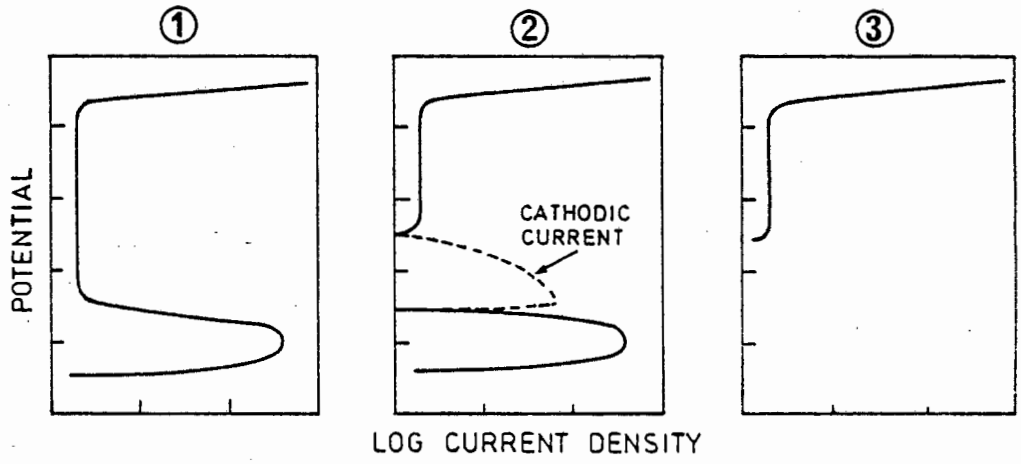

FIGURE 3.11 : Experimental polarization curves resulting from the three possible cases of intersection (after Greene, (1962))

Pourbaix (1973) has shown how the determination of polarization curves can be used in the construction of experimental E-pH diagrams. Figure 3.12 shows the regions of immunity, corrosion and passivation determined for iron by measuring polarization curves at a range of pH's in deaerated solutions.

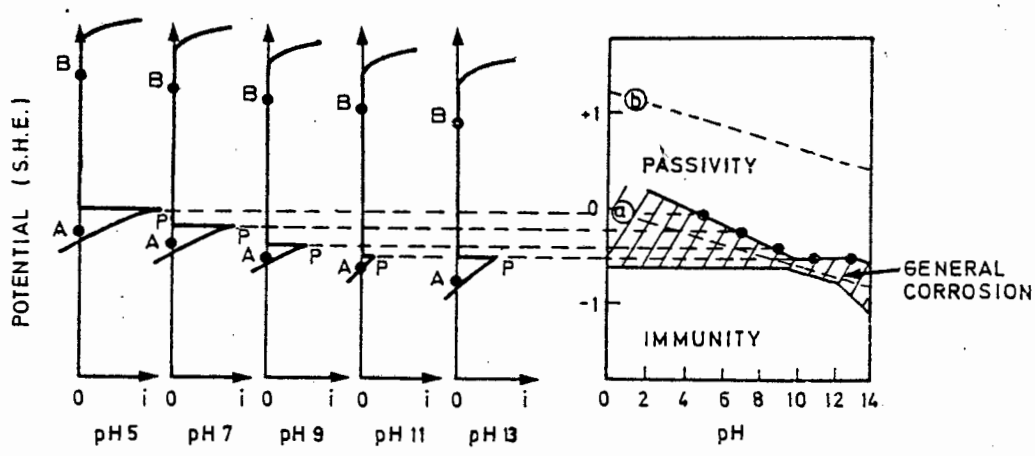

FIGURE 3.12 : Experimentally determined E-pH diagram for iron (after Pourbaix, (1973))

3.3 PITTING CORROSION OF STAINLESS STEELS

3.3.1 Introduction

The excellent general corrosion resistance of stainless steel in the passive state is largely undermined by the occurrence of localized pitting corrosion in solutions containing aggressive anions (Hospadaruk and Petrocelli, (1966)). When evaluating the pitting corrosion resistance of a metal the determination of conditions under which pitting may occur is far more important than the determination of corrosion rates (Schwenk, (1964) and Pessall and Liu, (1971)).

3.3.2 Characteristic Potentials of Pitting Corrosion

3.3.2.1 Pitting Potential

In 1937 Brennert proposed an electrochemical technique for the determination of the "break-through potential" of stainless steel in chloride containing solutions. A simplified representation of his apparatus is shown in Figure 3.13. The technique involved increasing the anodic polarization of the specimen by moving the sliding contact of the resistance at a rate of 15 $V.h^{-1}$ in the direction from right to left. A potentiometer was used to measure the potential of the specimen with respect to a saturated calomel electrode (S.C.E.) and the current was monitored by an ammeter. At a certain potential a rapid increase in current was noted and on examining the surface of the specimen localized pitting attack was observed. The potential at which the current first increased was termed the "break-through potential" (Brennert, (1937)).

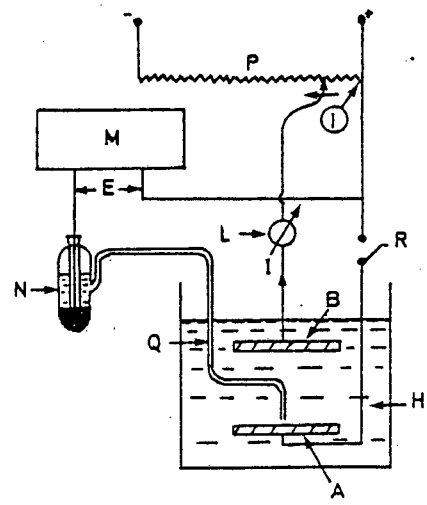

A - stainless steel specimen
B - cathode
H - test solution
L - milliammeter
M - valve potentiometer
N - saturated calomel electrode
P - resistance
Q - agar conductor
R - switch

FIGURE 3.13 : Simplified apparatus for determination of "break-through potential" (after Brennert, (1937))

In an analysis of electrochemical techniques Szklarska-Smialowska and Janik-Czachor (1971) listed a host of different terms - break-through potential, breakdown potential, Lochfraßpotential (directly translated to English as "hole-eating potential") critical potential and pitting potential - all of which describe the potential above which pitting can initiate on a passive metal surface.

For the purpose of this investigation the term pitting potential, E_p, will be used.

3.3.2.2 Protection Potential

Pourbaix et al (1963) introduced the concept of the protection potential, E_x, as being the potential above

which existing pits could continue to propagate. A specimen, initially polarized to a potential greater than its pitting potential, was then polarized in the reverse direction. The potential at which the resultant hysteresis loop closed, was identified as the protection potential.

3.3.2.3 The Validity of the Pitting and Protection Potentials

France and Greene (1970) and Wilde (1972) have questioned the validity of the pitting and protection potentials. Potentiostatic exposure tests (Pourbaix, (1970), Hospadaruk and Petrocelli,(1966), and Azzerri et al, (1982)) have confirmed the applicability of these potentials. Using specifically chosen conditions and a variety of redox systems Wilde and Williams (1970) confirmed the initiation of pits above E_p and the possible propagation of pits below E_p, by chemical means.

3.3.3 Techniques for Determining E_p and E_x

3.3.3.1 Potentiostatic Determination of Anodic Polarization Curves

Three variations of this technique are:-

1) Stationary - holding the specimen at each potential until a constant current is attained.
2) Potentiodynamic - changing potential at a constant rate.
3) Quasi-stationary - stepwise change of potential at a certain rate.

Figure 3.14 is a representative potential log current curve which would be obtained by these techniques, the scanning direction is indicated by arrows. E_p is determined by the sharp inflection of the curve during anodic polarization and E_x as the potential at which the

hysteresis loop is closed during reverse polarization (Szklarska-Smialowska and Janik-Czachor, (1971)).

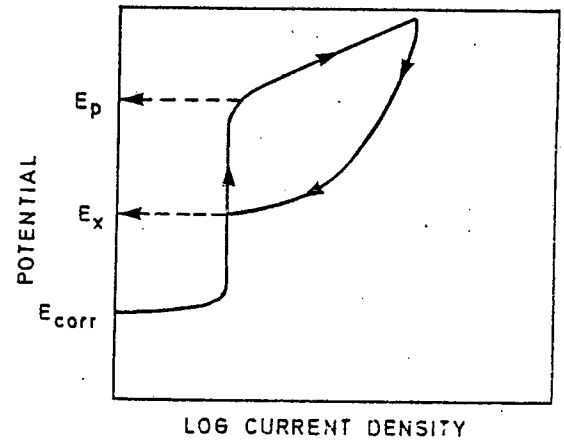

FIGURE 3.14 : The determination of E_p and E_x by anodic polarization (after Szklarska-Smialowska and Janik-Czachor, (1971))

3.3.3.2 The Effect of Rate of Potential Change on the Determination of E_p and E_x

In his pioneering work on pitting potentials, Brennert (1937) noted that an increase in the rate of potential change resulted in higher values of pitting potential. Leckie (1970) reported an increase of 280 mV in the value of the pitting potential as the scan rate was increased from 10 to 10^4 mV/hour. As seen in Figure 3.15 his results indicate that a limiting value of E_p exists at low scan rates. Broli et al (1973) and Man and Gabe (1981) also found E_p to increase with increasing scan rates. Lizlovs and Bond (1975) measured the pitting potentials of a range of ferritic stainless steels at scanning rates of 0.26V/hour and 50V/hour. They reported a good correspondence between the values of E_p and in some cases even noted lower E_p values at the fast scan rate.

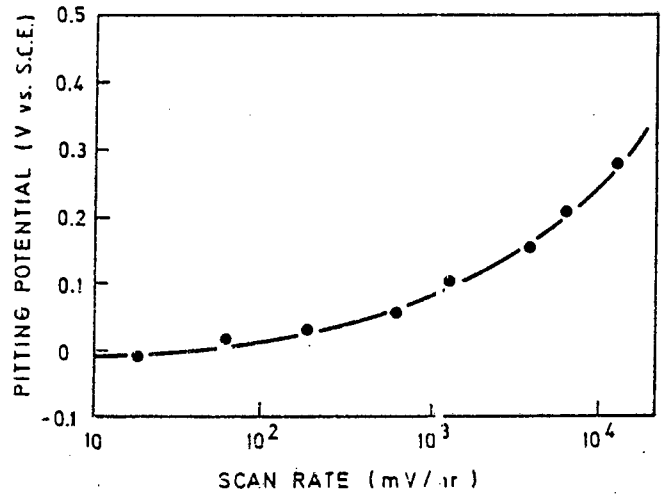

FIGURE 3.15 : The effect of scan rate on E_p (after Leckie, (1970))

3.3.3.3 Other Methods for Determining E_p and E_x

Szklarska-Smialowska and Jan k-Czachor (1971) described the application of current/time curves at constant potential for the determination of E_p and E_x. The time which elapses before a current increase due to pit initiation is known as the induction time, τ. They also outlined the use of galvanostatic measurement of anodic polarization curves and potential/time curves at constant current density. Pessall and Liu (1971) developed the "scratch technique" which entails the scratching of the specimen surface at constant potential using a silicon carbide crystal. The pitting potential is determined by measuring the repassivatior time/potential and the induction time/potential data as shown in Figure 3.16. A statistical estimate of the pitting potential, indicating both the mean value and the cumulative probability of the value obtained, has been suggested by Fratesi (1985) for the analysis of pitting potentials measured by both the scratch and potentiodynamic methods.

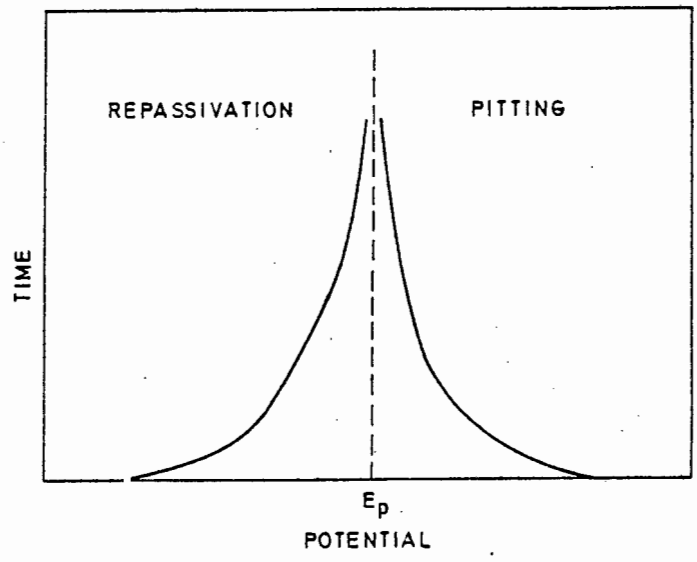

FIGURE 3.16 : Determination of E_p by the scratch method (Pessall and Liu, (1971))

3.3.4 A Comparison of the Electrochemical Methods Discussed

Little agreement on which method is most suitable for measuring the pitting behaviour of stainless steels can be found in the literature. Szklarska-Smialowska and Janik-Czachor (1971) favoured the determination of current/time curves at constant potential for measuring E_p and E_x. Broli et al (1973) found that the stationary potentiostatic technique with a holding time of 10^4 minutes at each potential gave the most accurate results. The scratch technique and the potentiodynamic technique were compared by Lizlovs and Bond (1975) and Fratesi (1985), the former advocated the use of the scratch technique while the latter favoured the potentiodynamic technique with a scan rate of 10 mV/hour. Unanimous agreement is evident (Lizlovs and Bond, (1975), Broli et al, (1973), Wilde, (1972) and Atrens, (1983)) that the minimization of crevice corrosion at the edge of the specimen is essential if valid results are to be obtained.

Table 3.1 lists some of the work performed on the pitting of metals and gives an indication of the variety of techniques and conditions used.

TABLE 3.1 : Various methods and conditions used by different authors for determining E_p and E_x

AUTHOR	METHOD	SCAN RATE/ STEP RATE	SPECIMEN	ENVIRONMENT
ASTM G61-78 (1980)[1]	Potentiodynamic	0.6 V/hr	AISI 304, Hastelloy, Alloy C-276	3.5% NaCl
Atrens (1983)	Potentiodynamic	3.6 V/hr	12% Cr Martensitic Stainless Steel	5×10^{-5} to 4N NaCl
Barbosa & Scully (1982)	Scratch		AISI 304	H_2SO_4+HCl or KCl, pH = 2
Bogaerts et al (1981)	Potentiodynamic	0.36V/hr	Fe-Cr-Ni alloys	NaCl, Na_2SO_4 KCl, $KHCO_3$
Dayal et al (1980)	Quasi-stationary	40 mV per 2 minutes	AISI 316	1N H_2SO_4 + 0.5N NaCl
France & Greene (1970)	Quasi-stationary	50 mV per 5 minutes	AISI 430, Zirconium	1N H_2SO_4, 1N NaCl
Hospadaruk & Petrocelli (1966)	Stationary		AISI 316, 301, 434	NaCl, Na_2SO_4 $CaCl_2$ pH = 2-8
Leckie and Uhlig (1966)	Quasi-stationary	50 mV per 5 minutes	18Cr-8Ni Stainless steel	NaCl + OH^-, SO_4^{2-}, NO_3^- or ClO_4^-
Man and Gabe (1981)	Potentiodynamic	3.6V/hr	AISI 304, 316, 321 and 15-7 PH	NaCl+Na_2SO_4
Stolica (1969)	Constant Potential I/t curves		Fe-Cr and Fe-Cr-Ni alloys	H_2SO_4 + NaCl
Szklarska-Smialowska (1971)	Constant Current E/t curves		Nickel	H_2SO_4 + NaCl
Szklarska-Smialowska & Janik-Czachor (1971)	Constant Potential I/t curves		Pure Iron	0.1 N KCl

3.3.5 Factors Influencing the Pitting Corrosion of Stainless Steels

3.3.5.1 The Effect of Chloride Concentration

The notoriety of chloride ions as a cause of pitting

corrosion is due to their great agressiveness as well as their widespread presence in natural and industrial waters (Kolotyrkin, 1963).

The decrease in pitting potential with increasing chloride concentration has often been studied; Brennert (1937) first reported the effect. Walker and Rowe (1969) found a similar decrease in pitting potentials when investigating a range of stainless steels intended for use as automobile trim materials. Man and Gabe (1981) reported that increasing chloride concentration caused a decrease in the pitting potentials of austenitic stainless steels in natural waters. A plot of E_p as a function of the logarithm of the chloride concentration indicated a linear dependence with a slope of 90 mV per decade for an 18-8 stainless steel (Leckie and Uhlig, (1966)). Verink and Pourbaix (1971) plotted E_p/E_b, E_x, E_{corr} and E_{pp} of a 12% Cr alloy as a function of the chloride ion concentration at a pH of 8.8. E_{pp}, E_x and E_{corr} did not vary significantly with chloride ion concentration, while E_p was found to decrease with increasing chloride ion concentration. In Figure 3.17 it can be seen that a chloride ion concentration of approximately 10^{-2} M was necessary for pitting corrosion to be recorded.

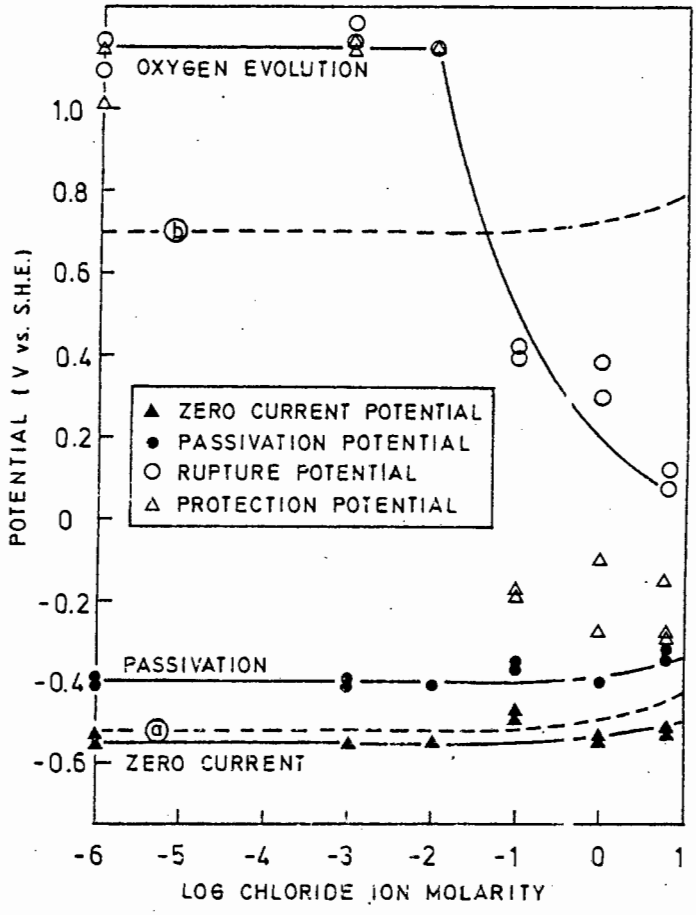

FIGURE 3.17 : Potential vs. Log chloride ion molarity at pH = 8.8 (after Verink and Pourbaix, (1971))

Similar diagrams have been constructed by Atrens (1983), who assessed the behaviour of a 12% Cr martensitic stainless steel in solutions typical of the condensate formed on low-pressure steam-turbine blades. Figure 3.18 shows one of his diagrams determined at 80°C. E_{corr} values measured in both aerated and dearated solutions have been plotted. A decrease of 183 mV/decade for E_p amd 142 mV/ decade for E_x was measured. From the position of the E_{corr} lines it can be seen that pit propagation can only be avoided in deaerated solutions with a chloride ion concentration less than about 2×10^{-4} N.

Azzerri et al (1982) have plotted diagrams, which incorporate the conditions inside an occluded cell (pit),

for a variety of stainless steels. Their results also indicate a linear dependence of E_p and E_x on the log of the chloride ion concentration.

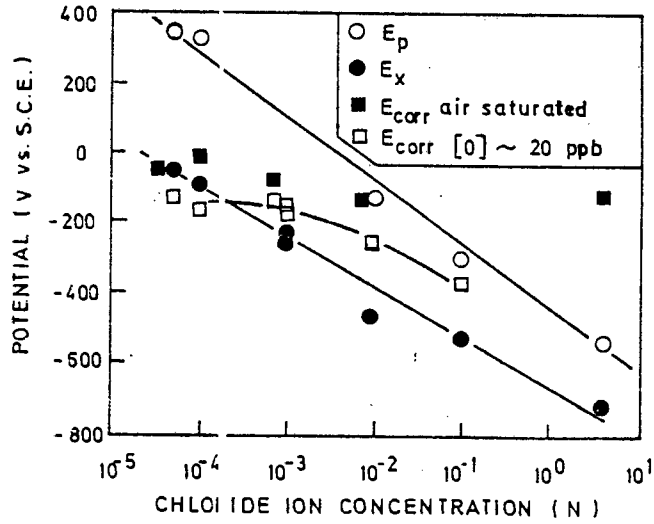

FIGURE 3.18 : Potential versus log chloride ion molarity at 80 °C for a 12% Cr martensitic stainless steel (after Atrens, (1983))

3.3.5.2 The Effect of pH

Figure 3.19 illustrates the dependence of the pitting potentials of AISI 316, 304 and 430 on the pH of a 3% NaCl solution (Szklarska-Smialowska, (1971)). E_p remains fairly constant in the pH range from 1 to about 10, above pH 10 a sharp increase in E_p occurs. Similar effects have been reported by Leckie and Uhlig (1966) for an 18-8 stainless steel in 0.1 N NaCl, and by Leckie for AISI 304 in 0.01, 0.1 and 1.0 M NaCl. They found that the sharp increase in E_p persisted to the point where general dissolution occurred by the transpassive formation of chromates. Pourbaix (1970) found that E_p increased with increasing pH for AISI 410 and AISI 304 in 0.1 M chloride solutions over a pH range from acidic to alkali. He also reported that the protection potential remained independent of pH over this range.

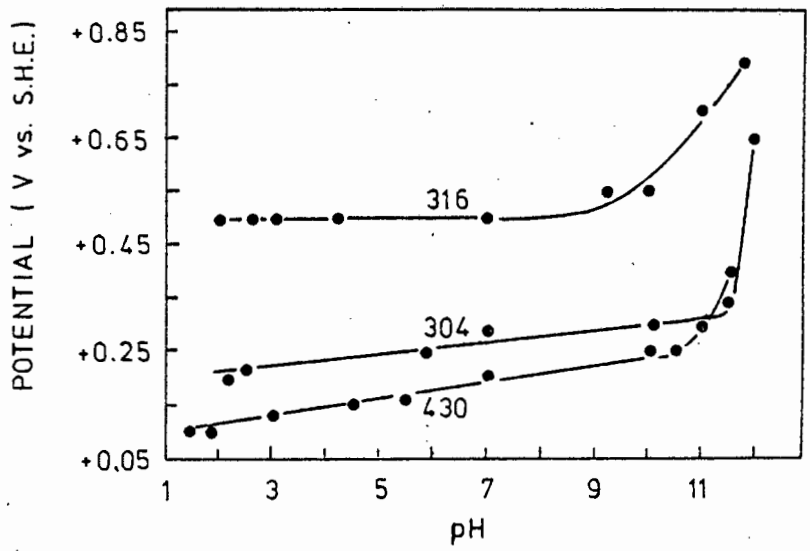

FIGURE 3.19 : The variation of E_p with pH in 3% NaCl solutions (after Szklarska-Smialowska, (1971))

3.3.5.3 The Effect of Secondary Ions

Immersion testing by Uhlig and Gilman (1964) has shown that chloride induced pitting of a 18-8 stainless steel can be effectively inhibited by a sufficiently high concentration of nitrate ions. A specimen exposed to a 10% $FeCl_3$ + 3% $NaNO_3$ solution showed no pitting over a period of 25 years, while a specimen exposed to a 10% $FeCl_3$ solution was severly pitted within hours. Leckie and Uhlig (1966) determined anodic polarization curves to assess the inhibitive effect of OH^-, NO_3^-, SO_4^{2-} and ClO_4^- on the pitting of an 18-8 stainless steel in chloride solutions. Complete inhibition was determined by the concentration of inhibitive ion required to increase E_p to the point where breakdown occurred due to transpassive dissolution rather than pitting corrosion. By plotting the logarithm of the minimum activity of the inhibitive ion required for complete inhibition as a function of the logarithm of the chloride ion activity they derived the following equations:

$$\log (Cl^-) = 1.62 \log (OH^-) + 1.84 \qquad \text{Equation 3.1}$$

$$\log (Cl^-) = 1.88 \log (NO_3^-) + 1.18 \qquad \text{Equation 3.2}$$

$$\log (Cl^-) = 0.85 \log (SO_4^{2-}) - 0.05 \qquad \text{Equation 3.3}$$

$$\log (Cl^-) = 0.83 \log (ClO_4^-) - 0.44 \qquad \text{Equation 3.4}$$

Figure 3.20 shows the curves obtained for inhibition by NO_3^- and OH^-.

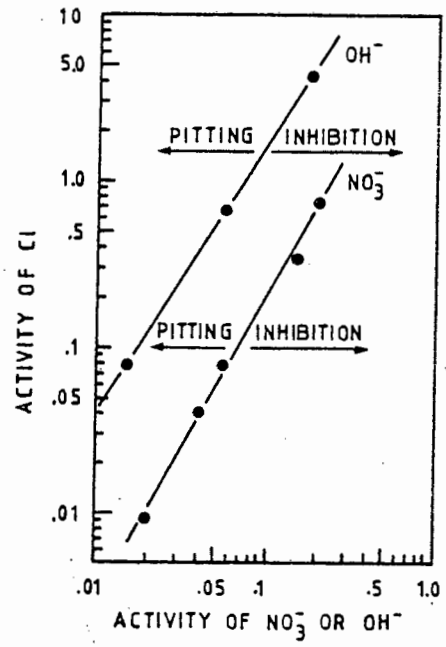

FIGURE 3.20 : The activity of NO_3^- or OH^- required to inhibit pitting by Cl^- (after Leckie and Uhlig, (1966))

The efficiency of inhibition thus decreased in the order $OH^- > NO_3^- > SO_4^{2-} > ClO_4^-$.

Herbsleb (1965) and Man and Gabe (1981) reported the inhibition of 18-8 stainless steel by NO_3^- and SO_4^{2-}. Bogaerts et al (1981) found that SO_4^{2-}, HCO_3^- and OH^- inhibited the pitting of AISI 304 and 316 at temperatures above and below 100°C.

3.3.5.4 The Effect of Temperature

Leckie and Uhlig (1966) found a dramatic decrease in E_p

between 0 and 25°C in a 0.1 N NaCl solution. Above 25°C a gradual decrease in pitting potential with increased temperature was noted. Szklarska-Smialowska (1971) determined the E_p of AISI 304, 316 and 430 over a temperature range of 30°C to 100°C and reported a change of about 200 mV in E_p over the 70°. Bogaerts et al (1981) have shown that E_p of AISI 316L measured at 60°C are lower than at 25°C in solutions of NaCl and Na_2SO_4.

3.3.5.5 Metallurgical Variables Affecting Pitting Corrosion

The beneficial effect of chromium, nickel and molybdenum content in stainless steels is well known (Szklarska-Smialowska, (1971)). Chen and Stephens (1979) have demonstrated the increase in pitting potential with increasing chromium content, as shown in Figure 3.21. A similar effect has been recorded by Bond and Lizlovs (1968) for molybdenum added in a range of 0 - 3 %. Lunarska et al (1975) found that the pitting potential of an 18 Cr - 5 Ni alloy decreased sharply when manganese was added in a content range of 0 to 10%. Sedriks (1984) has reviewed the effects of various alloying elements and discussed them in terms of their influence and on microstructural properties.

Baghdasarian and Ravitz (1975) also reported increased pitting potentials with increasing Mo content in a range of TRIP (Transformation-Induced Plasticity) steels. An interesting observation which emerged from their work was the fact that cold worked specimens showed greater resistance to pitting corrosion. They suggested that this was not due to the cold work itself but rather to the transformation of austenite to martensite during cold working. Mazza et al (1976), however, found that pitting resistance decreased with increasing degree of deformation.

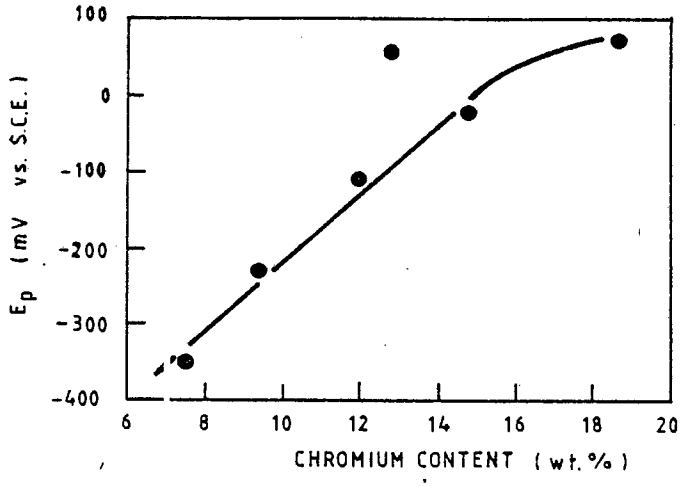

FIGURE 3.21 : The effect of Cr content on E_p in a modified 304 alloy (after Chen and Stephens, (1979))

Scotto et al (1979) and Sedriks (1983) have considered the effects of inclusions on the pitting of stainless steels. Sulphides and in particular manganese sulphides have been shown to be the most active sites for pit nucleation in commerical stainless steels. Manning et al (1979) explained a decrease in E_p with increasing surface roughness by assuming a greater exposure of sulphide inclusions in the higher surface roughness specimens.

3.3.6 Mechanisms of Pitting Corrosion

Pitting corrosion can be divided into two distinct stages, namely the initiation stage and the propagation stage (Szklarska-Smialowska, (1975)). A number of mechanisms which attempt to explain either one or both of these stages, have been suggested. Mechanisms explaining the inhibition of pitting by some anions have also been postulated.

3.3.6.1 The Initiation Stage

Kolotyrkin (1961) proposed that the activating adsorption of chloride ions competes with the passivating adsorption

of oxygen at the metal surface. Pitting corrosion is initiated when a sufficiently high potential, E_p, and chloride ion concentration, is attained. He explained the localized nature of pitting by assuming that a non-uniform distribution of current carries the chloride ions to the surface, resulting in higher chloride concentration at points of greater current. At these points the critical concentration of chloride ion necessary for pitting to initiate is achieved first. Leckie and Uhlig (1966) and Uhlig and Gilman (1964) supported this mechanism of competitive adsorption between chloride and oxygen ions. Hoar (1967) proposed a modified version of the adsorption theory. His "mechanical" theory suggests that the build up of adsorbed chloride ions causes a lowering of the interfacial tension resulting in cracks in the passive film at which pits are able to initiate. Janik-Czachor et al (1975) reported that the existence of islands of chloride ions at discrete sites on the passive surface were precursors of pit initiation.

Galvele (1976) reported that E_p was the minimum potential required to maintain local acidity inside a pit. Using simple transport equations he showed that a minimum product of the pit depth, x, and the current at the bottom of the pit, i, was necessary to sustain a pit. Assuming the "crack heal" nature of the passive film and a current density of 1 A/cm^2 at the bottom of a pit he calculated that for most metals a crack length of 10^{-6} cm in the passive film would be sufficient for the initiation of a pit.

Bearing in mind that the mechanisms discussed can explain the initiation of pitting corrosion on perfect surfaces, it must be remembered that a commercial stainless steel contains inclusions, second phases, and other heterogeneities (Sedriks, (1983)). The dissolution of inclusions, particularly sulphides, resulting in cavities

and microcrevices have been identified as preferential initiation sites for pits (Sedriks, (1983), Scotto et al, (1979)).

In an assessment of the processes leading to pit initiation Janik-Czachor et al (1980) concluded that for a precise model of pit nucleation to be constructed, clarification and confirmation of various aspects of the different proposed mechanisms was necessary.

3.3.6.2 Propagation

The autocalalytic nature of pit propagation, shown in Figure 3.22, is a generally accepted model (Fontana and Greene, (1967)). Consider a pit which has initiated on the surface of a metal, M, in an aerated solution. Rapid dissolution of metal ions occurs within the pit while the area surrounding the pit is protected by the cathodic oxygen reduction reaction occurring there. Now, the excessive positive charge within the pit, due to the accumulation of M^+ ions, is overcome by the influx of Cl^- ions. The subsequent hydrolysis of the metal ion

$$M^+Cl^- + H_2O \rightarrow MOH + H^+ Cl^-$$

results in a decrease in pH (Fontana and Greene, (1967)). Mankowski and Szklarska-Smialowska (1975) measured chloride concentrations as high as 12 N in the solution within pits formed on an 18 Cr - 12 Ni- 2 Mo- Ti austenitic stainless steel. Suzuki et al (1973) reported a chloride concentration range of 3.78 to 6.47 N and a pH range of 0.13 to 0.80 in the anolyte of pits studied on AISI 304L, AISI 316L and an 18Cr-16Ni-5Mo stainless steel.

Thus the fact that there exists a potential , E_x, (which is lower than E_p) above which pits can propagate is due to the local aggressive environment associated with the occluded nature of a pit (Jones, (1982)).

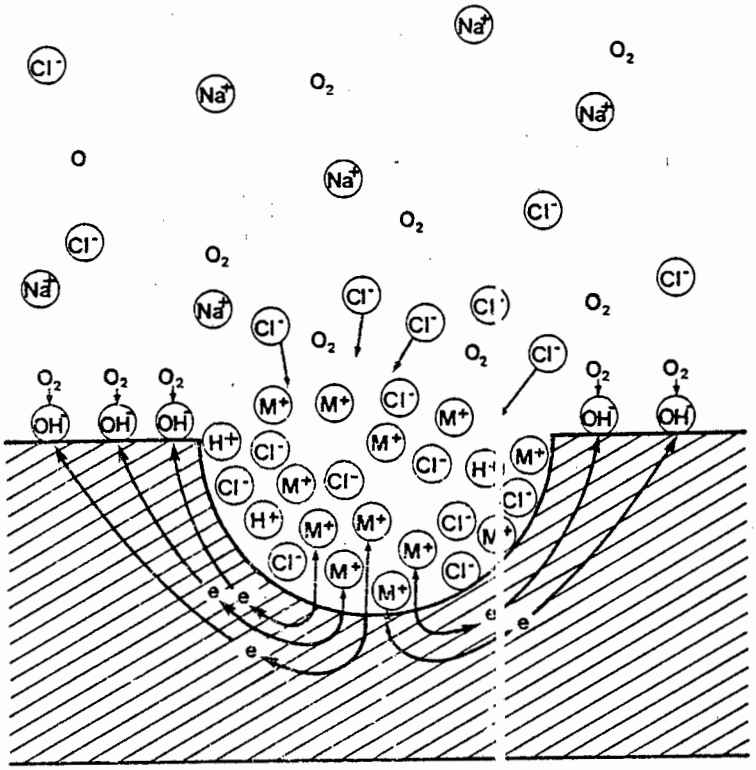

FIGURE 3.22 : The autocatalytic mechanism of pit propagation (after Fontana and Greene, (1967))

3.3.6.3 The Inhibition

Leckie and Uhlig (1966) and Uhlig and Gilman (1964) extended the competitive adsorption mechanism to explain the inhibition of pitting by nitrate ions. They suggested that nitrate ions compete with chloride ions and oxygen for adsorption sites, and that once adsorbed, nitrate ions do not attack the surface. As chloride ions have to compete with two non-reactive species a higher chloride ion concentration is required to initiate pits. They found that their data corresponded to the following form of equation which is predicted by the Freundlich adsorption isotherm:

$$\log (Cl) = \text{constant} + {}^{n1}/_{n2} \log (NO_3^-)$$

In this equation n_1 is the exponent in the Freundlich adsorption isotherm:

amount adsorbed = $k\ (Cl^-)^{1}/_{n1}$

and n_2 is the corresponding exponent for nitrate. Similar inhibitive behaviour was demonstrated for OH^-, SO_4^{2-} and ClO_4^- ions.

Galvele (1976) however proposed that the inhibitive effect was due to transport processes resulting in a build up of sulphate within the pit which would result in inhibition.

CHAPTER 4

EXPERIMENTAL TECHNIQUES

4.1 INSTRUMENTATION

An EG & G Princeton Applied Research Model 173 potentiostat/galvanostat was used for the polarization experiments. Direct conversion of current density to logarithm of current density was performed by a Model 376 logarithmic current convertor. The reference electrode was monitored by a Model 178 electrometer probe while the incorportation of a Model 178/41 noise filter eliminated the possible pick-up of noise in the power lines at the cell. Potentiodynamic Scanning was accomplished by an Elscint Model ABA-26 external automatic baseline advance. The polarization curves generated were directly plotted by an Houston Omnigraphic S-200 X-Y plotter. Figure 4.1 shows the instrumentation used during testing.

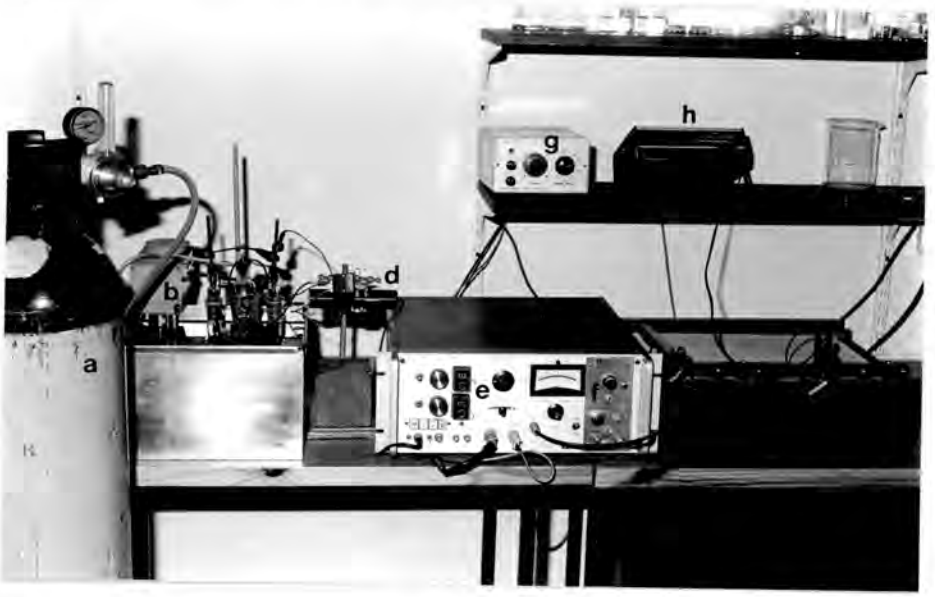

a - gas bottle
b - thermoregulator
c - corrosion flask
d - electrometer probe
e - potentiostat
f - logarithmic current convertor
g - automatic baseline advance
h - voltmeter
i - X-Y plotter

FIGURE 4.1 : A photograph of the potentiodynamic testing instrumentation

The corrosion cell and its accessories are shown in Figure 4.2 and were all acquired from Princeton Applied Research. The experiments were conducted in a glass corrosion flask with especially ground joints for accommodating the Lugin capillary probe, the graphite counter electrodes, the gas purge tube and the electrode holder. Potential measurements were recorded against a saturated calomel electrode which has a potential of 0.241 V with reference to the standard hydrogen electrode.

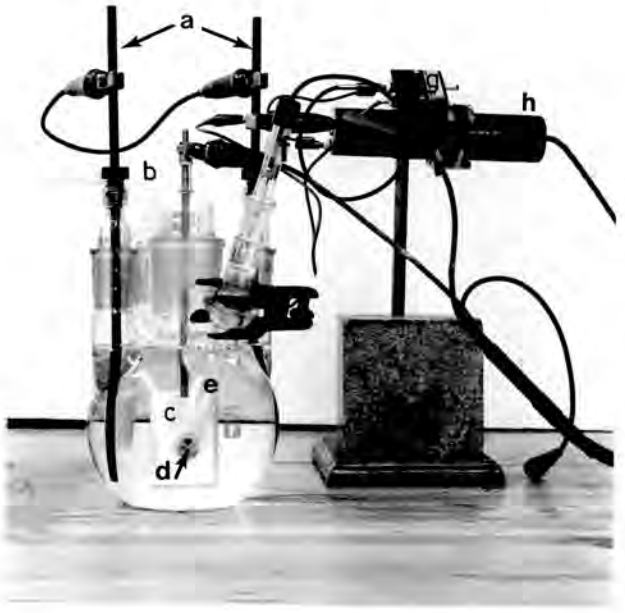

a - counter electrodes
b - gas inlet
c - specimen holder
d - specimen
e - Lugin capillary
f - saturated calomel reference electrode
g - noise filter
h - electrometer probe

FIGURE 4.2 : A photograph showing the arrangement of the components inside the corrosion flask

4.2 SPECIMEN MOUNTING TECHNIQUE

The following three techniques were considered for the mounting of specimens during potentiodynamic testing:

1) Hot Mounting Resin : A 20 mm long cylindrical specimen with an 11.3 mm diameter was prepared with a 4 mm threaded hole in the side. A screw was inserted into the hole and the specimen was hot mounted in resin using a mounting press. On completion of mounting the screw was removed, leaving a thread going through the resin into the specimen, in which the mounting rod of the working electrode could be accommodated.

2) Heat Shrunk Polytetrafluoroethylene (P.T.F.E.) : An 11.1 mm diameter hole was drilled 20 mm deep into a 30 mm long cylinder of P.T.F.E. The P.T.F.E. mounting was heated to about 160°C in an oven, causing the hole to expand. A 20 mm long specimen with an 11.3 mm diameter was inserted into the enlarged hole; on cooling the hole shrunk resulting in a tight seal between the specimen and the P.T.F.E.. A threaded hole for the mounting rod was made through the P.T.F.E. into the specimen.

3) Compression Gasket Specimen Holder : Figure 4.3 shows the specimen holder which was manufactured; it is a slight modification of similar holders described by France (1967) and Chance, Schreiber and France (1975). The casing was made from crystalline polyester to provide rigidity while P.T.F.E. was used for the compression gasket and bolt. On tightening the bolt a seal is created between the gasket and the specimen.

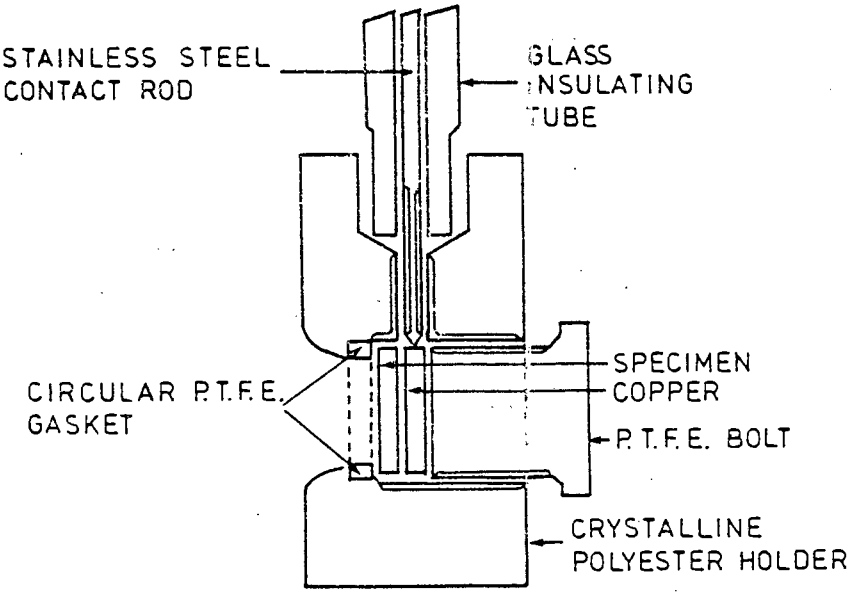

FIGURE 4.3 : The specimen holder

The three mounting techniques, shown in Figure 4.4, have the following in common:

1) They expose 1 cm^2 of specimen for easy determination of current density.

2) All exposed surfaces (excluding the specimen) are inert in the testing media used.

3) The specimen can be re-used simply by grinding and polishing the exposed surface.

For the first two techniques it was noted that the integrity of the seal between the specimen and the mounting material was undermined by the grinding, polishing an ultrasonic cleaning processes. The deterioration in the seal was assumed to be the cause of crevice corrosion encountered during tests conducted in chloride solutions. On the other hand, the specimen holder allows for removal of the specimen which can then be polished and cleaned independently of the mounting medium. Instances of crevice corrosion did occur while using the specimen holder but were of a less serious nature. Often these crevices were associated with a worn P.T.F.E. gasket which was then replaced. A further advantage was the facilitation of microscopic examination once the specimen had been removed from the holder. For the above reasons the specimen holder was used for specimen mounting during corrosion testing. The Stern-Makrides gasket recommended by the ASTM Standard G5-78 (ASTM, (1980)[2]) was not considered due to the difficulty involved in specimen manufacture and polishing, and the achievement of a constant surface area for the determination of current density.

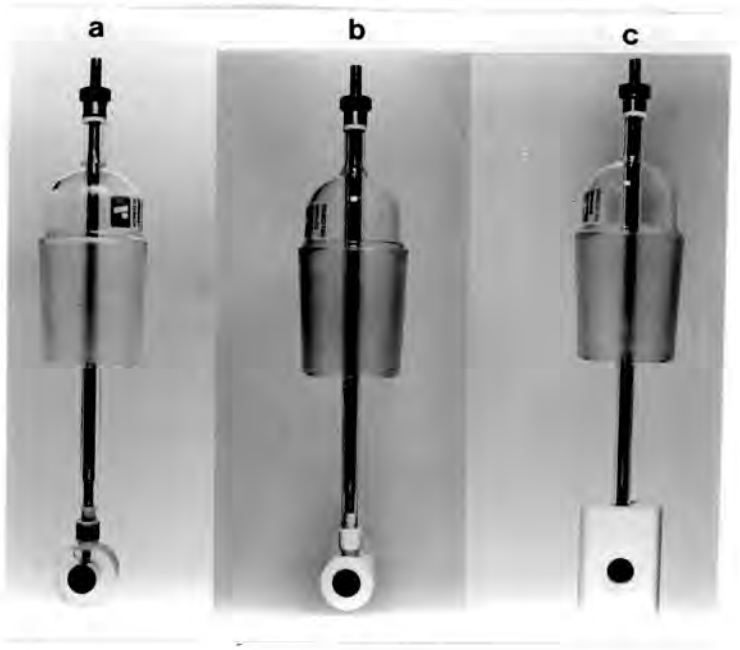

FIGURE 4.4 : A photograph showing the 3 mounting techniques a - hot mounted resin, b - heat shrunk P.T.F.E., c - specimen holder.

4.3 SPECIMEN PREPARATION

In an attempt to avoid any variation in the composition of the alloy a single bar of material, from which all specimens were manufactured was acquired. The bar was turned to 15.8 mm diameter and parted into 4 mm thick disc-shaped specimens. The specimens were ground on silicon carbide pads and finally polished to a 3 m diamond finish. The diamond polish allowed easier microscopic examination of the corroded surface. After polishing, the specimens were degreased in a beaker of alcohol placed in an ultrasonic bath. Immediately prior to testing the specimens were swabbed with alcohol and then with distilled water.

4.4 PREPARATION OF SOLUTIONS

All chemicals used were of analytical reagent grade. Testing solutions were made up in one litre volumetric flasks using glass distilled water. A concerted effort was made to minimise solution contamination; this was

done by washing all glassware after use and thorough rinsing with distilled water before making up the solutions. Once a solution was prepared the pH was determined to an accuracy of 0.1 pH units using a Schott Geräte pH meter. The chemicals used for achieving desired ionic concentrations depended on the composition of the test solution:

1) Experimental E-pH Diagram

500 ppm of sulphate was added as H_2SO_4. The pH was varied by addition of $Ca(OH)_2$. This procedure was followed in an attempt to reproduce the real situation in the mines.

2) Chloride Solutions

Chloride was added as NaCl. The desired pH was attained by addition of a predetermined amount of HCl for acidic solutions or $Ca(OH)_2$ for alkaline solutions.

3) Chloride plus Nitrate Solutions

Chloride was added as NaCl and nitrate as $Ca(NO)_3.4H_2O$. The desired pH was attained by addition of a predetermined amount of HNO_3 for acidic solutions or $Ca(OH)_2$ for alkaline solutions.

4) Chloride plus Sulphate Solutions

Chloride was added as NaCl and sulphate as H_2SO_4. The desired pH was attained by addition of a predetermined amount of $Ca(OH)_2$

5) The Effect of Cu^{2+} and Fe^{3+}

The correct pH, chloride concentration and nitrate concentration were achieved as described previously. Ferric, Fe^{3+}, and cupric, Cu^{2+}, ions were introduced into solution as $FeCl_3$ and $CuCl_2.2H_2O$ respectively. $FeCl_3$ could only be added in trace amounts as its tendency to form hydrated complexes results in a drastic reduction in the pH of the solution.

4.5 TESTING PROCEDURE

4.5.1 Standard Test

To ensure that the system was functioning correctly, a test was performed on AISI 430 in 1N H_2SO_4 according to ASTM standard G5-78 (ASTM, (1980)[2]). Figure 4.5 shows that the potentiodynamic curve obtained corresponds well to the ASTM standard reference curve.

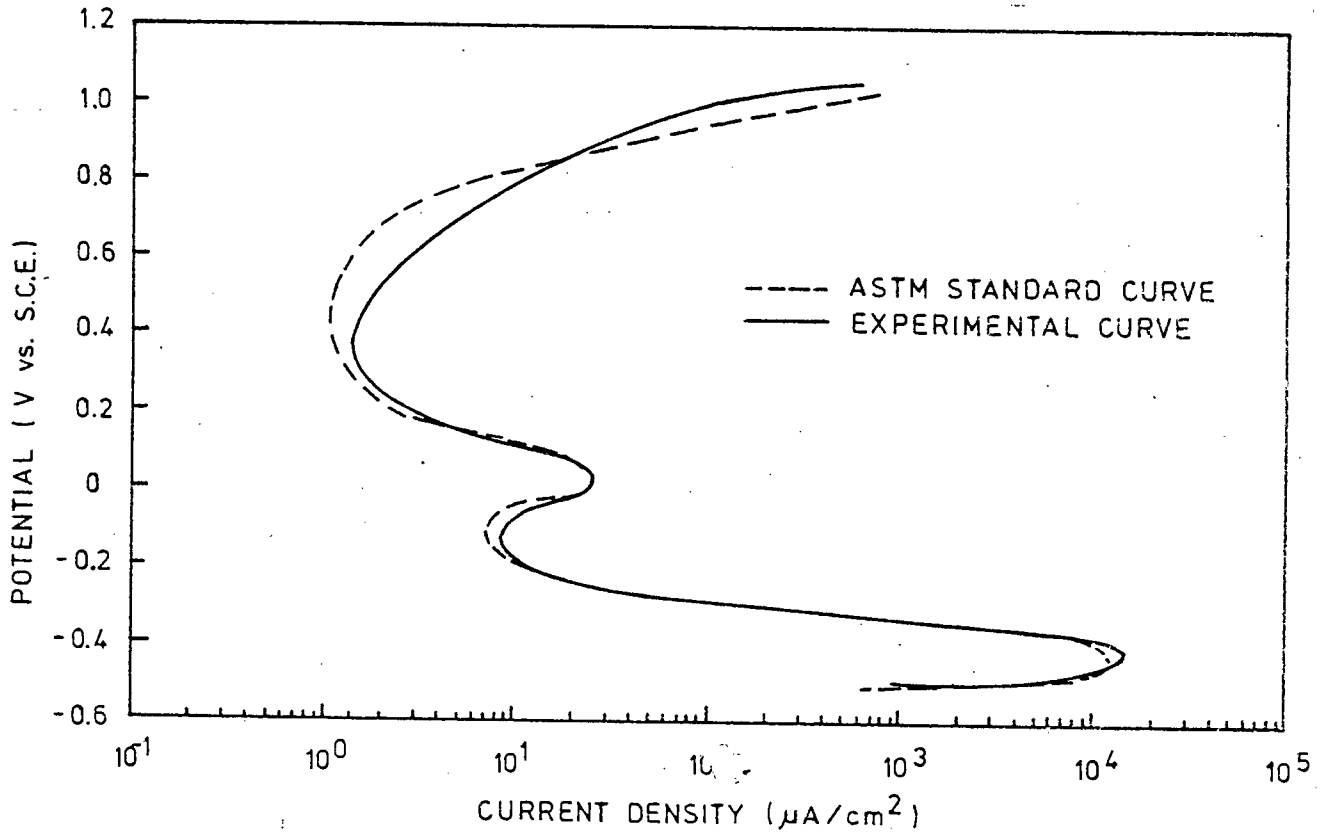

FIGURE 4.5 : Potentiodynamic scan of AISI 431 in 1N H_2SO_4 compared to ASTM standard reference test.

4.5.2 Construction of E-pH Diagram

The solution was maintained at a constant temperature of 30°C using a thermoregulator. Deaeration was achieved by purging the solution with ultra-high purity nitrogen for two hours before the test was started. The specimens were polarized to a cathodic potential of approximately -1.4V vs S.C.E. thirty minutes prior to

commencement of the test. Potentiodynamic scanning was performed at a rate of 0.12 mV/second in the positive direction and once the potential had reached a value greater than the breakdown potential, E_b, the test was terminated.

The experimental E-pH diagram was constructed by plotting the corrosion potential, E_{corr}, the breakdown potential, E_b, and , if present, the Flade potential E_F. Figure 4.6 illustrates the experimental determination of an E-pH diagram.

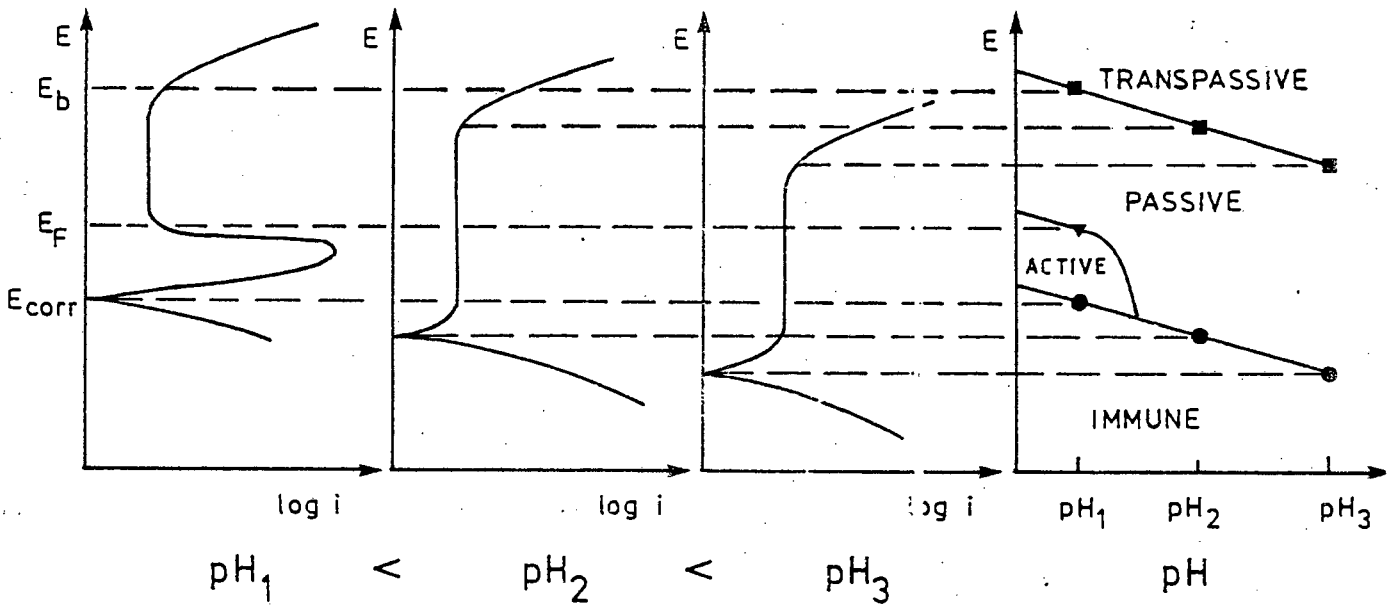

FIGURE 4.6 : The construction of an experimental E-pH diagram

4.5.3 Pitting Corrosion Tests and Determination of the Critical Chloride Concentration

The tests were performed in oxygen saturated solutions. This was achieved by bubbling oxygen through the solutions for thirty minutes before initiating the anodic scan. Fifteen minutes prior to initiation of scanning, the specimen was polarized to a cathodic potential of about 50 mV below its corrosion potential. The potentiodynamic anodic scan was performed at a rate of

0.12 mV/second. The pitting potential, E_p, or the breakdown potential, E_b, was identified as the potential at which a rapid increase in current density occurred. Once the current had reached a value of about 1 mA, due to either pitting corrosion or transpassivity, the direction of scanning was reversed. The test was terminated in either of the following instances:

i) The reverse scan retraced the forward scan without any hysteresis

or

ii) once the hysteresis loop, formed during reverse scanning, intersected the trace of the forward scan at the protection potential, E_x.

The chloride concentration above which localized breakdown of passivity occurred due to pitting and below which uniform breakdown of passivity occurred due to transpassivity was defined to be the critical chloride concentration, $[Cl^-]_{crit}$. Figure 4.7 illustrates the determination of the $[Cl^-]_{crit}$ using the potentiodynamic polarization technique. The schematic polarization curve on the left represent a solution in which the chloride concentration is less than $[Cl^-]_{crit}$ and breakdown of passivity occurs at the breakdown potential E_b, due to transpassive dissolution. The schematic polarization curve on the right represents a solution in which the chloride concentration is greater than $[Cl^-]_{crit}$ and breakdown of passivity occurs at the pitting potential, E_p, due to pitting corrosion. The determination of the protection potential, E_x, and the corrosion potential, E_{corr}, is also demonstrated. These characteristic potentials are determined at increasing chloride concentrations in a series of solutions with constant pH, nitrate concentration and sulphate concentration. E_{corr}, E_p/E_b and E_x (if any) are plotted as a function of chloride concentration in order to ascertain the value of the $[Cl^-]_{crit}$ as shown in the centre figure.

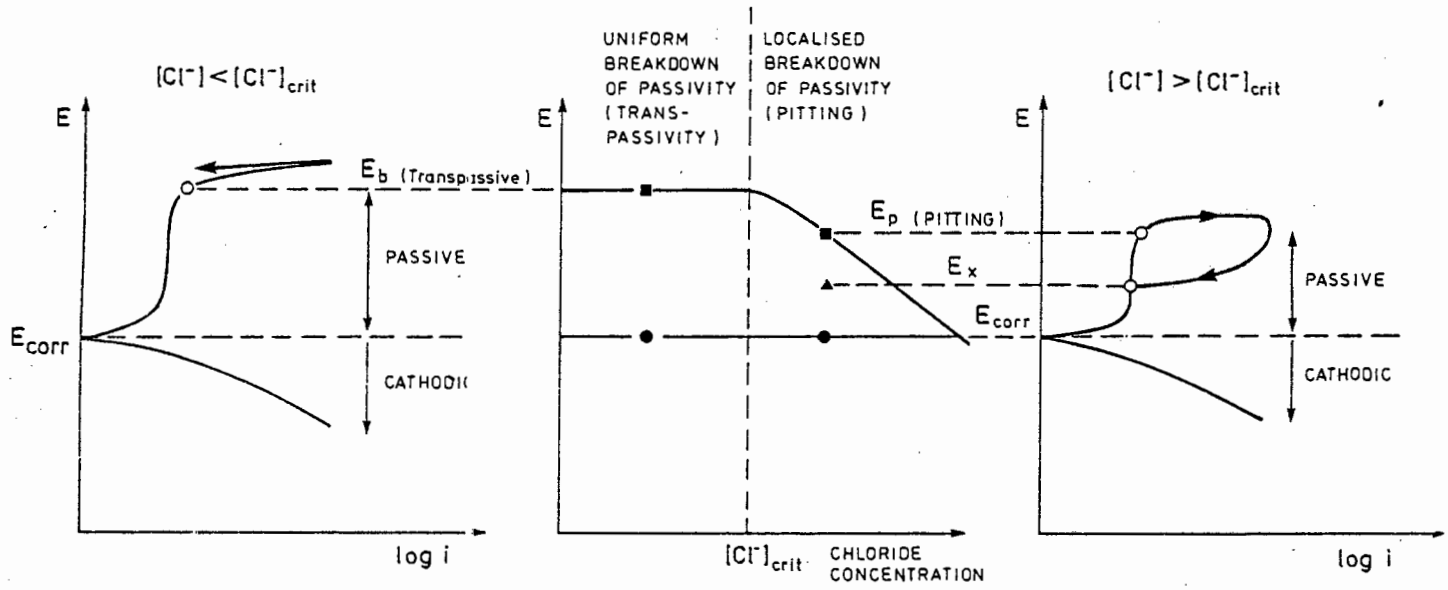

FIGURE 4.7 : The determination of $[Cl^-]_{crit}$

4.5.4 Corrosion Potential-Time Tests in Real Mine Water

Due to the difficulty in transporting real mine water from Johannesburg to Cape Town this experimental work was conducted by the Research Organisation of the Chamber of Mines in Johannesburg. The composition of the mine water was determined at the Chamber of Mines Research Organisation.

A specimen of AISI 431 was immersed in a flask of mine water which was aerated by bubbling oxygen through the solution. The E_{corr} of the specimen was monitored on a daily basis over a period of approximately 5 weeks using a saturated calomel reference electrode.

4.6 MICROSCOPIC EXAMINATION

All specimens were cleaned after testing and their surfaces were examined using the optical microscope. This examination procedure revealed whether breakdown of passivity was due to pitting or transpassive corrosion. Figure 4.8(a) shows a typical pitting surface and Figure 4.8(b) a typical transpassive surface as seen uder the optical microscope.

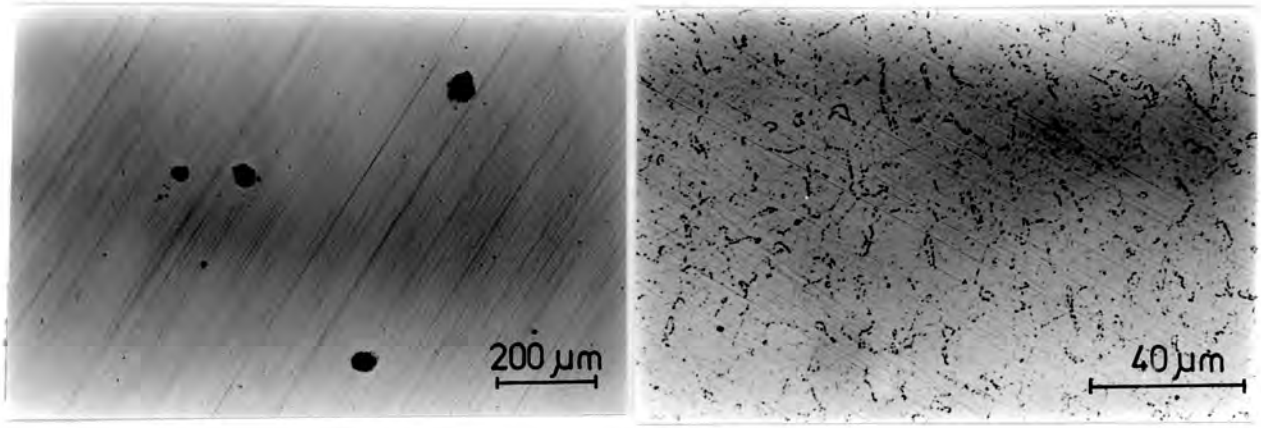

FIGURE 4.8(a) : Pitted surface of AISI 431

(b) Transpassive surface of AISI 431

The optical microscopy was complemented by the use of the scanning electron microscope (SEM). Specimens were gold coated prior to examination by the SEM. Photographs of the characteristic corrosion surfaces were taken using the camera facility available on the SEM.

CHAPTER 5

RESULTS AND DISCUSSION

5.1 CONSTRUCTION OF AN EXPERIMENTAL E-pH DIAGRAM

In the mining situation acidification of the water, due to the formation of H_2SO_4, is usually neutralized by the addition of $Ca(OH)_2$. To determine the E-pH behaviour of AISI 431 under similar conditions potentiodynamic polarization curves were recorded in a series of solutions containing 500 ppm of sulphate ions (added as H_2SO_4), and increasing amounts of $Ca(OH)_2$ to vary the pH. These curves were measured in deaerated solutions at 30°C using a scan rate of 0.12 mV/second.

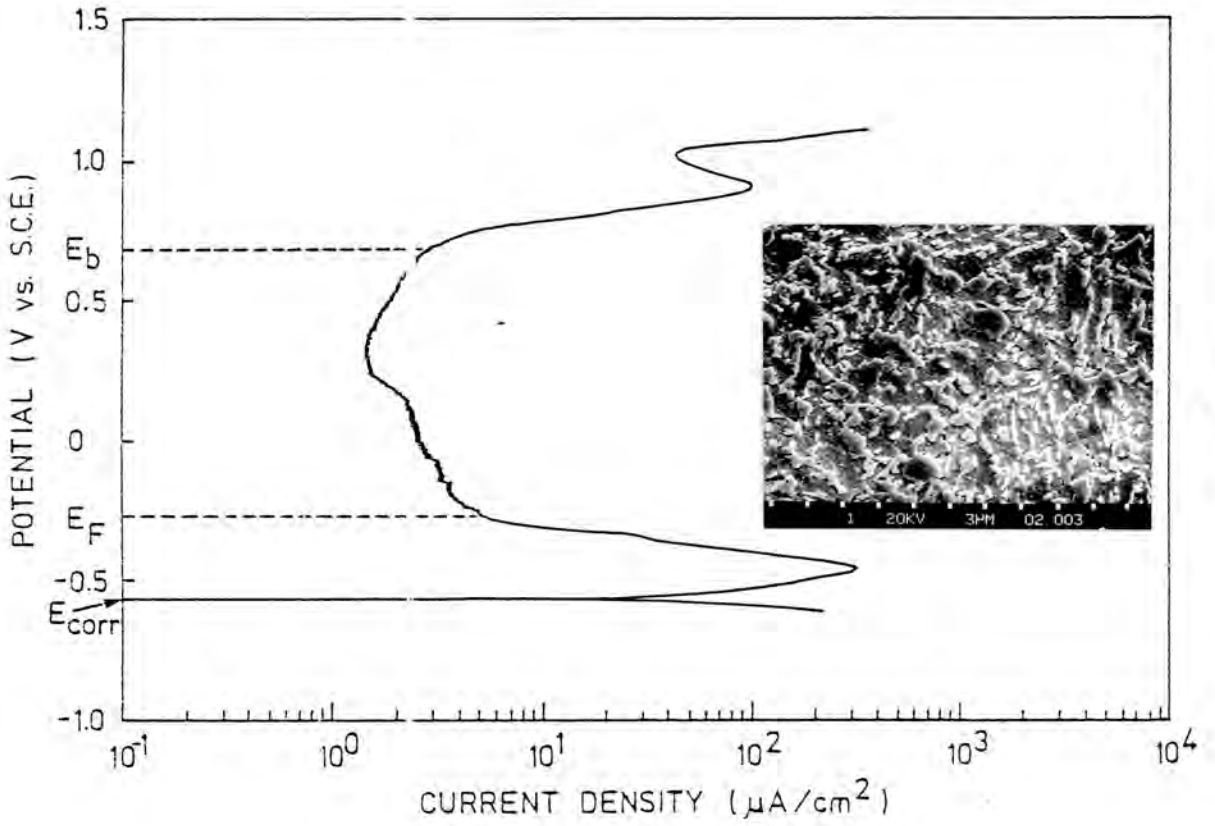

FIGURE 5.1 : Potentiodynamic polarization curve for AISI 431 in pH 2.7 solution, showing E_{corr}, E_F and E_b and an SEM micrograph of the actively corroded surface

Below a pH of 3.8 typical active/passive polarisation behaviour was observed. Examination of the specimen after testing showed that general corrosion of the exposed surface had occurred. Figure 5.1 shows the polarization curve obtained in a solution with a pH of 2.7. The determination of the corrosion potential (E_{corr}), the Flade potential (E_F) and the breakdown potential (E_b) is indicated. The inset SEM micrograph shows the typical appearance of the surface due to general corrosion in the active region.

In the solutions with a pH equal to or greater than 3.8 the E_{corr} of the specimen was found to lie within the passive range. Figure 5.2 shows a potentiodynamic polarization curve obtained at a pH of 7.2. It is clear that, due to the absence of an active loop in the curve, the intersection of the anodic and cathodic curves has occurred within the passive range of the steel. The transpassive breakdown of the passive film results in a corrosion surface with an appearance typified by the inset micrograph in Figure 5.2.

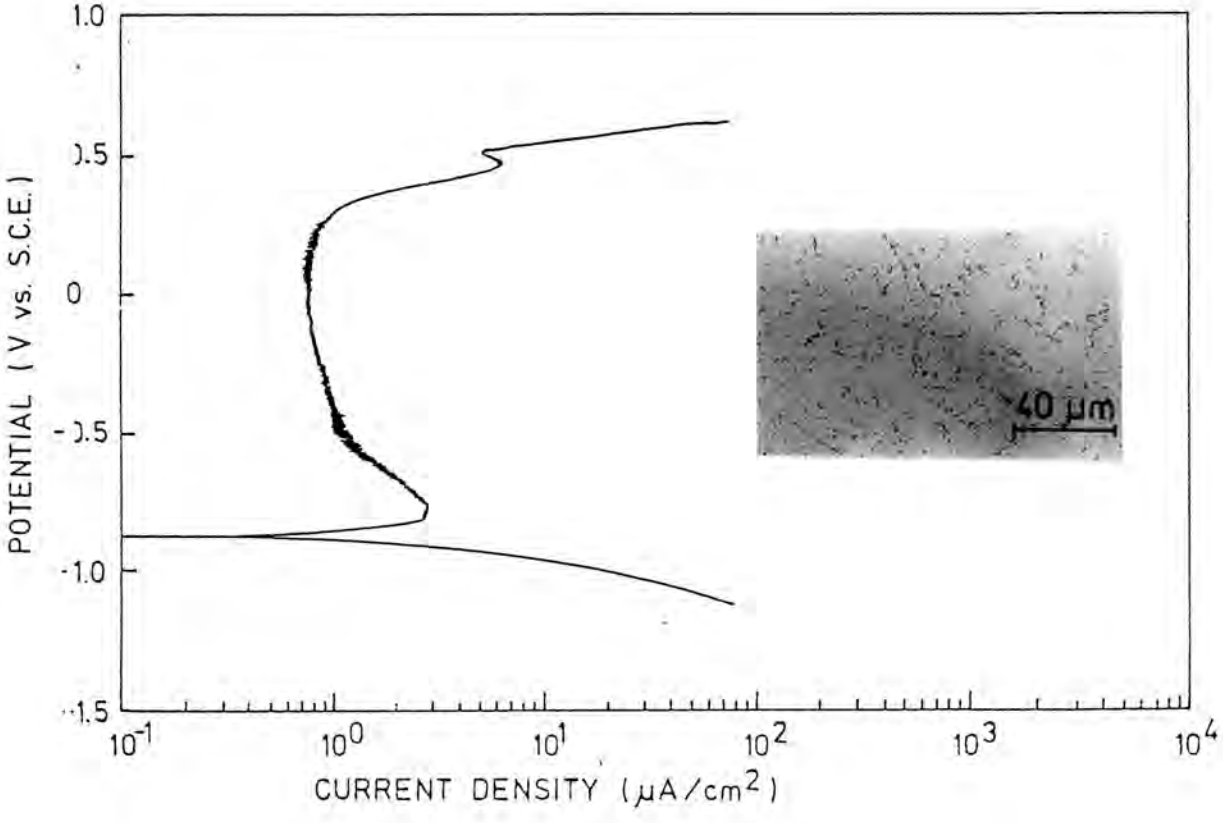

FIGURE 5.2 : Potentiodynamic curve for AISI 431 in pH 7.2 solution and a micrograph of the corroded surface due to transpassive breakdown

From the potentiodynamic curves obtained in the pH range of 2.3 to 10 an experimental E-pH diagram was constructed. For pH below 3.8 E_{corr}, E_F and E_b were plotted while at pH equal to or greater than 3.8 E_F did not exist and hence only E_{corr} and E_b were plotted. Figure 5.3 is the resultant experimental E-pH diagram indicating the potential with reference to both the saturated calomel electrode (S.C.E.) and the standard hydrogen electrode (S.H.E.).

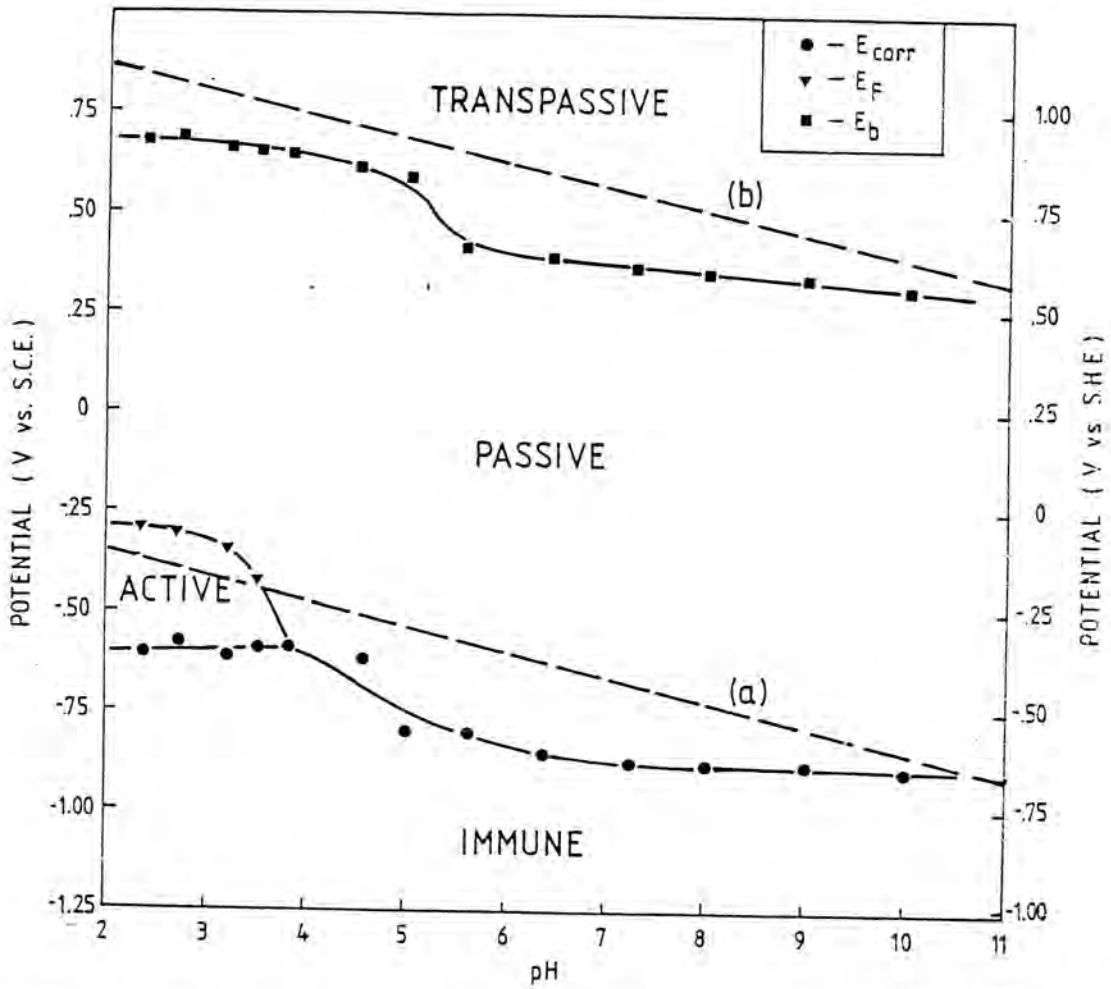

FIGURE 5.3 : Experimental E-pH diagram for AISI 431 in 500 ppm SO_4^{2-} + xmg $Ca(OH)_2$ solutions

Comparison of the experimental E-pH diagram of AISI 431 and the simplified theoretical E-pH diagram for chromium of Deltombe, de Zoubov and Pourbaix (1966), shown in Figure 5.4, indicates the similar corrosion behaviour of chromium and AISI 431 stainless steel. Line 'a' represents the hydrogen evolution reaction while line 'b' represents the oxygen reduction reaction. In both cases active/passive behaviour is predicted for mildly acidic environments where the hydrogen evolution reaction

is the cathodic reaction. In these solutions the oxygen reduction reaction could, however, result in passivation of the surface. For neutral and mildly alkali solutions either cathodic process of the aqueous system would result in passivation of the surface. In all cases polarization of the passive surface to a sufficiently high potential would result in transpassive breakdown of the passive layer. The similarities in the corrosion behaviour of AISI 431 and chromium as predicted by their respective E-pH diagrams confirm that the corrosion resistance of AISI 431 can be ascribed to the chromium enrichment of the oxide layer. The presence of 16 per cent chromium in AISI 431 has been shown to be effective in promoting the formation of a stable passive oxide layer on the surface of the steel.

The E-pH diagram determined for AISI 431 may be regarded as a standard for a martensitic stainless steel. In the future the E-pH behaviour of the steels developed for the mining industry may be compared to that of AISI 431.

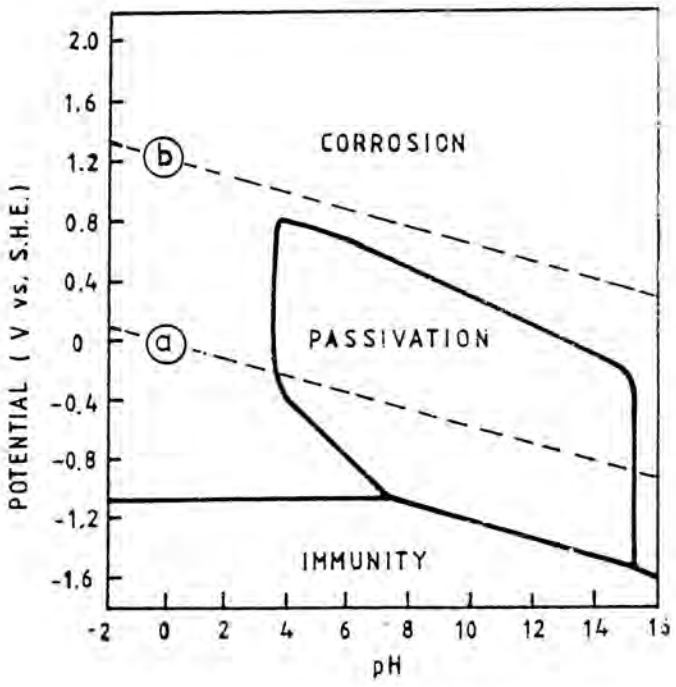

FIGURE 5.4 : Simplified E-pH diagram for chromium considering $Cr(OH)_3$ (after Deltombe, de Zoubov and Pourbaix (1966))

5.2 THE EFFECT OF CHLORIDE CONCENTRATION ON THE POLARIZATION BEHAVIOUR OF AISI 431

A series of tests was conducted to determine the effect of increasing chloride concentration on the polarization behaviour of AISI 431 at a pH of 6.2. The tests were run in fully aerated solutions at a scan rate of 0.12 mV/second.

At chloride concentrations of 100 ppm and less a constant breakdown potential, E_b, of 0.55 V vs S.C.E. was measured due to transpassive breakdown of the passive film. Reversing the direction of scanning indicated no hysteresis effect and microscopic examination of the specimen showed a typical transpassive surface. Figure 5.5 illustrates the polarization curves measured at a chloride concentration of 100 ppm. The absence of hysteresis during reverse scanning is evident, and the inset micrograph shows the resultant transpassive appearance of the surface.

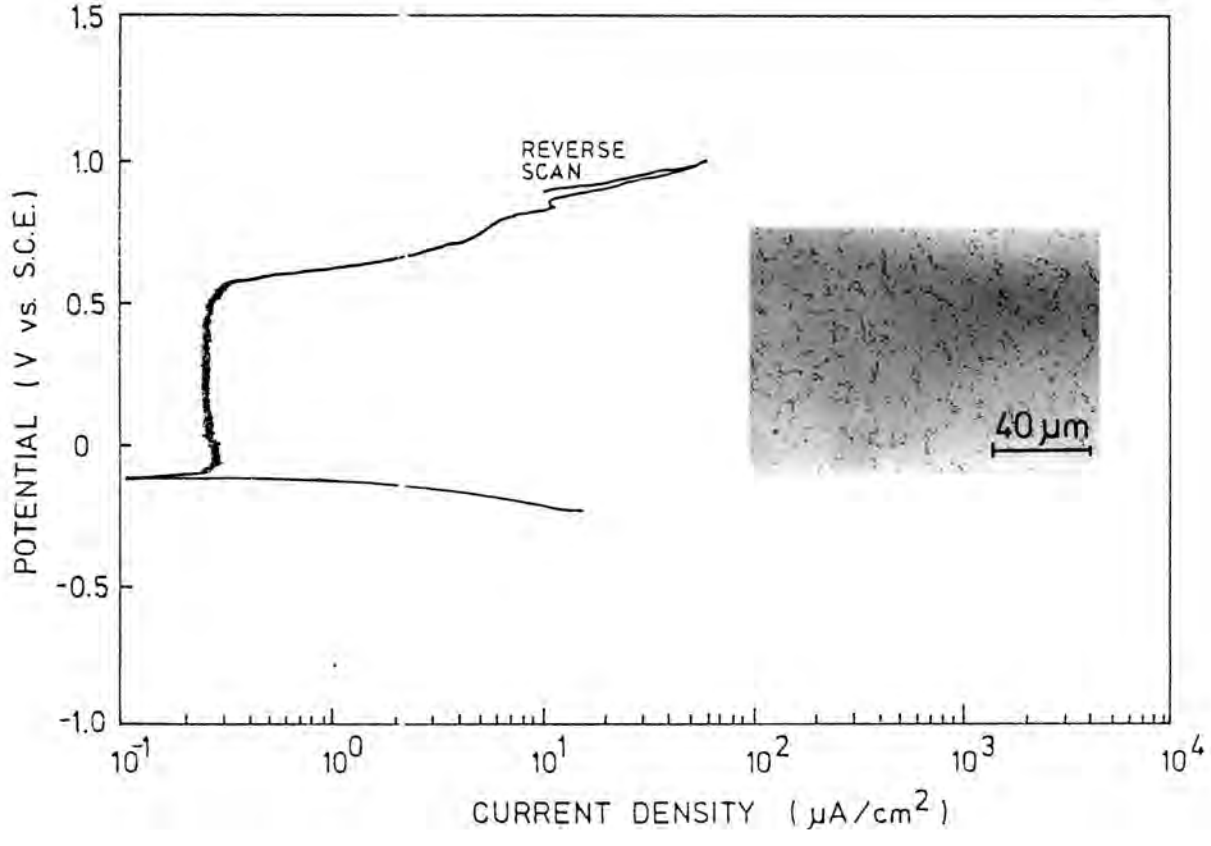

FIGURE 5.5 : Potentiodynamic polarization curve of AISI 431 in 100 ppm chloride solution - pH 6.2, and a micrograph of the transpassive surface

In the solutions with chloride concentration equal to or greater than 150 ppm, breakdown of passivity was due to the onset of pitting corrosion at specific pitting potentials. Evidence of pitting corrosion was revealed by the following factors:-

i) Breakdown of passivity at a pitting potential, E_p, which was lower than E_b.
ii) The hysteresis effect and determination of a protection potential, E_x, during reverse scanning.
iii) Numerous small pits on the exposed surface of corroded specimen.

The potentiodynamic polarization curve, showing the hysteresis effect and the determination of E_p and E_x, of AISI 431 in 1000 ppm chloride solution is illustrated in Figure 5.6. The typical pitted appearance of the polarized surface can be seen in the inset SEM micrograph.

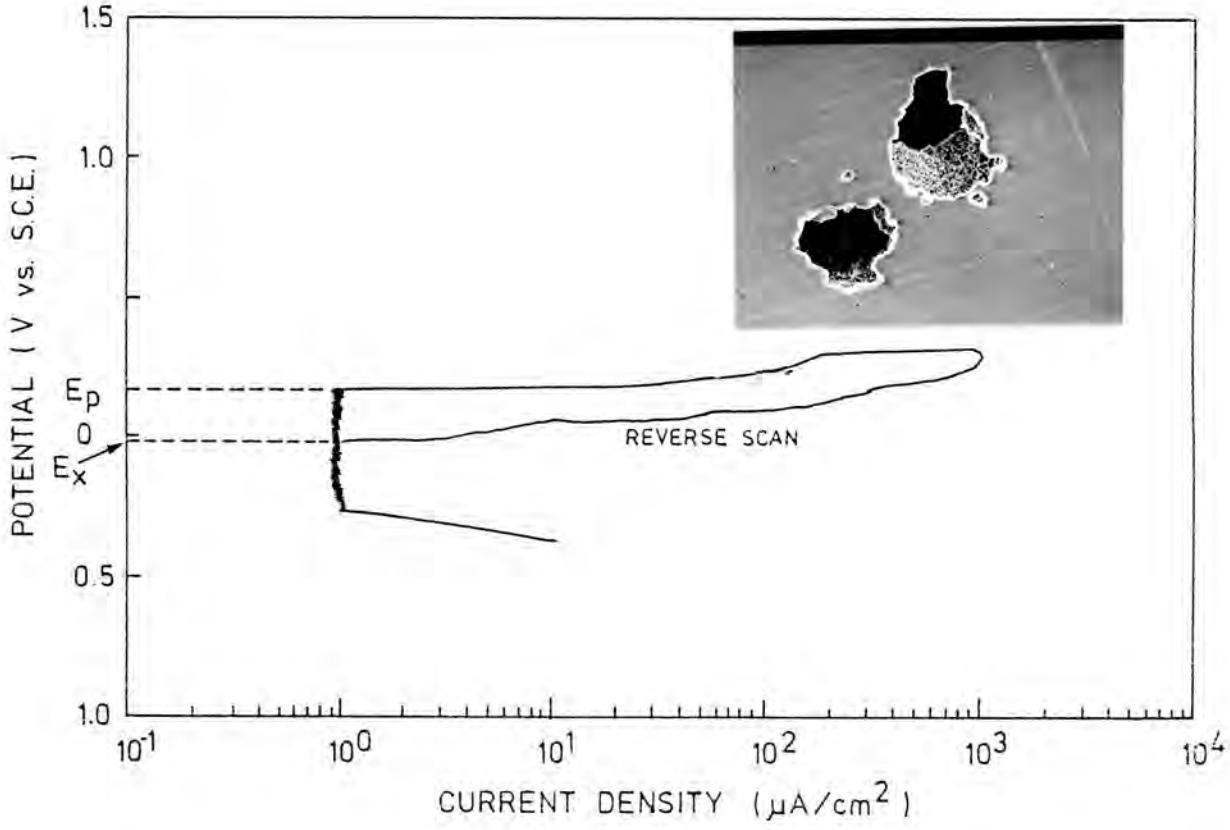

FIGURE 5.6 : Potentiodynamic polarization curve of AISI 431 in 1000 ppm chloride solution - pH 6.2 and SEM micrograph of pitted surface

In Figure 5.7 E_{corr}, E_x and E_p/E_b have been plotted as a function of the logarithm of the chloride concentration. Between chloride concentrations of 150 and 300 ppm E_p decreases sharply from 0.45 to 0.28 V vs S.C.E. Above a chloride concentration of 300 ppm, however, E_p decreases linearly, with a slope of 0.186 V/decade, with increasing chloride concentration. E_x decreases linearly with increasing chloride concentration and has a slope of 0.093 V.decade. These results can be compared to Figure 3.18 which shows a decrease of 0.183 V/decade in E_p and 0.143 V/decade in E_x for a 12% Cr martensitic stainless steel (Atrens, 1983).

In Figure 5.7 a critical chloride concentration, $[Cl^-]_{crit}$, has been defined to exist at 125 ppm i.e. midway between 100 and 150 ppm of chloride. $[Cl^-]_{crit}$ is the chloride concentration below which breakdown of passivity occurs at E_b due to transpassive corrosion, and above which breakdown of passivity occurs at E_p due to pitting corrosion.

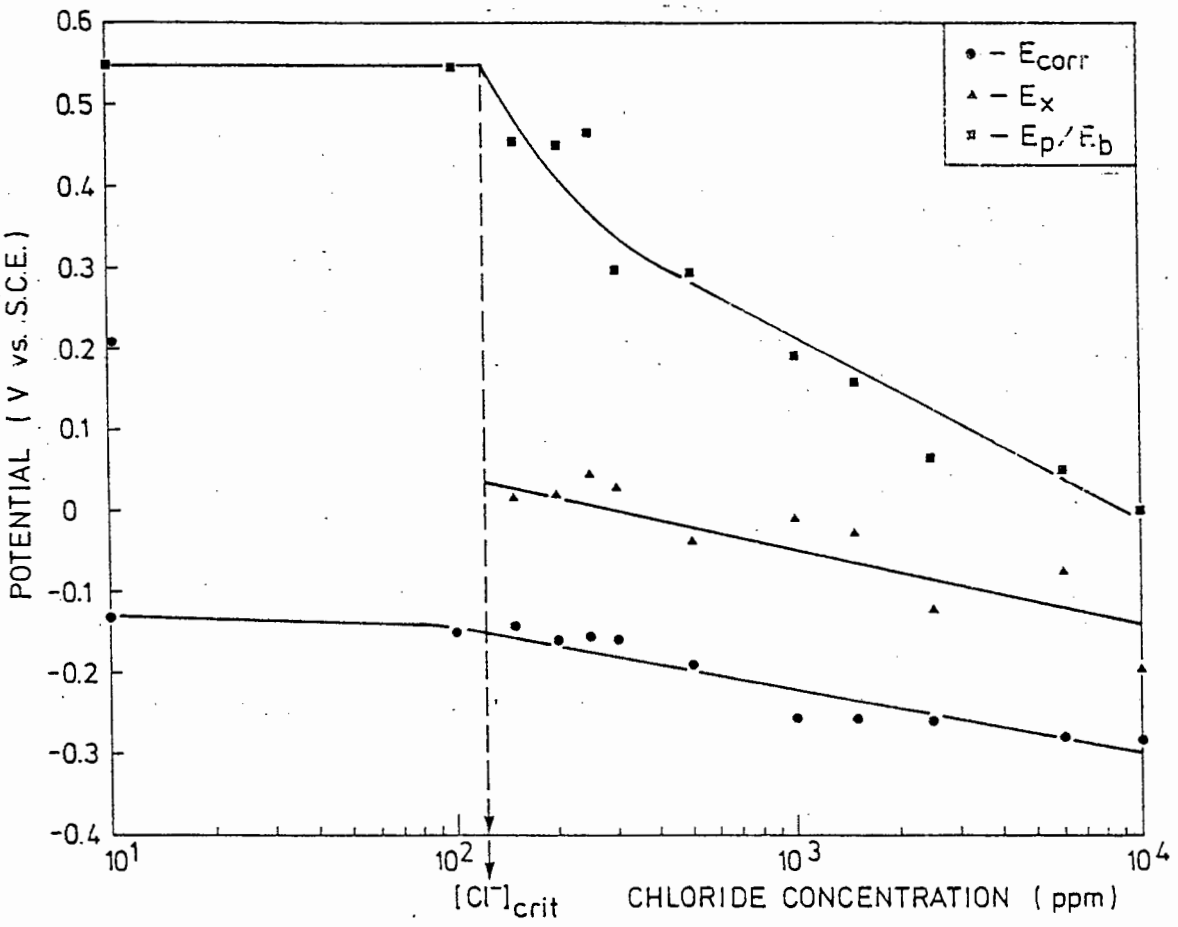

FIGURE 5.7 : E_{corr}, E_x and E_p/E_b of AISI 431 versus chloride concentration - pH 6.2

Increasing chloride concentration was also found to increase the magnitude of the passive current, I_{pass}. Figure 5.8 shows I_{pass} as a function of the logarithm of the chloride concentration at a pH of 6.2. At chloride concentrations of 200 ppm and less, I_{pass} approaches the value of I_{pass} measured in distilled water. Between a chloride concentration of 200 and 2500 ppm I_{pass} increases linearly with a slope of 0.81 μA decade. Above 2500 ppm chloride the passive current density approaches a limiting current density which could be governed by the rate of an adsorption or transport process involving the interaction between the passive film and the chloride ions. The alternative y-axis in Figure 5.8 indicates that these passive current densities represent very low corrosion rates.

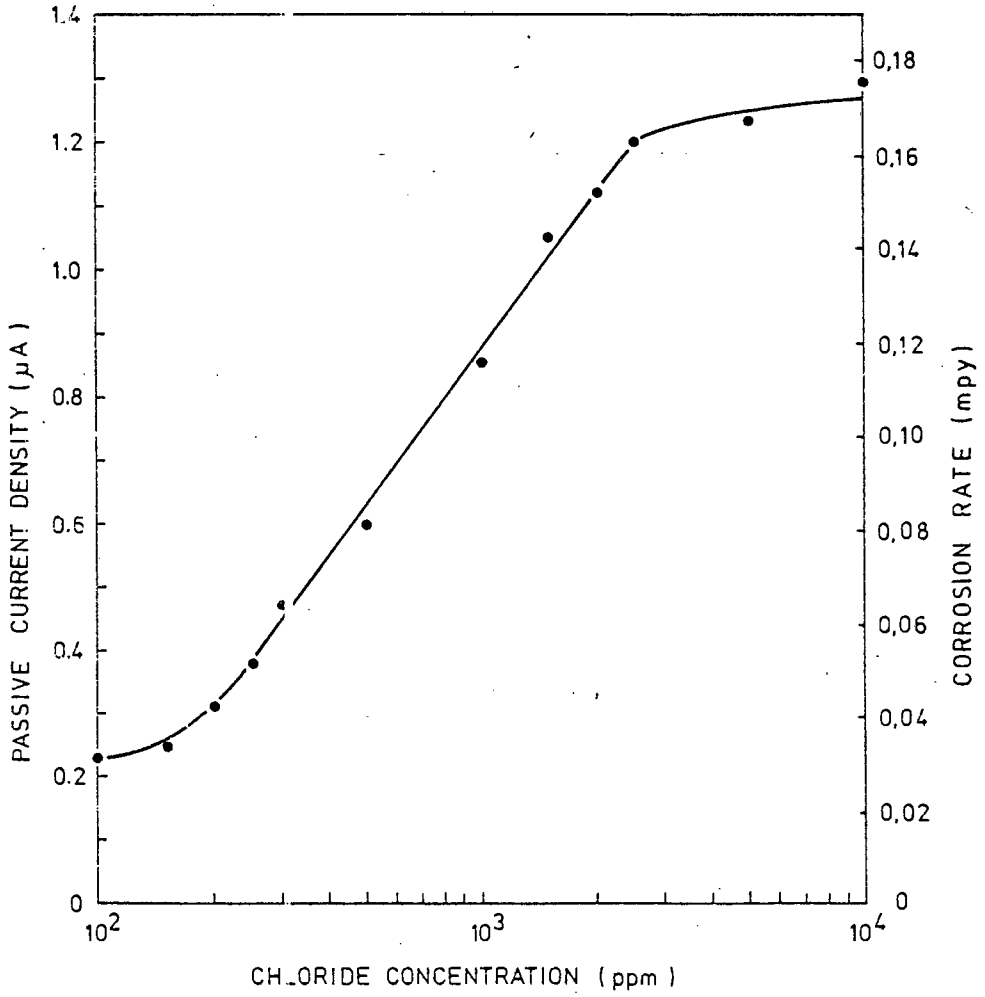

FIGURE 5.8 : I_{pass} of AISI 431 as a function of chloride ion concentration, pH 6.2

A decrease of 0.076 V/decade in E_{corr} can be measured from Figure 5.7. In the case of a metal existing in the passive state E_{corr} is determined by the potential at which the cathodic curve intersects the anodic curve in the passive region. Now as the passive current density increases with increasing chloride concentration so the potential at the intersection of the anodic and cathodic curves, and thus E_{corr}, decreases. Figure 5.9 illustrates this principle. As the chloride concentration is increased in order for curves 1, 2 and 3, there is a corresponding decrease in E_{corr}, in the order $E_{corr1} > E_{corr2} > E_{corr3}$.

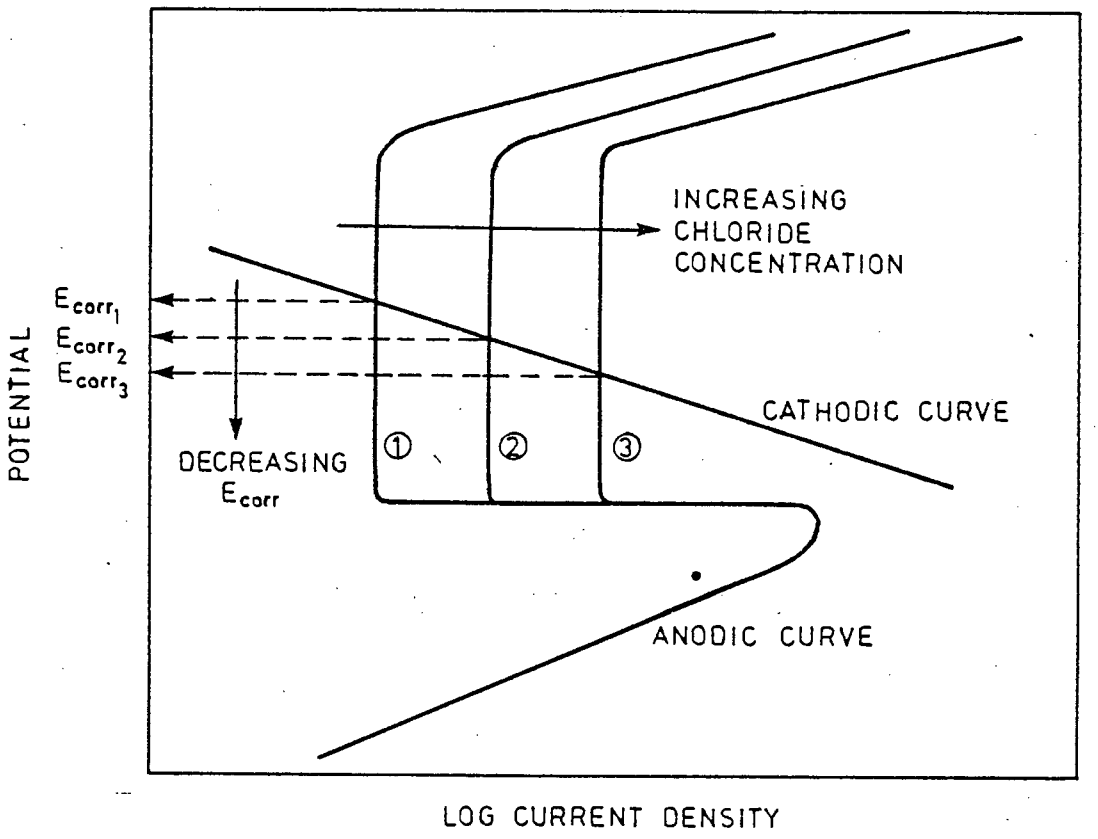

FIGURE 5.9 : An explanation for the decrease in E_{corr} with increasing chloride concentration

5.2.1 The Effect of pH on the Pitting Corrosion Behaviour of AISI 431 in Chloride Solutions

The effect of increasing chloride concentration on the

polarization behaviour of AISI 431 at pH 3.8 and pH 9.4 was determined and the resultant potential vs. chloride concentration curves are depicted in Figures 5.10 and 5.11 respectively.

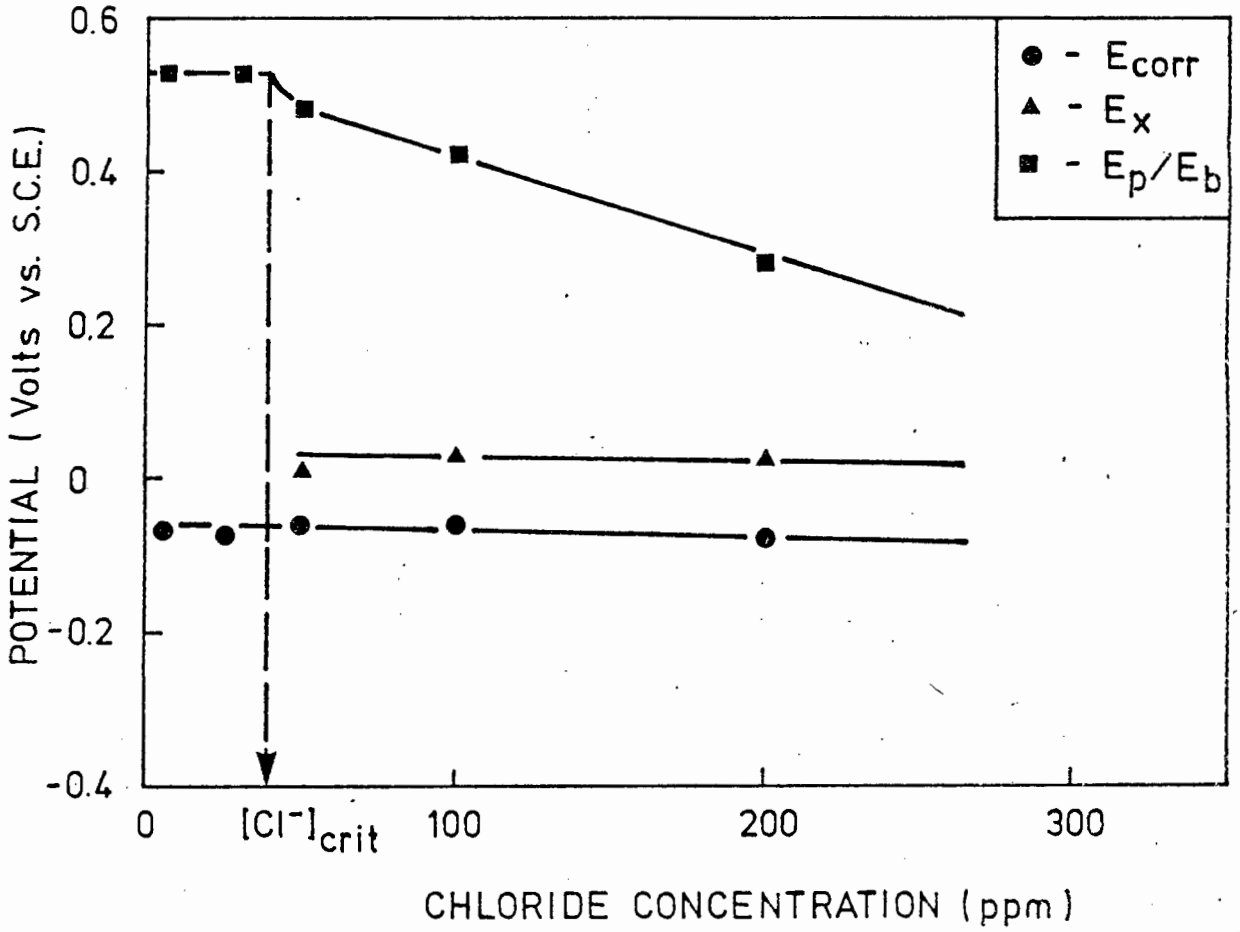

FIGURE 5.10 : E_{corr}, E_x and E_p/E_b of AISI 431 versus chloride concentration, pH 3.8

In Figure 5.10 it can be seen that for a pH of 3.8 the $[Cl^-]_{crit}$ lies between 25 and 50 ppm chloride. It is possible that in solutions of lower pH inclusions on the metal surface become less stable and tend to dissolve. This would result in the nucleation and subsequent propagation of pits at lower chloride concentrations. The lower pH of the bulk solution would also help to maintain the low pH of the localized medium which is present within a propagating pit (Suzuki, (1973)).

At pH 9.4 the critical chloride concentration was found to be about 425 ppm chloride as seen in Figure 5.11.

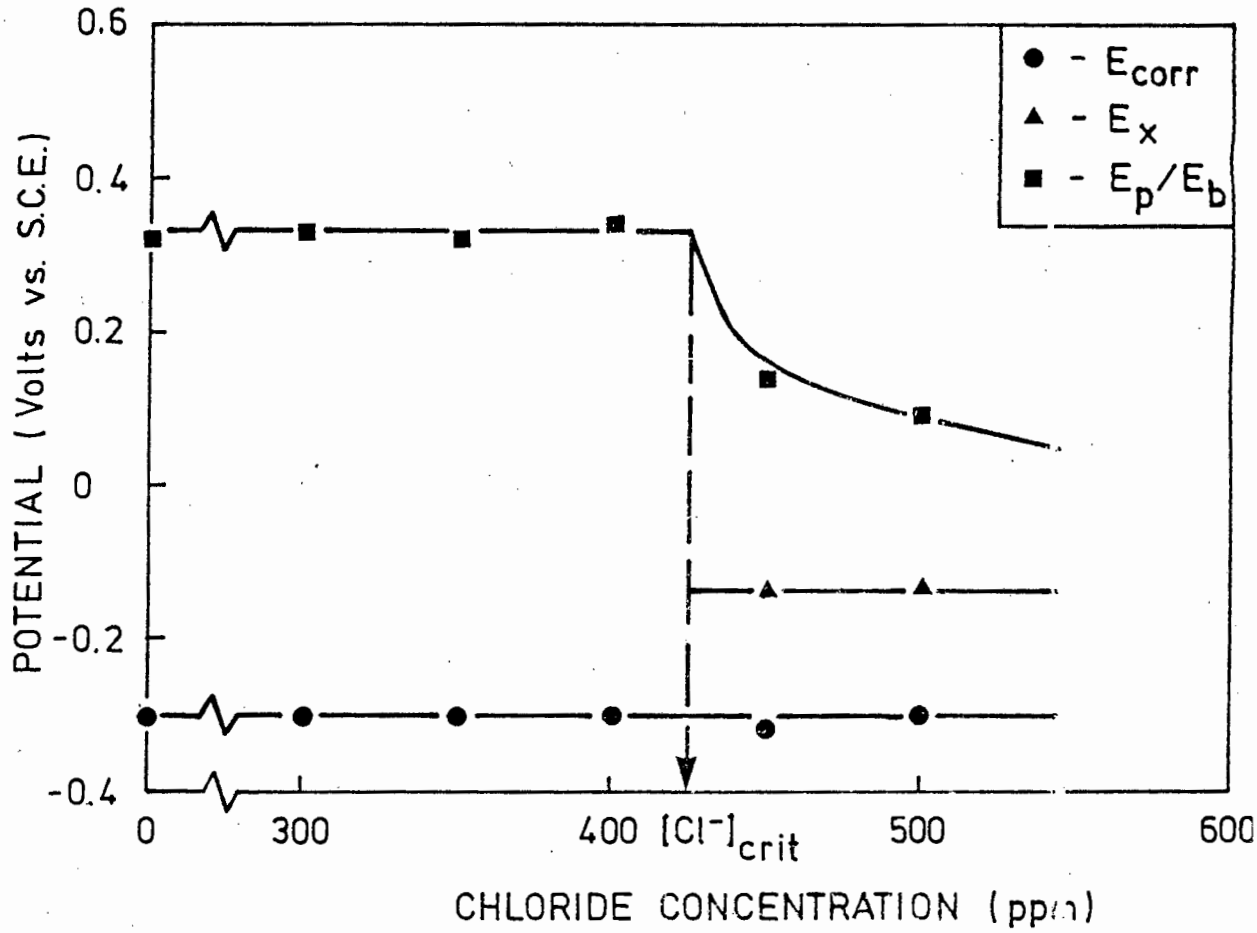

FIGURE 5.11 : E_{corr}, E_x and E_p/E_b of AISI 431 versus chloride concentration, pH 9.4

The increase in $[Cl^-]_{crit}$ at pH 9.4 compared to $[Cl^-]_{crit}$ at pH 6.2 is probably due to the inhibitive effect of OH^- ions on pitting corrosion. This effect was reported by Leckie and Uhlig (1966) who determined the following relationship between the critical chloride ion activity and the activity of OH^- ions for an 18-8 stainless steel:-

$$\log (Cl^-) = 1.62 \log (OH^-) + 1.84 \qquad \text{Equation 3.1}$$

The relationship indicates that the inhibitive effect of OH^- ions only becomes significant at pH greater than 10, as demonstrated in Table 5.1 where the critical chloride concentrations have been calculated for various pH's using equation 3.1 assuming an activity coefficient of 1.

TABLE 5.1 : Critical chloride concentration at various pH's - calculated from data of Leckie and Uhlig (1966)

pH	CRITICAL CHLORIDE CONCENTRATION (ppm)
8	5×10^{-4}
9	0.02
10	0.81
11	33.85
12	1411
13	5883

These results were extrapolated from a limited range of OH^- concentration, 0.016 - 1.0 M (272-17000 ppm), and are therefore not directly applicable but do serve to highlight the fact that the inhibitive effect of OH^- ions can only be expected to manifest itself above a sufficiently high pH. Furthermore, the propagation of a pit is associated with an acidic localized environment (Suzuki, (1973)), thus a pit initiating in an alkali environment will tend to repassivate due to the neutralization of the localized acidic medium by the bulk solution. Verink and Pourbaix (1971) measured a $[Cl^-]_{crit}$ of about 350 ppm for a 12% Cr alloy at pH 8.8, this value compares well with the $[Cl^-]_{crit}$ of 425 ppm at pH 9.4 determined in this study

In Figure 5.12 the results of this study have been compared to the data calculated from equation 3.1 of Leckie and Uhlig (1966) and the result of Pourbaix (1971). Clearly the extrapolated data of

Leckie and Uhlig only predicts the inhibitive effect of OH^- at pH's higher than determined in this study. The result of Pourbaix (1971) for a 12% Cr steel however corresponds well to the results determined for AISI 431 (16.3% Cr).

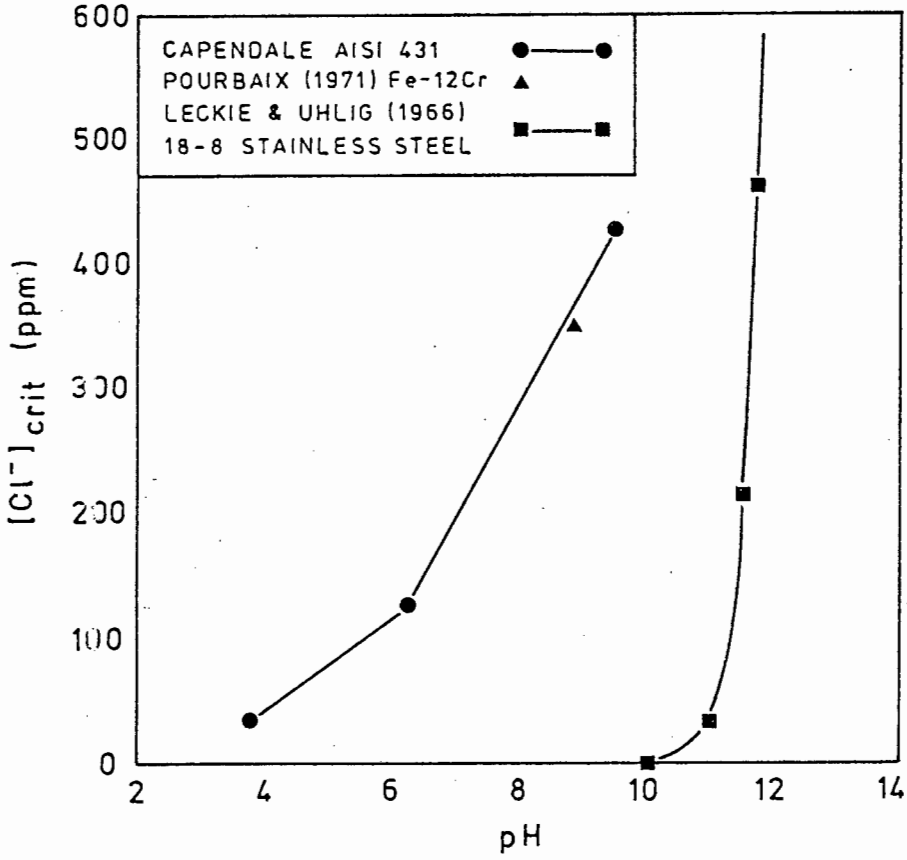

FIGURE 5.12 : $[Cl^-]_{crit}$ as a function of pH

5.3 THE EFFECT OF NITRATES ON THE POLARIZATION BEHAVIOUR OF AISI 431

A series of tests was conducted to determine the effect of increasing nitrate concentration on the potentiodynamic polarization behaviour of AISI 431 at pH 6.2.

The results of the tests at various nitrate concentrations are presented in Table 5.2. E_{corr} and E_b were found to be independent of increasing nitrate concentration and in no case did pitting corrosion occur. I_{pass} increased with increasing nitrate concentration.

TABLE 5.2 : I_{pass}, E_{corr}, E_b of AISI 431 for increasing nitrate concentration

NITRATE CONCENTRATION	I_{pass} (μA)	E_{corr} (V vs. S.C.E.)	E_b (V vs. S.C.E)	NATURE OF REVERSE SCAN	APPEARANCE OF SPECIMEN SURFACE
500	0.68	-0.170	0.525	No hysteresis	Transpassive
1000	0.80	-0.150	0.550	No hysteresis	Transpassive
1500	0.88	-0.160	0.530	No hysteresis	Transpassive
2000	0.94	-0.155	0.542	No hysteresis	Transpassive

In a concentration range of 500 - 2000 ppm, nitrate ions, as in the case of chloride ions, increase the rate of corrosion in the passive state. In this concentration range however nitrates did not cause pitting corrosion and breakdown of the passive state was due to transpassive corrosion.

5.3.1 The Effect of Nitrate Ions on the Pitting Corrosion of AISI 431 in Chloride Solutions

Figure 5.13 shows E_{corr}, E_x and E_p/E_b as a function of chloride concentration in solutions with a pH of 6.2 and a nitrate concentration of 1000 ppm. The behaviour of E_{corr} and E_x is similar to that in Figure 5.7. The effect of adding 1000 ppm nitrate to the solution has clearly been to increase the $[Cl^-]_{crit}$ from 125 ppm, in the case of nitrate-free solution, to 1275 ppm chloride. Similar curves, shown in Appendix D, were determined for 500 and 1500 ppm nitrate where $[Cl^-]_{crit}$ was determined to be 625 and 1875 ppm respectively.

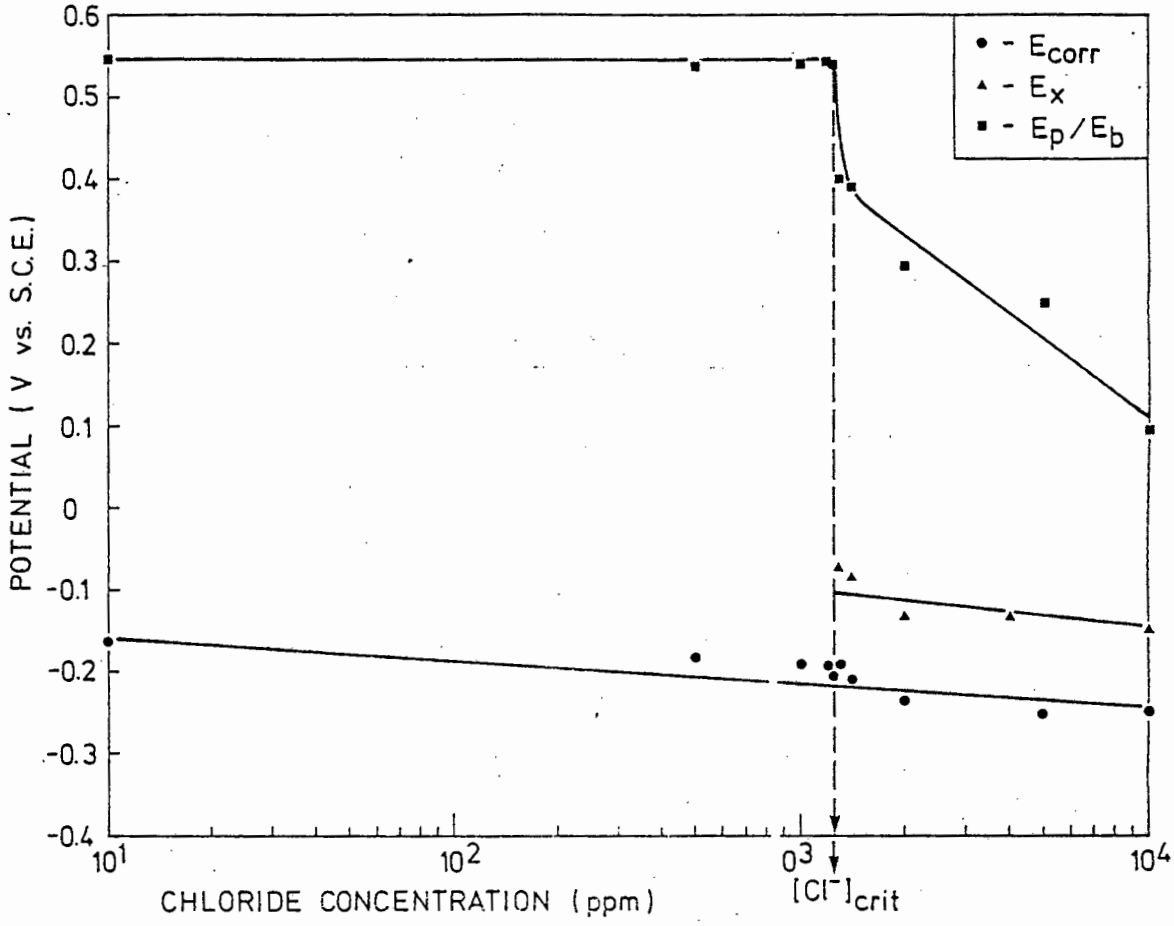

FIGURE 5.13 : E_{corr}, E_x and E_p/E_b of AISI 431 versus chloride concentration in 1000 ppm nitrate solution, pH 6.2

From curve (a) in Figure 5.14 the following linear relationship beweeen $[Cl^-]_{crit}$ and nitrate concentration has been determined:

$$[Cl^-]_{crit} = 1.18\ [NO_3^-] + 95 \qquad \text{Equation 5.2}$$

Leckie and Uhlig (1966) found the following relationship for inhibition of pitting by nitrates for an 18-8 stainless steel:-

$$\log (Cl^-)_{crit} = 1.88 \log (NO_3^-) + 1.18 \qquad \text{Equation 3.2}$$

where $(Cl^-)_{crit}$ and (NO_3^-) are the activity of chloride and nitrate respectively.

Their results were converted to concentration (ppm) using an activity coefficient of 1, and have been plotted in Figure 5.14, curve (b), for purposes of comparison. It can be seen that for the concentration range 0 - 1500 ppm nitrate the current results indicate more effective inhibition of pitting of AISI 431 than Leckie and Uhlig found for the pitting of an 18-8 stainless steel. Calculations show that above a nitrate concentration of about 6300 ppm the results of Leckie and Uhlig predict more effective inhibition of an 18-8 stainless steel than the current results, if extrapolated, predict for AISI 431.

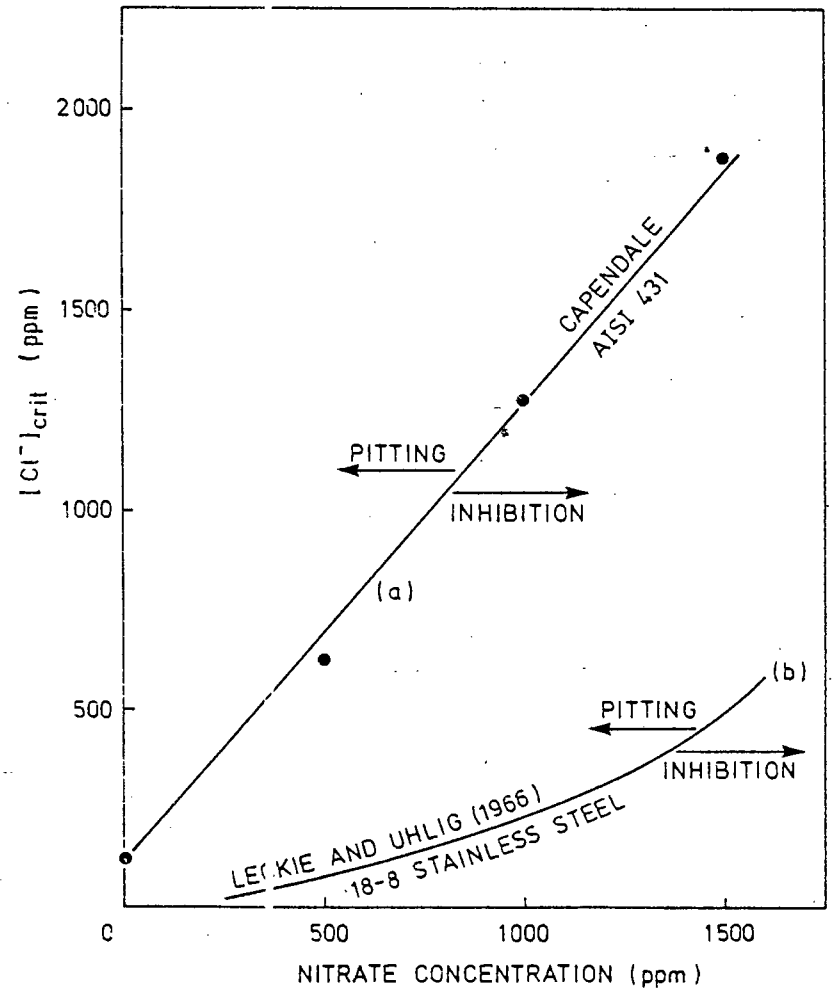

FIGURE 5.14 : $[Cl^-]_{crit}$ plotted as a function of nitrate concentration for AISI 431 compared to Leckie and Uhlig's (1966) results for an 18-8 stainless steel

5.3.2 The Effect of pH on Pitting Inhibition by Nitrates in Chloride Solutions

E_{corr}, E_x and E_p/E_b of AISI 431 were plotted as a function of chloride concentration in solutions containing 500, 1000 and 1500 ppm nitrate at pH 3.8 and 9.4. From these curves, shown in

Appendix D, the $[Cl^-]_{crit}$ was determined at each nitrate concentration and pH.

In Figure 5.15 $[Cl^-]_{crit}$ has been plotted as a function of nitrate concentration for pH 3.8, 6.2 and 9.4. From these curves the following linear relationships were formulated:

pH = 3.8	$[Cl^-]_{crit} = 1.02\ [NO_3^-] + 74$	Equation 5.2
pH = 6.2	$[Cl^-]_{crit} = 1.18\ [NO_3^-] + 95$	Equation 5.1
pH = 9.4	$[Cl^-]_{crit} = 2.32\ [NO_3^-] + 385$	Equation 5.3

It can be seen that nitrates inhibit pitting far more effectively at pH 9.4 than at pH 6.4 and 3.8. As discussed in section 5.2.1, this can be ascribed to the additional inhibitive effect of the OH^- ions at pH 9.4 as well as the tendency of the bulk solution to neutralize the local acidity which exists inside a pit.

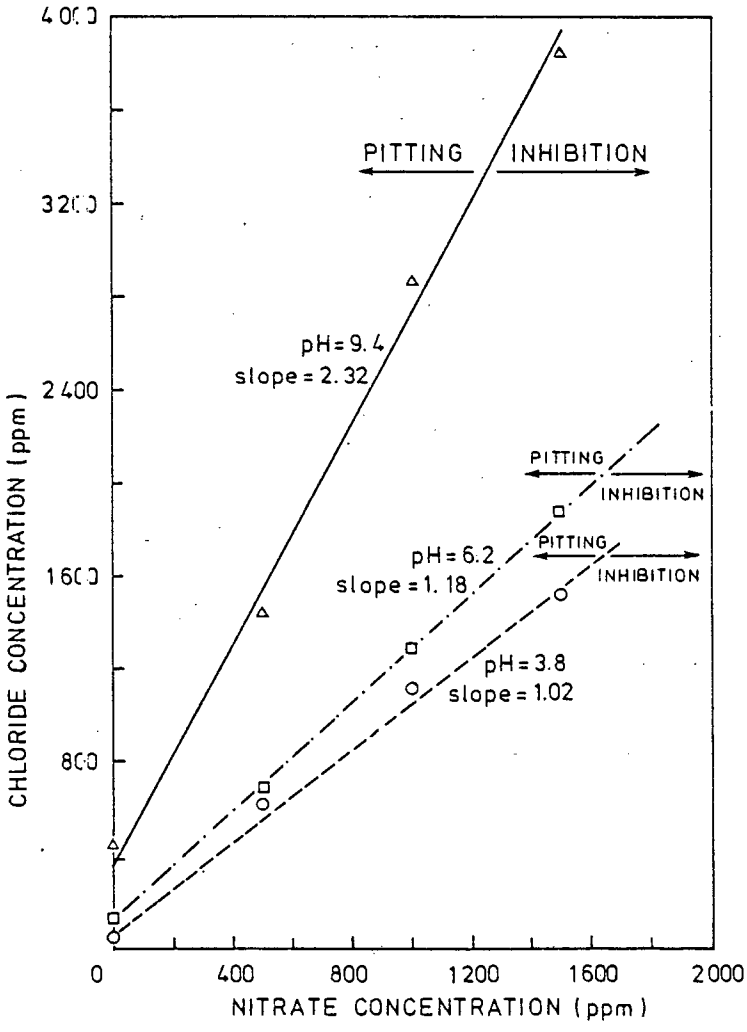

FIGURE 5.15 : $[Cl^-]_{crit}$ as a function of nitrate concentration at pH 3.8, 6.2 and 9.4

The greater inhibitive effect of the nitrates at higher pH is further illustrated in Figure 5.16 where the slopes of the lines determined in Figure 5.15 have been plotted as a function of pH. These slopes are a measure of the chloride to nitrate ratio above which pitting corrosion may occur.

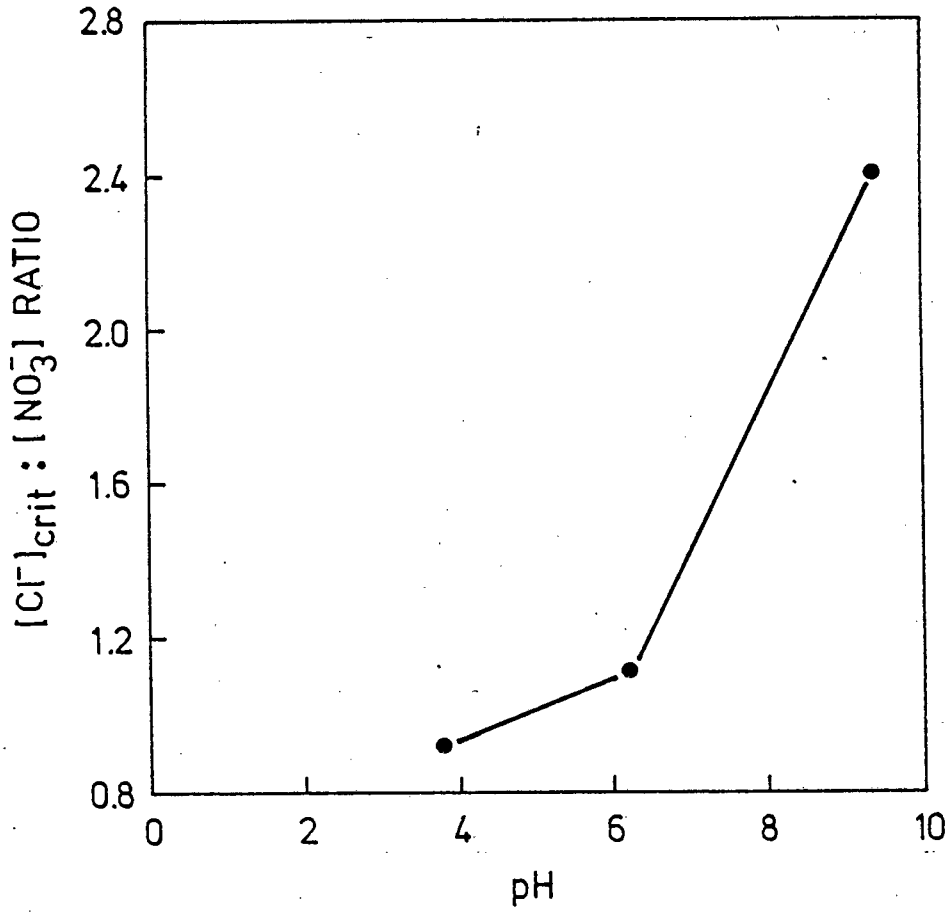

FIGURE 5.16 : $[Cl^-]_{crit}$ to NO_3^- ratio as a function of pH

Figure 5.17 shows the $[Cl^-]_{crit}$ is plotted as a function of pH in solutions without nitrates as well as for solutions containing 1000 ppm nitrate. The superimposed dotted line indicates the $[Cl^-]_{crit}$ values which would be anticipated if the inhibitive effects of pH and nitrates could be simply added together. However at a pH of 9.4 it is evident that the inhibitive effect of nitrates on pitting is greatly enhanced. The shaded area in Figure 5.17 indicates the extent to which the $[Cl^-]_{crit}$ is increased above the value obtained by simply adding the inhibitive effect of nitrates and pH. Clearly there is a synergistic

interaction between NO_3^- and OH^- ions which substantially increases the inhibition of pitting in alkaline solutions which contain nitrate ions.

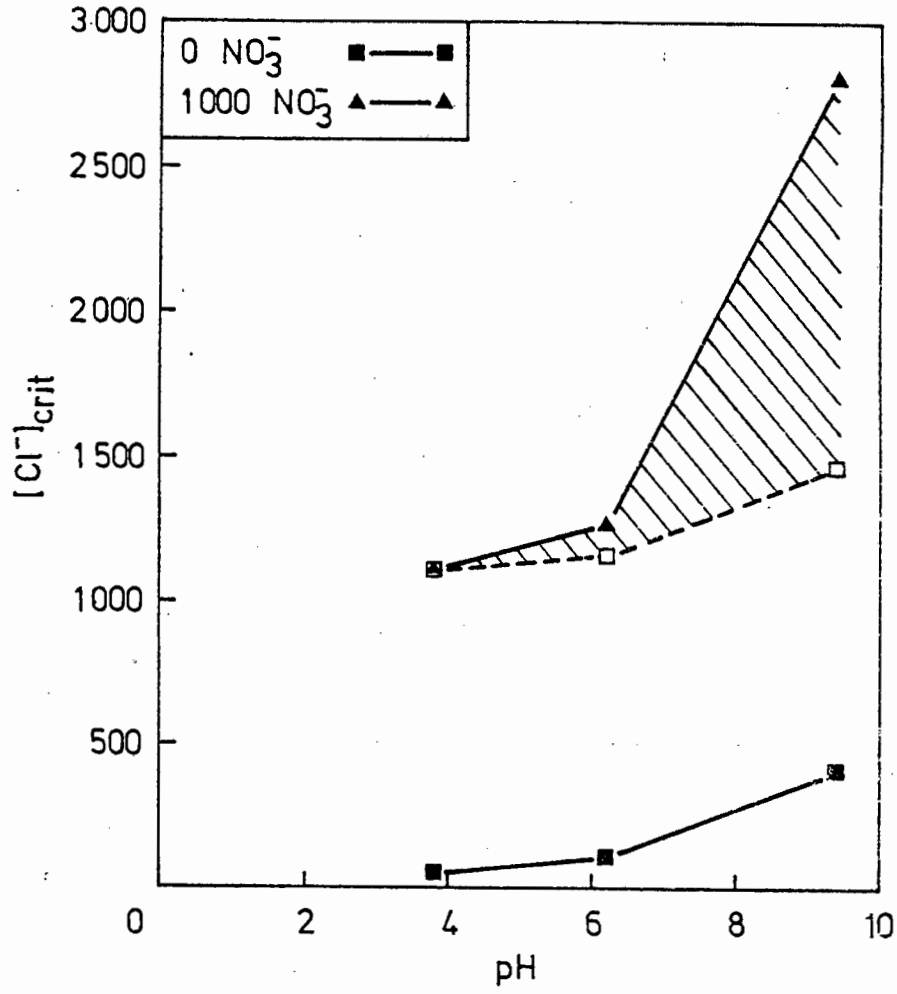

FIGURE 5.17 : The enhanced inhibition by nitrates of pitting at higher pH

5.4 THE EFFECT OF SCAN RATE ON $[Cl^-]_{crit}$

A scan rate of 12 mV/sec was used in a series of tests to determine $[Cl^-]_{crit}$ of AISI 431 at pH 6.2 and nitrate concentration of 500, 1000 and 1500 ppm. In Figure 5.18 $[Cl^-]_{crit}$ determined at the high scan rate has been plotted as a function of nitrate concentration and is compared to the results obtained at the slow scan rate. The slope of the curves is 2.13 and when compared to the slope of 1.18 measured at a scan rate of

0.12 mV/sec it is evident that the high scan rate grossly over-estimates the inhibition of pitting by nitrates. This effect could be due to insufficient being available for the accommodation of an induction time, τ, necessary for pit initiation. I_{pass} and E_p/E_b were also found to be higher at the fast scan rate than at the slow scan rate.

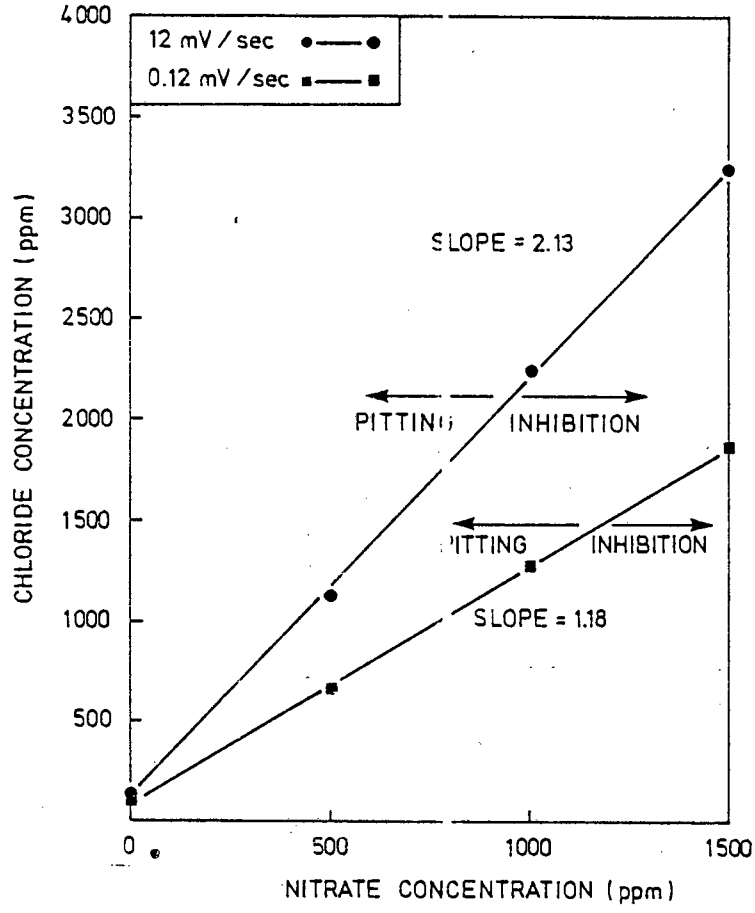

FIGURE 5.18 : $[Cl^-]_{crit}$ plotted as a function of nitrate concentration for fast and slow scan rates.

5.4.1 The Effect of Sulphates on $[Cl^-]_{crit}$ at Fast Scan Rate

Due to the time involved in performing the slow scan rate tests a fast scan rate, 12 mV/sec, was used to determine $[Cl^-]_{crit}$ for AISI 431 in solutions containing 500, 1000 and 2000 ppm sulphate at pH 6.2. By plotting $[Cl^-]_{crit}$ as a function of sulphate concentration in Figure 5.19 the following relationship was derived:

$$[Cl^-]_{crit} = 0.27\ [SO_4^{2-}] + 120 \qquad \text{Equation 5.5}$$

Sulphates thus also inhibit pitting corrosion by increasing $[Cl^-]_{crit}$, but their inhibitive power is substantially weaker than determined for nitrates. Figure 5.19 also shows the results of Leckie and Uhlig (1966) which were calculated from equation 3.3 using an activity coefficient of 1. Their results indicate more effective pitting inhibition by sulphates for an 18-8 stainless steel than was determined for AISI 431 in this study. They also, however, found that sulphates are less effective than nitrates in the inhibition of pitting corrosion.

To confirm the inhibition of pitting of AISI 431 by sulphates the $[Cl^-]_{crit}$ was determined for 1000 ppm sulphate solutions using the slow scan rate. The result has been plotted in Figure 5.19 and it can be seen that the difference in the results between the fast and slow scan rate tests is not as great as was found for the nitrate solutions.

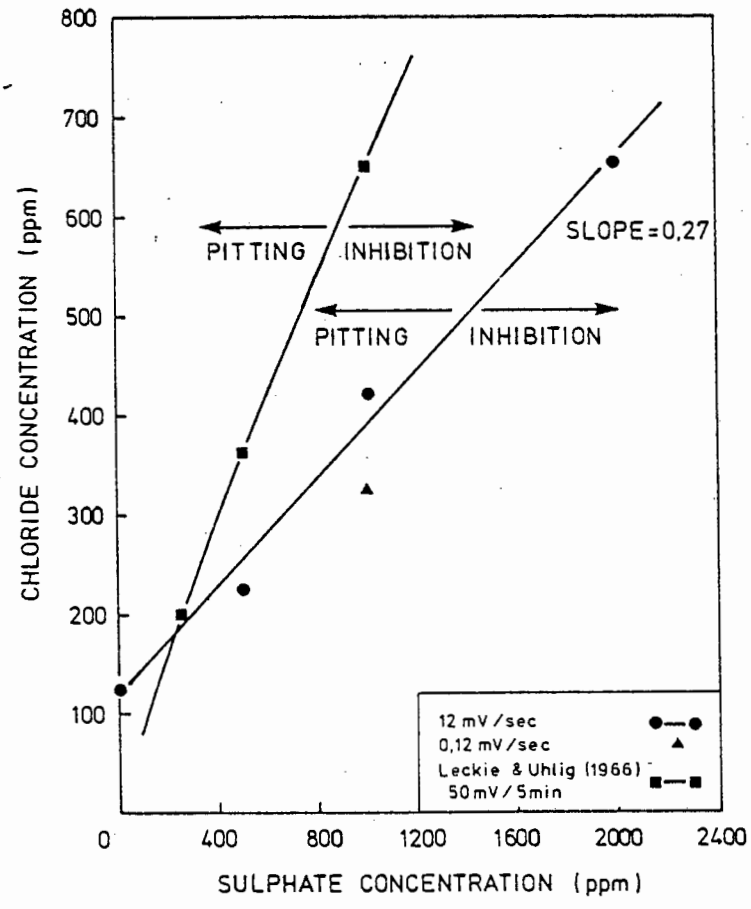

FIGURE 5.19 : $[Cl^-]_{crit}$ plotted as a function of sulphate concentration

5.5 THE SIGNIFICANCE OF THE RESULTS AND THEIR APPLICATION TO THE REAL MINE WATER SITUATION

The high cost of stainless steels is justified by their low rates of corrosion in the passive state. When considering the use of stainless steels it is therefore essential to ensure that the material will indeed be in the passive state when exposed to its service environment.

The experimental E-pH diagram, shown in Figure 5.3, which was constructed for AISI 431, underlines the importance of careful control of the pH of mine water. To ensure that this steel remains in the passive state it would be necessary to maintain a pH greater than 4 in the mine water. Neutralization of mine waters using $Ca(OH)_2$ has been successfully practised for many years and hence should not present a problem.

In many cases the minimal contribution which pitting corrosion makes to the overall corrosion rate is entirely acceptable. There are, however instances where, due to its insidious nature, pitting corrosion is not easily detected and this could lead to the unexpected failure of equipment. Pitting corrosion of pipes and cylinders in hydraulic systems could, for example, lead to eventual perforation and loss of pressure The presence of pits on components subjected to stress often facilitates the initiation of environment-sensistive cracking such as corrosion fatigue and stress corrosion cracking. The preferential initiation of such cracking at pits has been reported to be due to both the stress concentration associated with the pit geometry as well as the localized change in composition and potential which exists inside a pit (Parkins (1985)).

To avoid the occurrence of pitting corrosion E_{corr} should be at a potential lower than both E_p and E_x. If E_{corr} is greater than E_p, pits will be able to initiate and propagate, while if E_{corr} is less than E_p but greater than E_x, any existing pit or similar defect on a metal surface will be able to propagate (Pourbaix, 1970). In Figure 5.7 it can be seen that even at a chloride concentration of 10000 ppm, which exceeds the highest chloride concentrations reported in the survey of mine waters, pitting corrosion would not be predicted on AISI 431 as E_{corr} is less than E_x.

In some situations such as crevices or areas where excessive evaporation occurs a localized accumulation of ions takes place. Consider a water in which chloride and nitrate ions are present and the chloride concentration is greater than the $[Cl^-]_{crit}$ for that specific nitrate concentration and pH. As the chloride and nitrate ions accumulate proportionally in a build-up situation the chloride ion concentration will always be greater than the $[Cl^-]_{crit}$ and if sufficient build-up occurs a situation will eventually be reached where pitting corrosion may occur. Now, in the case where the chloride concentration in the water is less than the $[Cl^-]_{crit}$, the same argument may be applied and the chloride concentration will never exceed the $[Cl^-]_{crit}$ and hence a situation where pitting corrosion may occur will not be reached. This reasoning depends on the following three assumptions:

i) The build-up of ions occurs in the same proportion as they are present in the bulk solution.
ii) No significant change in pH is caused by the build-up of ions.
iii) The linear relationships which were derived between $[Cl^-]_{crit}$ and nitrate concentrations may be extrapolated to higher nitrate concentrations.

The value of E_x was always found to be about 0.15 V greater than E_{corr} in the tests conducted in synthetic mine waters and hence pitting corrosion was never predicted. In real mine waters however, E_{corr} can be affected by factors such as microbial activity, the presence of strongly oxidising metallic ions Fe^{3+} and Cu^{2+}, bimetallic contact, temperature and the flow velocity of the solution. Figure 5.20 shows a plot of the E_{corr} of an AISI 431 specimen immersed in a sample of water obtained from mine J. The composition of the water is given in Table 5.3.

TABLE 5.3 : The composition of mine J water

PROPERTY	LEVEL
pH	4.76
Conductivity (S/cm)	20180
T.D.S. (ppm)	5616
Suspended Solids (ppm)	40
Total Hardness (ppm)	3700
Calcium (ppm)	2100
Magnesium (ppm)	1600
Chlorides (ppm)	3704
Sulphates (ppm)	3354
Nitrates	3035

As can be seen in Figure 5.20 E_{corr} increases with time and reaches a constant value of about -0.01 V vs. S.C.E. after approximately 30 days. The values of E_x determined in the synthetic mine waters generally were in the region of 0.0 V vs. S.C.E.. Such an increase in the E_{corr} of a steel in a real mine water which has a chloride concentration greater than the $[Cl^-]_{crit}$ could therefore result in E_{corr} reaching a value greater than E_x thereby making the propagation of pits possible. If, however, the chloride concentration of the mine water was less than the $[Cl^-]_{crit}$ for that solution, pitting corrosion would be completely inhibited and an increase in E_{corr} would not be dangerous.

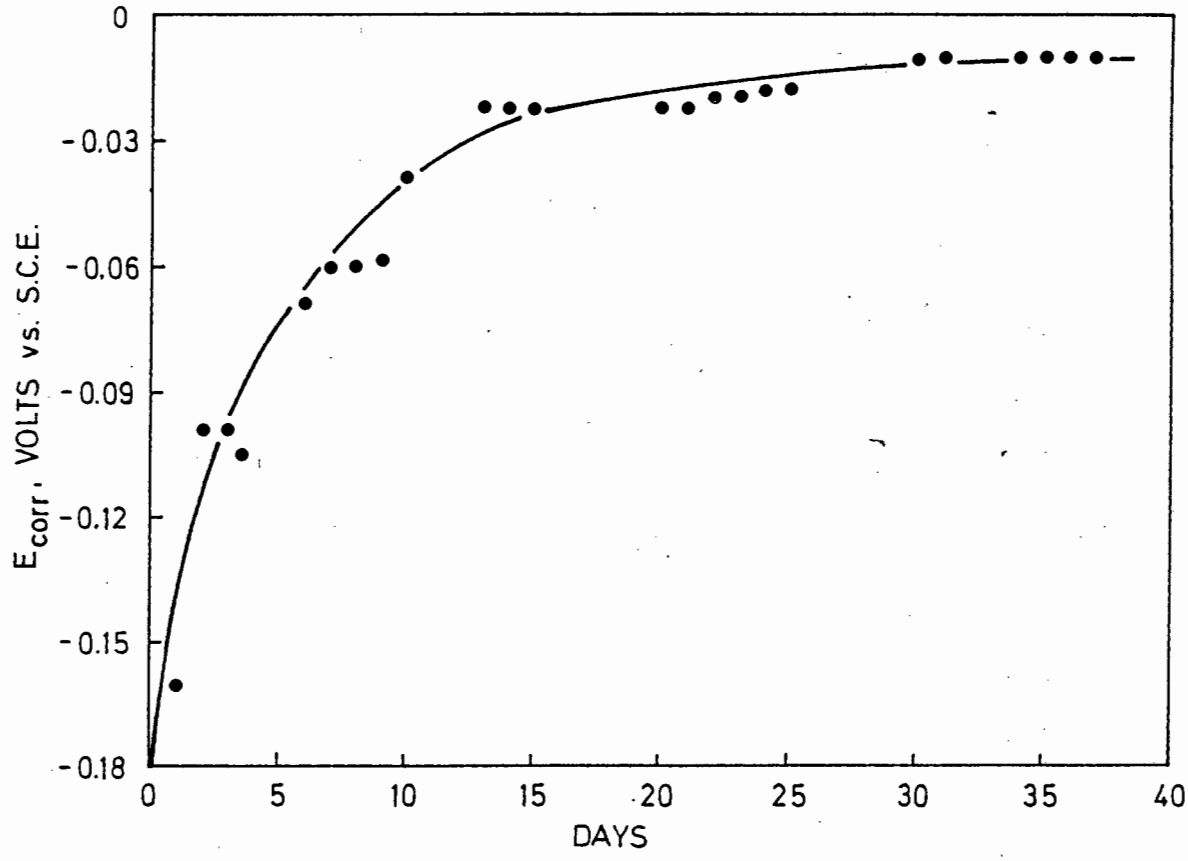

FIGURE 5.20 : E_{corr} of AISI 431 as a function of time in mine J water (Experimental work performed by the Chamber of Mines Research Organisation)

To further demonstrate this effect a potentiodynamic polarization test of AISI 431 was performed in a solution containing 1000 ppm NO_3^-, 2000 ppm Cl^-, 3 ppm Cu^{2+} and 1.7 ppm Fe^{3+} at a pH of 6.2. The E_{corr} measured in this test has been superimposed on the potential versus chloride concentration diagram for 1000 ppm NO_3^-, pH 6.2 solutions as shown in Figure 5.21. Reduction of Cu^{2+} and Fe^{3+} has provided an alternative

cathodic reaction and the resultant change in the cathodic kinetics has increased E_{corr} to a value greater than E_x making the propagation of pits possible. Another test was carried out with 100 ppm Cu^{2+} in solution and the E_{corr} was increased to a potential of 0.125 V vs. S.C.E. as indicated in Figure 5.21. Hence, while the presence of oxygen is desirable insofar as it stabilized the passive state of the steel, the effect of stronger oxidising agents is deleterious in that they may be the cause of pitting corrosion.

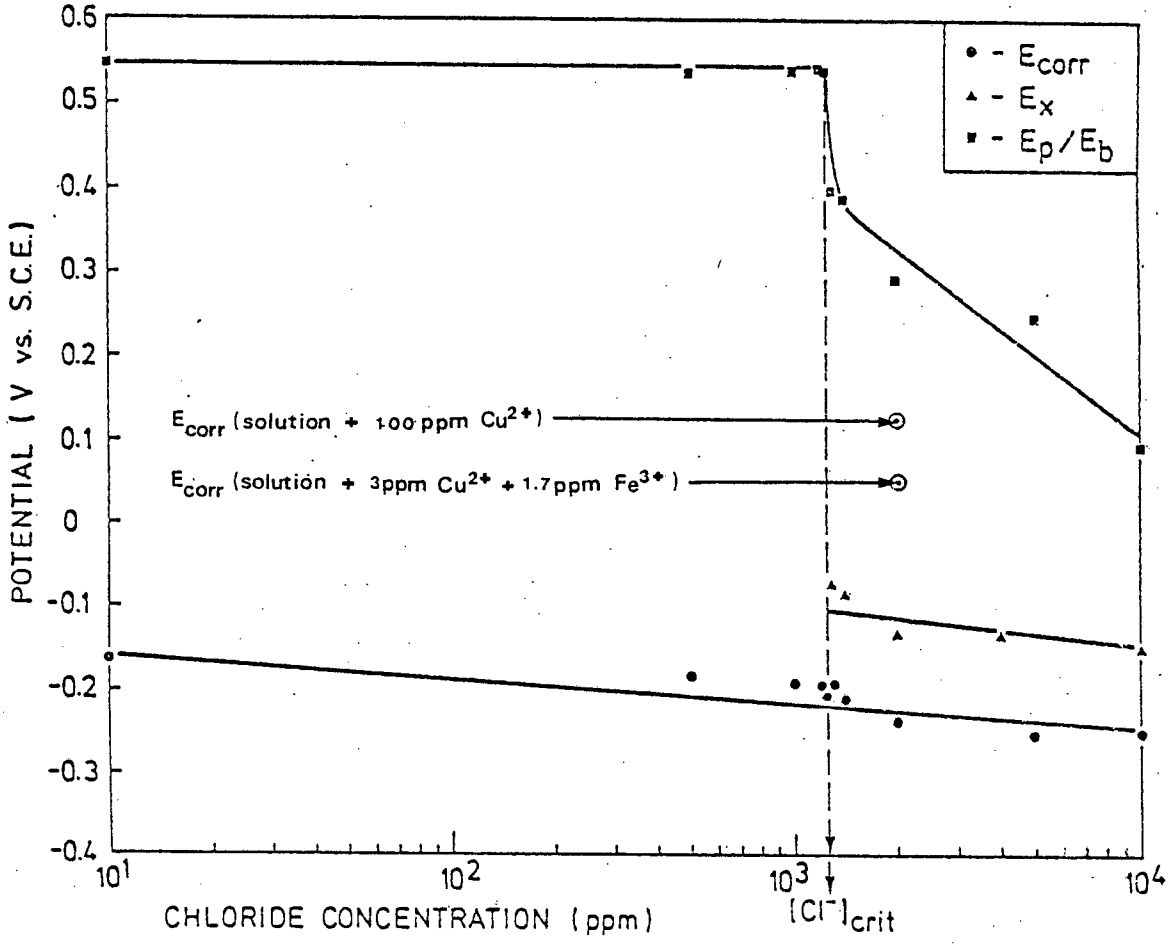

FIGURE 5.21 : The effect of oxidisers Fe^{3+} and Cu^{2+} on the E_{corr} of AISI 431 in a solution containing 1000 ppm nitrate and 2000 ppm chloride, pH = 6.2

The relatively simple compositions of the synthetic solutions in which the potentiodynamic tests were carried out raised the question of whether the relationships which were determined between $[Cl^-]_{crit}$ and nitrate concentration could be applied to the real mine water situation. The

only mine water available for potentiodynamic testing was acquired from mine J and contained 3704 ppm Cl^-, 3354 ppm SO_4^{2-} and 3035 ppm NO_3^- and had a pH of 4.76 (further details of the composition are given in Table 5.3). The potentiodynamic test performed in this mine water on AISI 431 did not result in the occurrence of pitting corrosion. A synthetic solution of mine J water was made up in the laboratory and the potentiodynamic test performed on AISI 431 in this solution failed to indicate the occurrence of pitting corrosion. A further test in a solution from which the sulphate ions were excluded also did not produce pitting corrosion. By applying the relationship (equation 5.1) determined between the $[Cl^-]_{crit}$ and the nitrate concentration at a pH of 6.2 to the compositon of the mine J water a $[Cl^-]_{crit}$ of 3676 ppm may be calculated. The chloride concentration in the mine J water (3704 ppm) is very close to the calculated $[Cl^-]_{crit}$ and probably represents a borderline case in which there is only just sufficient nitrate to inhibit pitting corrosion.

These tests showed that the inhibition of pitting corrosion of AISI 431 is also apparent in real mine water. This was, however, only demonstrated for an isolated case and further tests in real mine waters are required to confirm the result. Ideally it would be necessary to perform tests in samples of real mine water which have a chloride concentration greater than the $[Cl^-]_{crit}$, as well as in samples which have a chloride concentration less than $[Cl^-]_{crit}$.

This discussion has highlighted the advantages of maintaining the chloride concentration of a solution at a level lower than the $[Cl^-]_{crit}$ of that specific solution. The potentiodynamic polarization technique provides a rapid means of determining the $[Cl^-]_{crit}$ of a specific water composition/alloy combination and could provide useful input to water treatment engineers in determining the concentration levels to which mine water needs to be treated. Unfortunately the seeded reverse osmosis technique removes all ions in equal proportions and hence a mine water with a chloride concentration greater than $[Cl^-]_{crit}$ prior to treatment will be in the same position after treatment. Consideration should thus be given to either the possibility of selective removal of chloride ions or the more feasible solution of adding inhibitive ions (i.e. nitrates and sulphates) thereby increasing the $[Cl^-]_{crit}$. Either of these options could then be used in conjunction with the treatment of the water by

seeded reverse osmosis. The variation in a mine water during a cycle through a mine and the fact that potentiodynamic testing is a non-equilibrium situation would require that stringent safety factors be imposed on the values of $[Cl^-]_{crit}$ determined by this technique.

Since commercially produced steels will be used in the mines it is likely that pits will initiate at inclusion sites as suggested by Sedriks (1983). Furthermore it has been shown by Pessall and Liu (1971) and Burstein and Davis (1980) that scratches provide preferential pit initiation sites. In the mines the abrasive conditions provide an abundance of scratches for pit initiation. For these reasons it is important to create conditions in which the propagation of pits is completely inhibited. This study has shown that for the inhibition of pitting corrosion careful control of the parameters associated with the solution is as important as the consideration given to the choice of the material. Figure 5.22 summarises those factors which have been found to be important with respect to pitting corrosion. The most desirable situation is indicated by the area on the left of Figure 5.22 where complete inhibition of pitting occurs due to the chloride concentration of the solution being below the critical chloride concentration. This is achieved by maintaining the correct ratio of inhibitor ions (NO_3^- and SO_4^{2-}) to chloride ions at a specific pH. The area on the right of Figure 5.22 represents the situation where the chloride concentration of the solution is greater than the critical chloride concentration and in this case the value of E_{corr} in relation to the value of E_x is important. Those factors which may cause E_{corr} to increase to a value greater than E_x, thereby making the propagation of pits possible, are indicated.

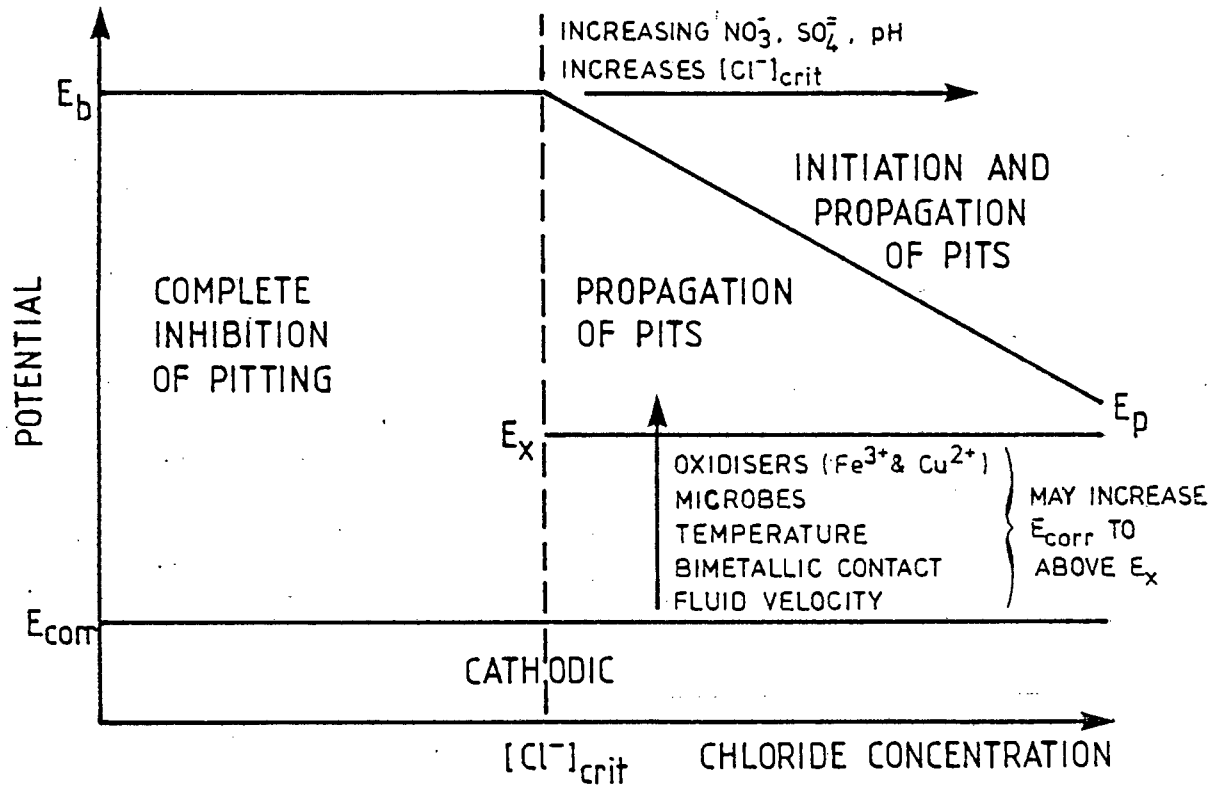

FIGURE 5.22 : A diagram summarising the factors which affect the possibility of pitting corrosion of a material in mine water solutions

The experiments conducted were not designed to establish the mechanisms of pitting and pitting inhibition. In the past a number of different mechanisms have been proposed (Kolotyrkin, (1961); Leckie and Uhlig, (1966); Hoar, (1967); Galvele, (1976)). In the author's opinion the most acceptable mechanisms are those which suggest that pitting and inhibition of pitting occurs due to a process of competitive adsorption between the various ions involved (Kolotyrkin, (1961); Leckie and Uhlig, (1966); Hoar, (1967)). To either confirm or disprove the validity of these mechanisms sophisticated techniques such as Auger electron spectroscopy would have to be used for studying the changes in the passive film which occur due to these processes. Such research would provide a greater degree of understanding of the mechanisms involved and could possibly reveal further means of manipulating the variables to the advantage of the mining industry.

CHAPTER 6

A SUMMARY OF FINDINGS AND CONCLUSIONS

The objectives of this study were:

i) To establish an electrochemical technique for determining the influence of the composition of synthetic mine water on the corrosion behaviour of AISI 431 stainless steel.

ii) To determine what effect those ions most commonly encountered in mine waters have on the corrosion behaviour of AISI 431.

The potentiodynamic polarization technique using a scan rate of 0.12 mV/second was found to be suitable for evaluating the corrosion behaviour of AISI 431 in synthetic mine water solutions. The use of this technique has resulted in the following findings:

1. An experimental E-pH diagram was constructed for AISI 431 in deaerated solutions. In solutions with a pH greater than or equal to 3.8, AISI 431 was found to be in the passive state. In solutions with a pH less than 3.8 AISI 431 was found to corrode in the active state. The E-pH diagram of AISI 431 will serve as a standard when evaluating other alloys.

2. Chloride ions were found to be responsible for the breakdown of passivity due to pitting corrosion during potentiodynamic polarization tests. Pitting corrosion during potentiodynamic scanning only occurred above a critical chloride concentration, $[Cl^-]_{crit}$.

3. The effect of pH, nitrate concentration and sulphate concentration on the $[Cl^-]_{crit}$ of AISI 431 was studied and it was found that:

   i) $[Cl^-]_{crit}$ increased with increasing pH, particularly when the pH was increased from 6.2 to 9.4. This is attributed to the inhibitive effect which OH^- ions have on pitting corrosion.

ii) Increasing nitrate concentration resulted in an increase in the $[Cl^-]_{crit}$ of AISI 431 in solutions of a particular pH. The inhibitive effect of nitrate ions on pitting corrosion was greatly enhanced in solutions with a pH of 9.4. Nitrate and hydroxyl ions are synergistic in their action in inhibiting pitting corrosion.

iii) Increasing the rate of potentiodynamic scanning from 0.12 mV/second to 12 mV/second resulted in an overestimation of the effectiveness of pitting inhibition by nitrate ions. The fast scan rate is therefore not recommended for the determination of $[Cl^-]_{crit}$.

iv) A series of tests using a scan rate of 12 mV/second showed that increasing the concentration of sulphate ions also increases the $[Cl^-]_{crit}$ of AISI 431. Even though the tests were conducted at a fast scan rate, sulphate ions were found to be less effective than nitrate ions in the inhibition of pitting corrosion.

4. Solutions containing up to 10 000 ppm chloride ions were investigated by the potentiodynamic polarization technique and in no case was the corrosion potential, E_{corr}, found to be greater than either the pitting potential, E_p, or the protection potential, E_x. This indicated that neither the initiation nor the propagation of pits could occur in synthetic mine water solutions containing chloride, sulphate and nitrate ions.

5. Immersion tests conducted in actual mine water showed that the corrosion potential of AISI 431 increased with time before attaining a constant potential after 30 days. This increase, which is thought to be due to microbial activity, is sufficient to ennoble the corrosion potenial to a value greater than the protection potential. Microbial activity can therefore be an important factor in the occurrence of pitting corrosion.

6. The presence of the strongly oxidising metallic ions, Fe^{3+} and Cu^{2+}, has been reported in mine waters. Potentiodynamic polarization tests performed in synthetic solutions containing Fe^{3+} and Cu^{2+} showed that these ions ennoble the corrosion potential of AISI 431 to potentials greater than its protection potential. Therefore, the presence of Fe^{3+} and Cu^{2+} can increase the probability of pitting corrosion of a stainless steel.

7. In real mine waters it is possible that either microbial activity or the presence of Fe^{3+} and Cu^{2+} could result in the corrosion potential being greater than the protection potential. To avoid the possibility of pitting corrosion the chloride concentration of the water should be kept below the critical chloride concentration, $[Cl^-]_{crit}$.

8. The water treatment processes used by the mines remove all ions in equal proportions. It is therefore important that the attention of water treatment engineers be drawn to the fact that water having a chloride concentration greater than $[Cl^-]_{crit}$ prior to treatment will still have a chloride concentration greater than $[Cl^-]_{crit}$ after treatment. Such water treatment will thus not necessarily decrease the susceptibility of a steel to pitting corrosion.

9. The relationships derived between $[Cl^-]_{crit}$ and the nitrate and sulphate ion concentrations successfully predicted the inhibition of pitting of AISI 431 during a potentiodynamic polarization test conducted in real mine water.

10. Mine waters are known to contain a complex variety of ions. This study has shown that is is important to ascertain the effect of individual ions before considering what effects interactions between the ions have on the corrosion behaviour of a steel. The potentiodynamic polarization technique provides a rapid means of evaluating the various factors contributing to the corrosivity of mine water.

CHAPTER 7

RECOMMENDATIONS FOR FUTURE WORK

This project must be seen as a contribution to an ongoing research programme. It is important that the results of this study and future work may be translated into practical terms by mining engineers. There is, however, also the need for fundamental research which will provide a basic understanding of the mechanisms involved in the processes under investigation.

Besides providing important information relevant to the mining industry this study has raised a number of questions of academic interest regarding the mechanisms involved in pitting corrosion and the inhibition of pitting corrosion.

In order to understand the mechanisms further research on the subject is essential. Time/current relationships could be performed to determine the existence and duration of pit initiation times in solutions where pitting inhibition has been predicted. It would also be of interest to establish whether nitrate and sulphate ions are able to inhibit the propagation of actively corroding pits. The determination of E_x and its position relative to E_{corr} has been suggested to be of great importance, and attention should thus be given to the exact nature and validity of this characteristic potential of pit propagation.

The influence of corrosion in abrasion-corrosion, corrosion fatigue and stress corrosion cracking is important as these processes involve mechanical breakdown of the passive film to expose virgin metal surfaces to the environment. The scratch techniques used by Pessall and Liu (1971) and Burstein and Davies (1980) would provide valuable input in the study of these mechanically accelerated corrosion processes.

Fundamental research into passive films and pitted surface using sophisticated techniques such as Auger electron spectroscopy would have to be undertaken to determine the exact nature and sequence of those events which occur on a passive surface during pitting corrosion and the inhibition of pitting corrosion.

To provide additional information to mining engineers, future research should be directed in the area of the effect of solution composition as well as in the field of alloy development.

A simple means of monitoring mine water compositions should be investigated in order that the corrosion behaviour of a "stainless" type steel may be predicted in situ. Higginson and White (1983) reported that the conductance and total dissolved solids (T.D.S.) of mine water are related by the following equation:

$$\text{T.D.S. (ppm)} = 0.76 \times \text{conductance } (\mu S)$$

If it is possible to relate the $[Cl^-]_{crit}$ to the total dissolved solids then by measuring the conductance and chloride concentration of the water it could be possible to establish whether the chloride concentration was greater than or less than the $[Cl^-]_{crit}$ for a specific alloy. The measurement of conductance is simple and reliable while chloride concentration could be determined by using a selective ion electrode.

In order to achieve the above and be able to predict pitting in real mine water the inhibitive effect of sulphate ions will have to be further investigated by the potentiodynamic polarization technique. The effect of sulphate ion concentration on the $[Cl^-]_{crit}$ should be determined using the slow scan rate in solutions by various pH. It should also be established whether the inhibitive effect of sulphate and nitrate ions may be added when these ions are together in solution. To determine the validity of these results potentiodynamic polarization tests should be conducted in real mine waters where the chloride concentration is less than $[Cl^-]_{crit}$ as well as in mine waters where the chloride concentration is greater than $[Cl^-]_{crit}$.

The experimental alloys which are developed should be tested using the potentiodynamic polarization technique and the results compared to those of AISI 431.

A recently developed 8 per cent chromium alloy (designated Alloy A) was subjected to exposure tests in a corrosion loop (described by Capendale, (1983)) containing a synthetic solution of mine F water. Alloy A was found to undergo severe crevice corrosion which propagated in the rolling direction of

the steel as shown in Figure 7.1. This result clearly indicates that the corrosion behaviour of such an experimental alloy should be investigated before it can be used effectively in the mines. AISI 431 was subjected to the same corrosion loop test and did not undergo any corrosion.

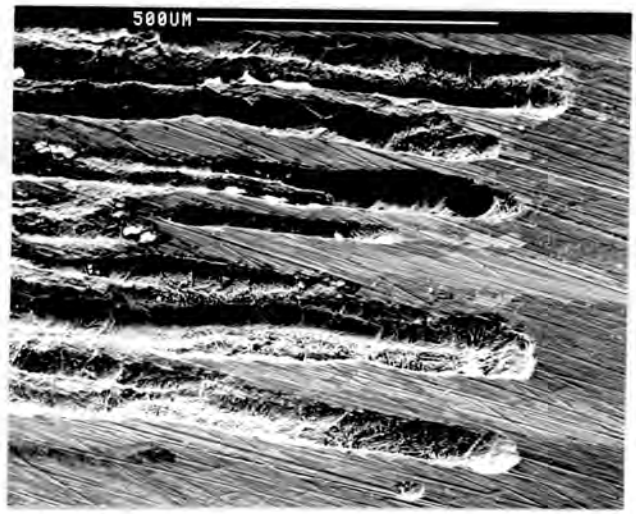

FIGURE 7.1 : Crevice corrosion of Alloy A, 8 per cent chromium alloy, the rolling direction is indicated by the arrow

REFERENCES

ASTM (1980)[1], "Conducting Cyclic Potentiodynamic Polarization Measurements for Localized Corrosion", Annual Book of Standards, Part 10, G61-78, p. 1033.

ASTM (1980)[2], "Standard Reference Method for Potentiostatic and Potentiodynamic Anodic Polarization Measurements", Annual Book of Standards, Part 10, G5-78, p. 816.

ATRENS A. (1983), "Environmental Conditions Leading to Pitting/Crevice Corrosion of a Typical 12% Chromium Stainless Steel at 80°C", Corrosion, 39, p. 483.

AZZERI N., MANCIA F., TAMBA A. (1982), "Electrochemical Prediction of Corrosion Behaviour of Stainless Steels in Chloride-Containing Water", Corrosion Science, 22, p. 675.

BAGHDASARIAN A., RAVITZ S.F. (1975), "Corrosion Resistance of Trip Steels", Corrosion, 31, p. 182.

BARBOSA M., SCULLY J.C. (1982), "The Role of Repassivation Kinetics in the Measurement of the Pitting Potential of AISI 304 Stainless Steel by the Scratch Method", Corrosion Science, 22, p. 1025.

BARKER K.C. (1986), "The Development of Abrasive-Corrosive Wear Resistance of Steels by Microstructural Control", PhD thesis to be submitted.

BOGGARTS W., VAN HAUTE A., et al (1981), "Influence of Cl^-, HCO_3^- and SO_4^{2-} on the Corrosion of Fe-Cr-Ni Alloys in Hot Water Systems", Proc. 8th Int. Congress on Metallic Corrosion, Dechema, Fed. Rep. of Germany, 2, p. 1887.

BOND A.P., LIZLOVS E.A. (1968), "Anodic Polarization of Austenitic Stainless Steels in Chloride Media", J. Electrochemical Society, 115, p. 1130.

BRENNERT S. (1937), "Method for Testing the Resistance of Stainless Steel to Local Corrosive Attack", J. Iron and Steel Institute, 35, p. 101.

BROLI A., HOLTAN H., MIDJO M. (1973), "Use of Potentiokinetic and Potentiostatic Methods for the Determination of Characteristic Potentials for Pitting Corrosion of an Fe-Cr Alloy", Br. Corrs. J., 8, p. 1025.

BURSTEIN G.T., DAVIES D.H. (1980), "The Effect of Anions on the Behaviour of Scratched Iron Electrodes in Aqueous Solutions", Corrosion Science, 20, p. 1143.

CAPENDALE A.E. (1983), "The Corrosion of Stainless Steels in Synthetic Mine Waters", Honours Thesis, U.C.T.

CHANCE R.L., SCHREIBER T.P., FRANCE W.D. Jr. (1975), "Anomalous Effects of Temperature on the Polarization Characteristics of Type 409 Stainless Steel", Corrosion, 31, p. 296.

CHEN W.Y.C., STEPHENS J.R. (1979), "Anodic Polarization Behaviour of Austenitic Stainless Steel Alloys with Lower Chromium Content", Corrosion, 35, p. 443.

DAYAL R.K., PARVATHAVARTHINI N., GNANAMOORTHY J.B. (1980), "A Study of Various Critical Pitting Potentials for Type 316 Stainless Steel in Sulfuric Acid Containing Chloride Ions", Corrosion, 36, p. 433.

EDELNAU C. (1958), "A Potentiostat Technique for Studying the Acid Resistance of Alloy Steels", J. Iron and Steel Institute, 56, p. 122.

DELTOMBE E., DE ZOUBOV N., POURBAIX M. (1966), Atlas of Electrochemical Equilibria, Pourbaix M., ed., Brussels, Cebelcor, pp. 97-105.

EL-BASIOUNY M.S., HARUYAMA S. (1976), "The Polarization Behaviour of Fe-Cr Alloys in Acidic Sulphate Solutions in the Active Region", Corrosion Science, 16, p. 529.

FELLONI L., FRATESI R., et al (1985), "Pitting and Crevice Corrosion Potentials of Solar Panel Stainless Steels in Seawater 0.6 M NaCl", Corrosion, 41, p. 169.

FONTANA M.G., GREENE N.D. (1967), Corrosion Engineering, New York, McGraw-Hill, pp. 297-346.

FRANCE W.D. Jr. (1967), "A Specimen Holder for Precise Electrochemical Measurements on Metal Sheets and Foils", J. Electrochemical Society, 114, p. 818.

FRANCE W.D. Jr., GREENE N.D. (1970), "Comparison of Chemically and Electrolytically Induced Pitting Corrosion", Corrosion, 26, p. 1.

FRATESI R. (1985), "Statistical Estimate of the Pitting Potential of AISI 316 L Stainless Steel in 3.5% NaCl Measured by Means of Two Electrochemical Methods", Corrosion, 41, p. 114.

GALVELE J.R. (1976), "Transport Processes and the Mechanism of Pitting in Metals", J. Electrochemical Society, 123, p. 464.

GOODING C.H. (1985), "Reverse Osmosis and Ultrafiltration Solve Separation Problems", Chemical Engineering, Jan. 7, p. 56.

GREENE N.D. (1962), "Predicting Behaviour of Corrosion Resistant Alloys by Potentiostatic Polarization Methods", Corrosion, 18, p. 136.

HERBSLEB G. (1965), "Die Inhibition der Chloridkorrosion (Lochfraß) auf Chemisch Bestandigen Stählen durch Nitrat-, Sulfate- und Chromationen und die Bestimmungstmethoden des Lochfraßpotentials", Werkstoffe und Korrosion, 16, p. 929.

HARRIES R.C. (1984), Private Communication.

HIGGINSON A. (1984), "The Effect of Physical and Chemical Factors on the Corrosivity of a Synthetic Mine Water", MINTEK Report No. M140.

HIGGINSON A., WHITE R.T. (1983), "A Preliminary Survey of the Corrosivity of Water in Gold Mines", MINTEK Report No. M65.

HOAR T.P. (1967), "The Production and Breakdown of the Passivity of Metals", Corrosion Science, 7, p. 341.

HOSPADARUK V., PETROCELLI J.V. (1966), "The Pitting Potential of Stainless Steels in Chloride Media", J. Electrochemical Society, 113, p. 878.

JANIK-CZACHOR M., SZUMMER A., SZKLARSKA-SMIALOWSKA Z. (1975), "Electron Microprobe Investigation of Processes Leading to the Nucleation of Pits on Iron", Corrosion Science, 15, p. 775.

JANIK-CZACHOR M., WOOD G.C., THOMPSON G.E. (1980), "Assessment of the Processes Leading to Pit Nucleation", Br. Corros. J., 15, p. 154.

JONES D.A. (1982), Corrosion Processes, Parkins R.N., ed., New York, Applied Science Publishers Ltd., pp. 161-207.

KOLOTYRKIN J.M. (1961), "Effects of Anions on the Dissolution Kinetics of Metals", J. Electrochemical Society, 108, p. 209.

KOLOTYRKIN J.M. (1963), "Pitting Corrosion of Metals", Corrosion, 19, p. 261.

LECKIE H.P. (1970), "A Contribution to the Applicability of Pitting Potentials", J. Electrochemical Society, 117, p. 1152.

LECKIE H.P., UHLIG H.H. (1966), "Environmental Factors Affecting the Critical Potential for Pitting in 18-8 Stainless Steel", J. Electrochemical Society, 113, p. 1262.

LIZLOVS E.A., BOND A.P. (1975), "An Evaluation of Some Electrochemical Techniques for the Determination of Pitting Potentials of Stainless Steel", Corrosion, 31, p. 219.

LUNARSKA E., SZKLARSKA-SMIALOWSKA Z., JANIK-CZACHOR M. (1975), "Susceptibility of Cr-Ni-Mn Stainless Steels to Pitting in Chloride Solutions", Corrosion, 31, p. 231.

MAN H.C., GABE D.R. (1981), "Pitting Tendency of Austenitic Stainless Steels in Various Natural Waters - A Potentiodynamic Technique", Proc. 8 Int. Congress on Metallic Corrosion, Dechma, Fed. Rep. of Germany, 1, p. 163.

MAN H.C., GABE D.R. (1981), "The Determination of Pitting Potentials", Corrosion Science, 21, p. 323.

MANAGER MAB (1983), Private Communication, Manager Engineering Materials Branch, Chamber of Mines Research Organisation.

MANKOWSKI J., SZKLARSKA-SMIALOWSKA Z. (1975), "Studies on Accumuation of Chloride Ions in Pits During Anodic Polarization", Corrosion Science, 15, p. 493.

MANNING P.E., DUQUETTE D.J., SAVAGE W.F. (1979), "The Effect of Test Method and Surface Condition on Pitting Potential of Single and Duplex Phase 304 L Stainless Steel", Corrosion, 35, p. 151.

MAZZA B., PEDEFERRI P., et al (1976), "Relationship between the Electrochemical and Corrosion Behaviour and the Structure of Stainless Steels Subjected to Cold Plastic Deformation", J. Electrochemical Society, 123, p. 1157.

NOËL R.E.J., ALLEN C., BALL A. (1984), "The Development and Use of In-situ and Laboratory Tests as a Guide to the Selection of Materials for the Gold Mining Industry", Proc. Int. Conference on Tribology in Mineral Extraction, Nottingham, England, p. 23.

PARKINS R.N. (1985), "Significance of Pits, Crevices and Cracks in Environment-sensitive Crack Growth", Materials Science and Technology, 1, p. 480.

PESSALL N., LIU C. (1971), "Determination of Critical Pitting Potentials of Stainless Steels in Aqueous Chloride Environments", Electrochimica Acta, 16, p. 1987.

POURBAIX M. (1973), "Lectures on Electrochemical Corrosion", Brussels, Cebebelcor.

POURBAIX M. (1966), Atlas of Electrochemical Equilibria, Pourbaix M., ed., Brussels, Cebelcor, pp. 70-83.

POURBAIX M. (1970), "Significance of Protection Potential in Pitting and Intergranular Corrosion", Corrosion, 26, p. 431.

POURBAIX M., DE ZOUBOV N. (1966)[1], Atlas of Electrochemical Equilibria, Pourbaix M., ed., Brussels, Cebelcor, pp. 97-105.

POURBAIX M., DE ZOUBOV N. (1966)[2], Atlas of Electrochemical Equilibria, Pourbaix M., ed., Brussels, Cebelcor, pp. 307-321.

POURBAIX M., KLIMZACK-MATHIEU L.V. et al (1963), "Potentiokinetic and Corrosimetric Investigations of the Corrosion Behaviour of Alloy Steels", Corrosion Science, 3, p. 239.

RAWAT N.S. (1976), "Corrosivity of Underground Mine Atmospheres and Mine Waters : A Review and Preliminary Study", Br. Corrosion J., 11, p. 86.

SCHWENK W. (1964), "Theory of Stainless Steel Pitting", Corrosion, 20, p. 129.

SCOTTO V., DI CINTIO R., MARCENARO G. (1985), "The Influence of Marine Aerobic Microbial Film on Stainless Steel Corrosion Behaviour", Corrosion Science, 25, p. 185.

SCOTTO V., VENTURA G., TRAVERSO E. (1979), "The Influence of Non-Metallic Inclusion Nature and Shape on the Pitting Corrosion Susceptibility of 18Cr9Ni and 17Cr11Ni2Mo Austenitic Stainless Steels", Corrosion Science, 19, p. 237.

SEDRIKS A.J. (1983), "Role of Sulphide Inclusions in Pitting and Crevice Corrosion of Stainless Steels", International Metals Reviews, 28, p. 295.

SEDRIKS A.J. (1984), "Metallurgical Aspects of Passivation of Stainless Steels", Proc. Stainless Steels Conference, Göteberg, The Institute of Metals, England, 1, p. 125.

SHREIR L.L. (1979), Corrosion, Volume 1, Metal Environment Reactions, Shreir L.L., ed., London, Newnes Butterworth, pp. 1:52-1:113.

STARR K.K., VERINK E.D. Jr., POURBAIX M. (1976), "The Significance of the Protection Potential for Fe-Cr Alloys at Room Temperature", Corrosion, 32, p. 47.

STOLICA N. (1969), "Pitting Corrosior on Fe-Cr and Fe-Cr-Ni Alloys", Corrosion Science, 9, p. 455.

SUBRAHMANYAM D.V., HOEY G.R. (1975), 'Influence of Water Quality on the Corrosion and Electrochemical Behaviou· of Mild Steel in Synthetic Acid Mine Waters", Corrosion, 31, p. 202.

SUZUKI T., YAMABE M., KITAMURA Y. (1973), "Composition of Anolyte within Pit Anode of Austenitic Stainless Steels in Chloride Solutions", Corrosion, 29, p. 18.

SZKLARSKA-SMIALOWSKA Z. (1971), "Review of Literature on Pitting Corrosion Published Since 1960", Corrosion, 27, p. 223.

SZKLARSKA-SMIALOWSKA Z. (1975), "Various Forms of Localized Corrosion in Iron and Steel : Common Features and Differences", Br. Corros. J., 10, p. 11.

SZKLARSKA-SMIALOWSKA Z., JANIK-CZACHOR M. (1971), "The Analysis of Electrochemical Methods for the Determination of Characteristic Potentials of Pitting Corrosion", Corrosion Science, 11, p. 914.

TILLER A.K. (1982), Corrosion Processes, Parkins R.N., ed., New York, Applied Science Publishers Ltd, pp. 115-159.

TRUMAN J.E. (1976), "Corrosion Resistance of 13% Chromium Steel as Influenced by Tempering Treatments", Br. Corros. J., 11, p. 92.

UHLIG H.H., GILMAN J.R. (1964), "Pitting of 18-8 Stainless Steel in Ferric Chloride Inhibited by Nitrates", Corrosion, 20, p. 289.

VERINK E.D. Jr., POURBAIX M. (1971), "Use of Electrochemical Hysteresis Techniques in Developing Alloys for Saline Exposures", Corrosion, 27, p. 497.

WALKER M.S., ROWE L.C. (1969), "The Application of Electrochemical Techniques to the Study of Corrosion of Automotive Trim Materials", Corrosion, 25, p. 47.

WHITE R.T. (1985), "Water Treatment Practice in South African Gold Mines", J.S. Afr. Inst. of Mining and Metallurgy, 85, p. 81.

WILDE B.E. (1972), "A Critical Appraisal of Some Popular Laboratory Electrochemical Tests for Predicting the Localized Corrosion Resistance of Stainless Alloys in Sea Water", Corrosion, 28, p. 283.

WILDE B.E., WILLIAMS, E. (1970), "On the Correspondence between Electrochemical and Chemical Accelerated Pitting Corrosion Tests", J. Electrochemical Society, 117, p. 775.

APPENDIX A

Table A.1 gives the compositions of various mine waters as determined by a survey conducted by the Chamber of Mines (shown overleaf).

TABLE A.1 : Mine Water Compositions

IONIC SPECIES (concentration in ppm) / NAME OF MINE	pH	Total Dissolved Solids	Total Suspended Solids	Total Hardness (as $CaCO_3$)	Sulphate	Chloride	Sulphite	Sulphide	Nitrate	Free Saline Ammonia	Hypochlorite	Bicarbonate	Fluoride	Calcium	Magnesium	Sodium	Potassium	Ferrous Ion	Ferric Ion	Nickel	Copper	Langelier Index	Aluminium	Zinc	Nitrite	Conductivity (mS/m)	Total Alkalinity (as $CaCO_3$)	pH of Saturation	Calcium Hardness (as $CaCO_3$)	Magnesium Hardness (as $CaCO_3$)
MINE A	6.5	1130	26	457	425	172	*	*	49	0.7	*	44	0.4	115	25	166	6	0.1	0.3	1.05	*	-1.49	*	*	*	na	na	na	na	na
MINE B (SHAFT 1)	6.0	3502	64	811	711	1037	*	*	246	27	170	5	0.8	243	50	930	7.3	0.7	11.7	1.36	*	-2.67	2.7	0.64	12.1	460	4	na	672	139
MINE B (SHAFT 2)	6.5	3038	18	635	265	1203	*	*	144	12	157	31	1.1	182	44	790	5.5	0.2	2.9	0.21	*	-1.46	0.8	0.19	37	490	26	na	511	124
MINE C (DAY 1)	6.1	3790	7	448	153	1865	*	*	65	0.8	*	94	1.2	182	5.8	1040	12	0.1	0.1	*	*	-2.0	*	*	1.0	614	24	8.10	402	46
MINE C (DAY 2)	7.2	3520	22	414	150	1574	*	*	43	4.0	67	49	1.3	138	16	1290	7.6	0.3	2.9	0.22	*	-0.94	5.1	*	27.2	na	40	na	371	43
RAND WATER BOARD	7.4	364	32	184	102	38	*	0.3	*	0.8	*	201	0.3	48	12	37	4.5	0.1	0.2	*	*	-0.56	*	*	*	54.7	101	na	na	na
MINE D	6.5	2184	19	518	829	39	1.1	0.8	327	91	142	10	1.5	158	30	290	15.2	0.23	1.8	1.98	*	-2.02	0.3	1.77	18.6	255	8	8.52	435	83
MINE E	6.3	4975	42	1034	821	1812	*	0.9	228	36	*	39	1.0	368	28	1130	13.9	*	*	0.37	*	-1.37	*	*	6.5	700	32	7.67	961	73
MINE F	5.8	10870	4	3689	2008	2766	*	0.8	1650	55	0.1	40	0.9	1250	138	1520	70	*	*	0.46	*	-1.52	*	0.12	58	1200	33	7.32	3322	367
MINE G	6.3	4180	20	769	901	1220	*	*	191	0.8	*	14	1.0	268	18	900	31	0.1	0.1	0.51	*	-1.55	*	*	*	619	7	7	na	na
MINE I (DAY 1)	4.7	3490	4	2173	2300	36	0.8	*	22	3.9	9	2.5	0.6	620	152	69	2.3	*	*	10.7	0.23	-3.94	23	8.5	9.9	na	2	8.64	na	na
MINE I (DAY 2)	6.9	2824	4	1526	1586	36	1.0	*	9.5	3.1	2.2	49	0.7	600	6.9	70	2.4	*	1.5	*	*	-0.44	49	*	0.7	240	40	7.34	1508	18
MINE H (DAY 1)	5.5	740	204	849	760	92	1.0	2.0	194	10.6	*	4.9	0.7	276	39	111	21	0.16	0.12	1.60	*	-3.00	1.1	0.19	4.1	na	4	8.50	na	na
MINE H (DAY 2)	7.6	1820	2875	738	677	103	1.2	*	188	17.4	100	78	0.5	250	28	104	19.7	0.13	2.0	0.33	*	0.18	1.4	0.1	9.8	175	64	7.42	664	74
MINE J	6.5	6756	44	1785	2176	1564	*	*	1185	93	107	12	0.6	580	82	1480	187	0.8	1.6	1.83	*	-1.36	2.3	0.62	30.5	850	10	na	1564	221

* = LESS THAN 0.1 PPM

n.a. - NOT AVAILABLE

APPENDIX B

THE SATURATION (LANGELIER) INDEX

The saturation index (S.I.) is the difference between the measured pH and the saturation pH, (pH_s):

$$S.I. = pH_{(measured)} - pH_{s(computed)}$$

If S.I. is positive, water becomes saturated with calcium carbonate which deposites as a protective film on the metal surface. At negative values of S.I. protective $CaCO_3$ scale can be dissolved thus exposing fresh metal to attack.

pH_s can be calculated by the following equation:

$$pH_s = (pK_2 - pK_s) + pCa^{2+} + p_{alk} + \log [1 + 2K_2/(H^+)_s] \qquad (1)$$

where pH_s is the saturation pH value
pCA^{2+} is the logarithm of calcium concentration
p_{alk} is the negative logarithm of alkalinity to methyl orange
pK_2 is the negative logarithm of the ionisation constant of HCO_3^-

that is : $$K_2 = \frac{[H^+]\,[CO_3^{2-}]}{[HCO_3^-]}$$

and pK_s is the negative logarithm of the solubility product of $CaCO_3$

that is : $K_s = [Ca^{2+}]\,[CO_3^{2-}]$

When the pH of the solution falls within the range 6.5 to 9.5 the last term in equation(1) becomes very small and the equation reduces to:

$$pH_s = (pK_2 - pK_s) + p\,Ca^{2+} + p_{alk}$$

Charts and nomographs are available for obtaining the pH_s values of waters with a wide range of compositions (Rawat, (1976)).

APPENDIX C

TABLE C.1 : AISI 431 recommended composition and composition as determined by laboratory analysis

ELEMENT	C	Cr	Mn	Ni	P	Si
Recommended composition	).20	15-17	1.0	1.25-2.50	0.04	1.0
Analysed composition	).21	16.3	0.64	2.02	-	0.30

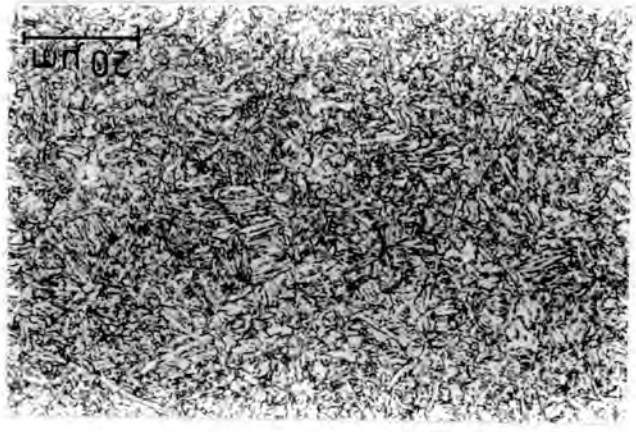

FIGURE 1 : Microstructure of AISI 431. Specimen etched in 100 ml of 1 in 5 volume/volume HCl + 2g ammonium bifluoride + 1g potassium metabisulfite for 6 seconds at room temperature

TABLE C.2 : The mechanical properties of AISI 431

UTS (MPa)	BRINELL HARDNESS	ELONGATION (%)	IZOD IMPACT STRENGTH (J)
800-950	225-275	14	40

APPENDIX D

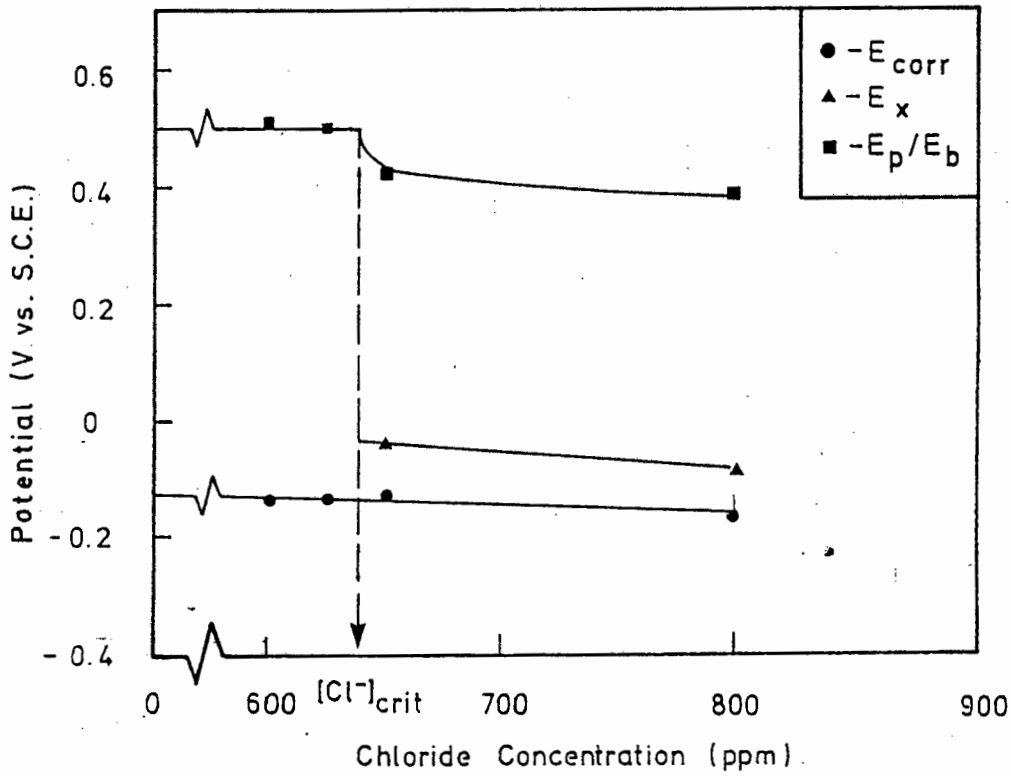

FIGURE D.1 : E_{corr}, E_x and E_p/E_b of AISI 431 versus chloride concentration in 500 ppm nitrate solution, pH 6.2.

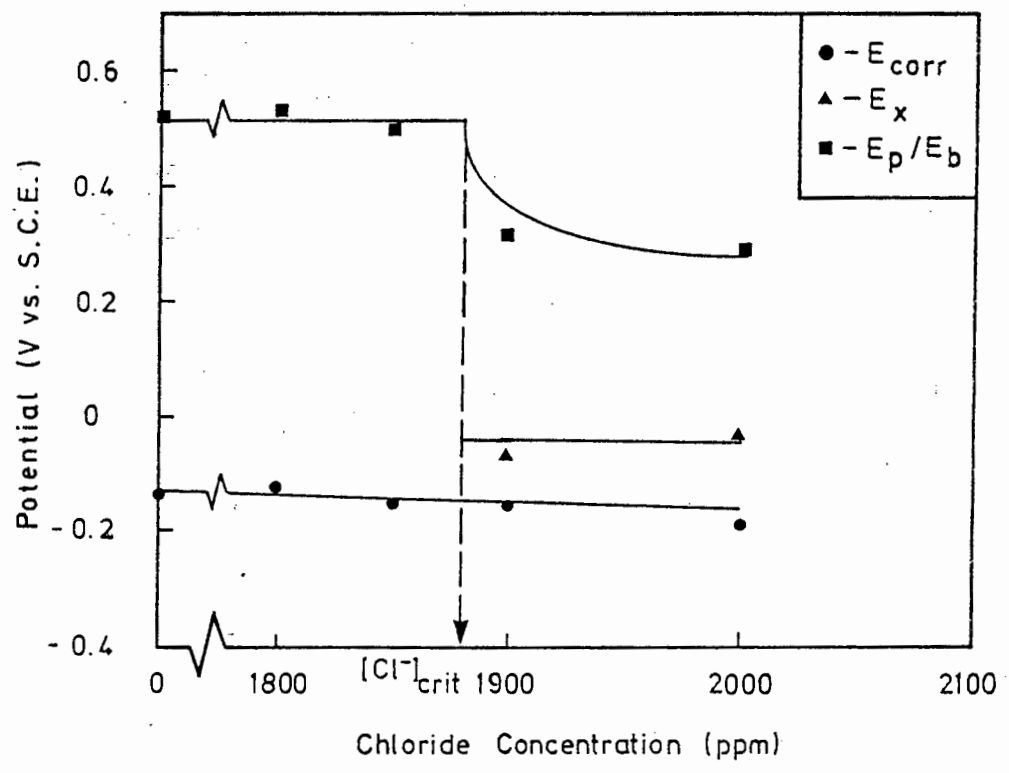

FIGURE D.2 : E_{corr}, E_x and E_p/E_b of AISI 431 versus chloride concentration in 1500 ppm nitrate solution, pH 6.2.

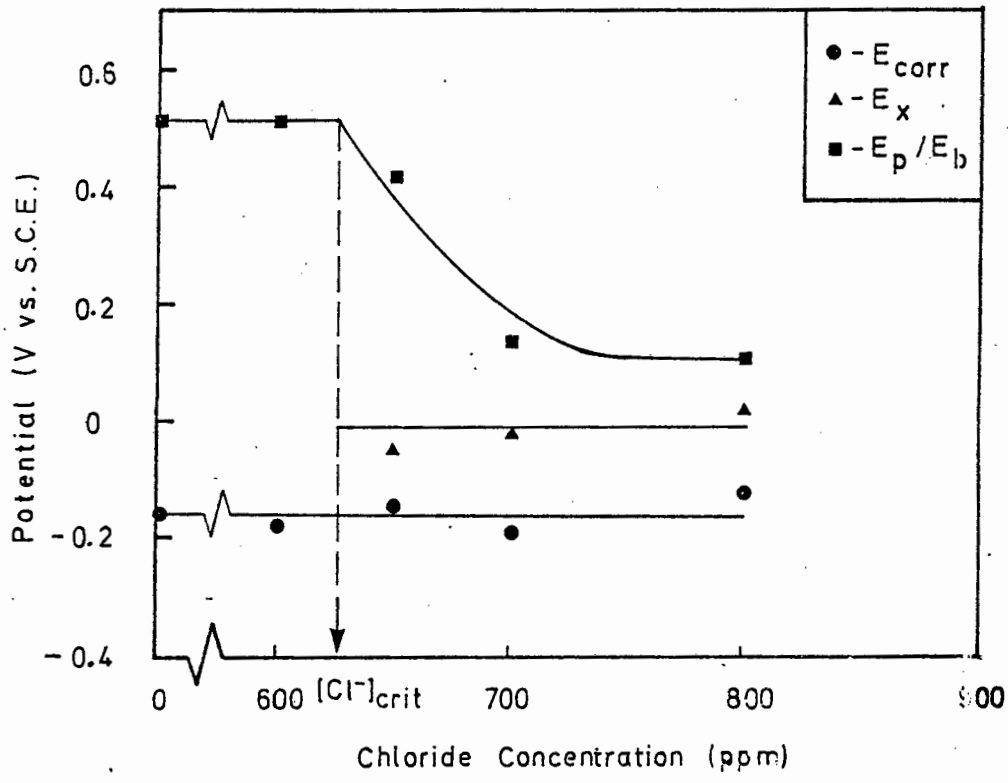

FIGURE D.3 : E_{corr}, E_x and E_p/E_b of AISI 431 versus chloride concentration in 500 ppm nitrate solution, pH 3.8.

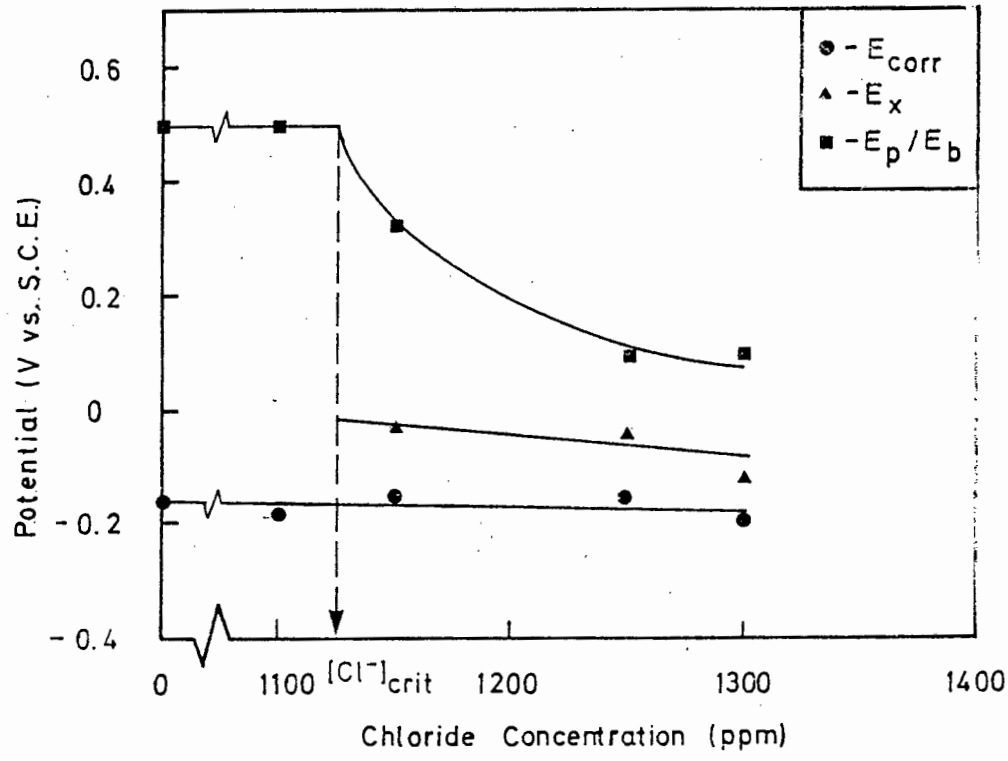

FIGURE D.4 : E_{corr}, E_x and E_p/E_b of AISI 431 versus chloride concentration in 1000 ppm nitrate solution, pH 3.8.

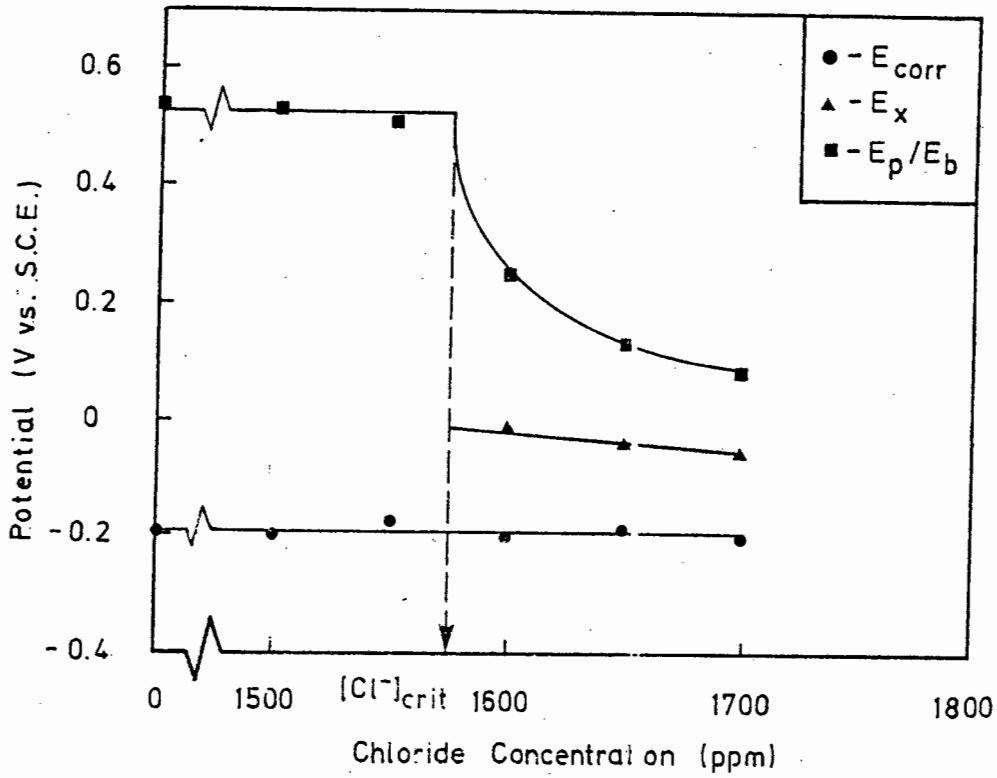

FIGURE D.5 : E_{corr}, E_x and E_p/E_b of AISI 431 versus chloride concentration in 1500 ppm nitrate solution, pH 3.4.

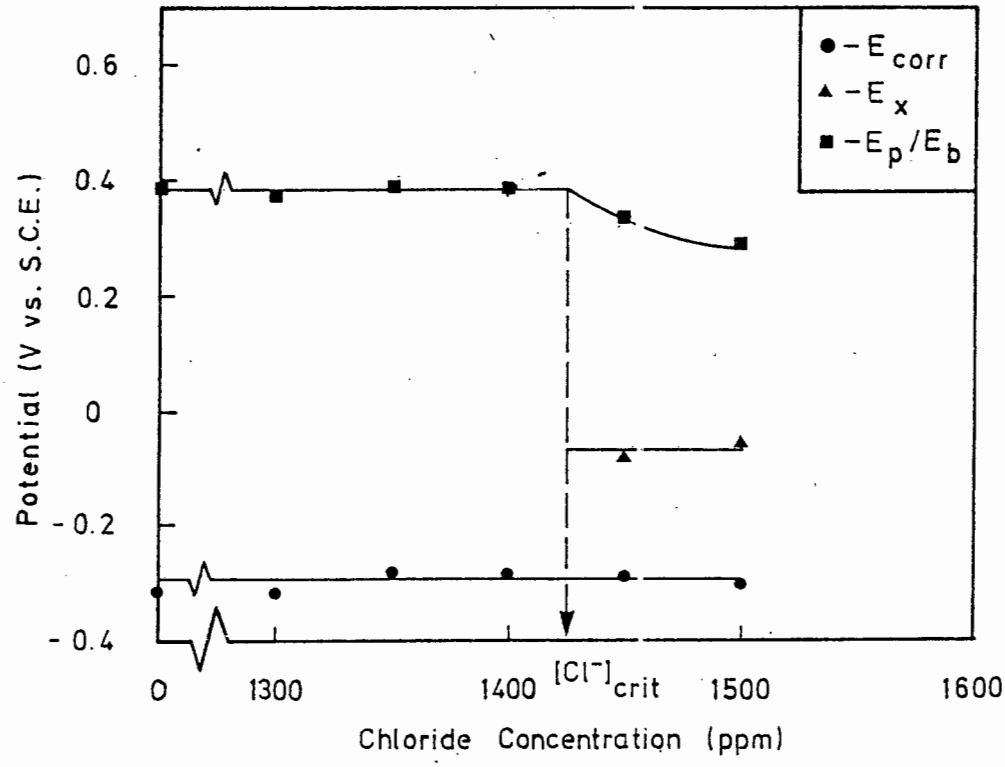

FIGURE D.6 : E_{corr}, E_x and E_p/E_b of AISI 431 versus chloride concentration in 500 ppm nitrate solution, pH 9.4.

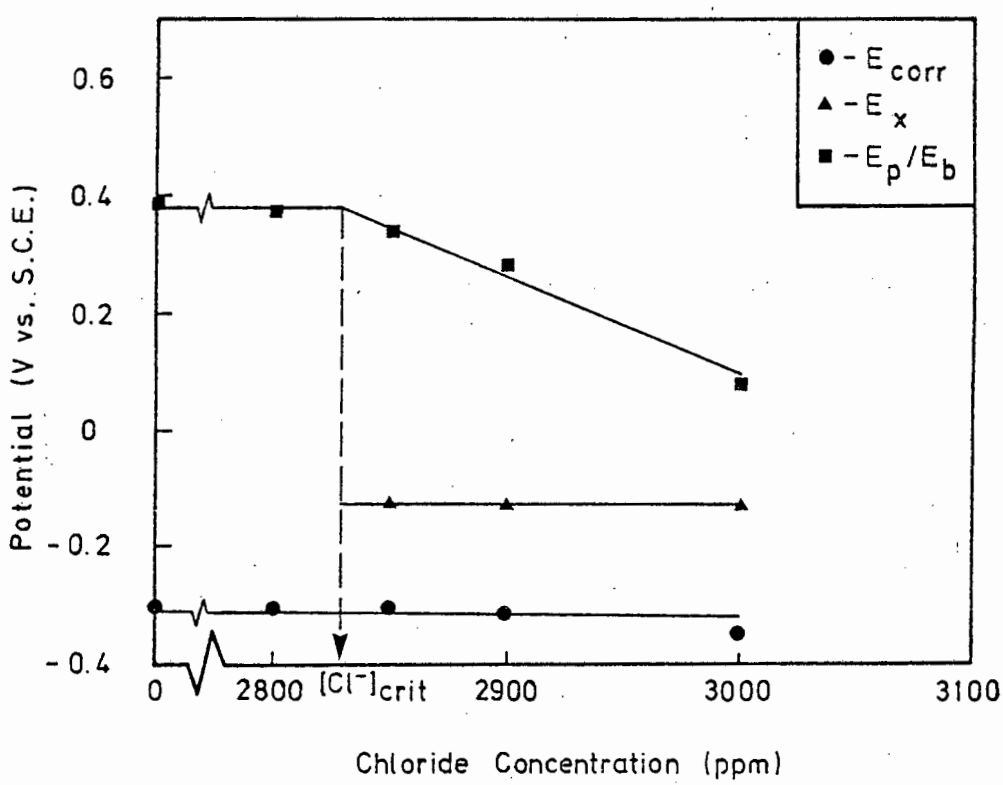

FIGURE D.7 : E_{corr}, E_x and E_p/E_b of AISI 431 versus chloride concentration in 1000 ppm nitrate solution, pH 9.4.

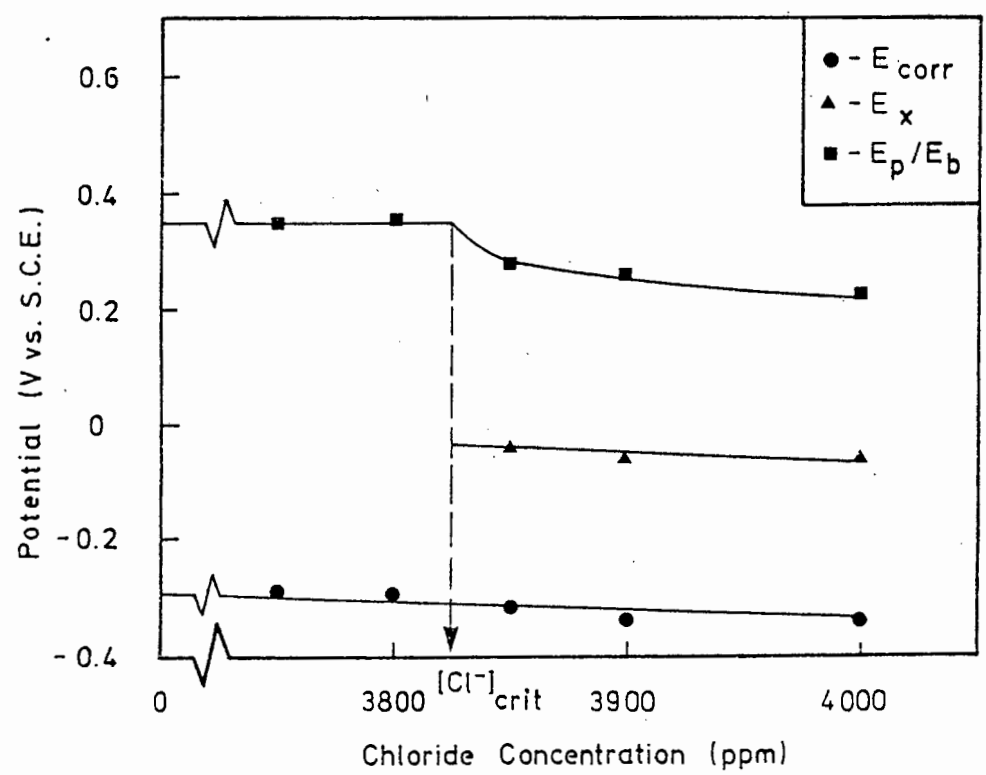

FIGURE D.8 : E_{corr}, E_x and E_p/E_b of AISI 431 versus chloride concentration in 1500 ppm nitrate solution, pH 9.4.